Cumulative Subject Index, Volumes 1–40

ISSN 0032–0633

PLANETARY AND SPACE SCIENCE

Editor-in-Chief: D. R. Bates (Belfast)
Honorary Editor: F. L. Whipple (Cambridge, Mass.)

Regional Editors:

Europe
M. Ackerman (Brussels)
M. I. Pudovkin (St Petersburg)

North America
M. H. Rees (Fairbanks, Alaska)
C. T. Russell (Los Angeles, Calif.)

Asia
H. Fukunishi (Sendai)

Southern Hemisphere
K. D. Cole (Victoria)

Cumulative Subject Index prepared by R. G. H. Greer (Belfast)

PERGAMON PRESS OXFORD NEW YORK SEOUL TOKYO

PLANETARY AND SPACE SCIENCE

Editor-in-Chief

Professor Sir David Bates

Department of Applied Mathematics and Theoretical Physics, The Queen's University, Belfast BT7 1NN, Northern Ireland (Fax No. (0232) 247895).

Assistant to the Editor-in-Chief

Mrs Shirley Laughlin

Honorary Editor

Dr F. L. Whipple. Astrophysical Observatory, 60 Garden Street, Cambridge, Massachusetts 02138, U.S.A.

Regional Editors

Europe

Dr M. Ackerman, Director, Institut d'Aeronomie Spatiale de Belgique, 3 Avenue Circulaire, B-l 180 Brussels, Belgium.

Professor M. I. Pudovkin, Institute of Physics, St Petersburg University, Stary Petergof 198904, St Petersburg, Russia.

North America

Professor M. H. Rees, Geophysical Institute, University of Alaska, Fairbanks, Alaska 99775-0800, U.S.A.

Professor C. T. Russell, Institute of Geophysics and Planetary Physics, University of California, Los Angeles, California 90024. U.S.A.

Asia

Professor H. Fukunishi, Upper Atmosphere and Space Research Laboratory, Tohoku University, Sendai 980, Japan.

Southern Hemisphere

Professor K. D. Cole, Division of Theoretical and Space Physics, La Trobe University, Melbourne, Victoria 3083, Australia.

Editorial Advisory Board

S. I. Akasofu (*College, Alaska*)
F. Arnold (*Heidelberg*)
W. J. Baggaley (*Christchurch, N.Z.*)
W. J. Beynon (*Aberystwyth*)
J. E. Blamont (*Verrières-le-Buisson*)
R. N. Bracewell (*Stanford, Calif.*)
J. W. Chamberlain (*Houston, Texas*)
J. Coulomb (*Paris*)
S. W. H. Cowley (*London*)
A. Dalgarno (*Cambridge, Mass.*)
A. J. Dessler (*Houston, Texas*)
T. M. Donahue (*Ann Arbor, Mich.*)
E. M. Dubinen (*Moscow*)
E. E. Ferguson (*Boulder, Colo.*)
B. J. Fraser (*New South Wales*)
R. Gendrin (*Issy-le-Moulineaux*)
R. M. Goody (*Cambridge, Mass.*)
R. G. Greer (*Belfast*)
M. Hayakawa (*Chofu, Tokyo*)
R. A. Helliwell (*Stanford, Calif.*)
W. J. Hughes (*Boston, Mass.*)
B. Hultqvist (*Kiruna*)
D. M. Hunten (*Tucson, Ariz.*)
F. S. Johnson (*Dallas, Texas*)
V. I. Krassovsky (*Moscow*)
E. J. Llewellyn (*Saskatoon, Sask.*)
R. Lundin (*Kiruna*)
K. Maeda (*Kyoto*)
M. B. McElroy (*Cambridge, Mass.*)
R. J. Moffett (*Sheffield*)
P. Moore (*Aston*)
E. Murad (*Hanscom, Mass.*)
K. Nagashima (*Nagoya*)
A. Nishida (*Kanagawa*)
E. N. Parker (*Chicago, Ill.*)
W. Priester (*Bonn*)
H. Rishbeth (*Southampton*)
S. S. Sazhin (*Sheffield*)
R. W. Schunk (*Logan, Utah*)
N. N. Shefov (*Moscow*)
G. G. Shepherd (*Toronto, Ont.*)
T. G. Slanger (*Menlo Park, Calif.*)
S. Solomon (*Boulder, Colo.*)
D. J. Southwood (*London*)
L. R. O. Storey (*Cucuron*)
M. Sugiura (*Tokyo*)
J. E. Titheridge (*Auckland, N.Z.*)
D. G. Torr (*Huntsville, Ala.*)
V. A. Troitskaya-Cole (*Melbourne*)
N. A. Tsyganenko (*St Petersburg*)
A. Vallance Jones (*Ottawa, Ont.*)
A. D. M. Walker (*Durban, S.A.*)
G. Witt (*Stockholm*)
K. Yumoto (*Nagoya*)
T. E. van Zandt (*Boulder, Colo.*)
E. C. Zipf (*Pittsburg, Penn.*)

Production Editor

Euan Stillie

Publishing and Advertising Offices: Pergamon Press Ltd, Headington Hill Hall, Oxford, OX3 0BW, U.K.; and Pergamon Press Inc., 660 White Plains Road, Tarrytown, NY 10591-5153, U.S.A.

Annual Subscription Rate (1993)

Annual Institutional Subscription Rate (1993) £745.00 (US $1192.00). Sterling price is definitive. US dollar price is quoted for convenience only, and is subject to exchange rate fluctuation. Prices include postage and insurance and are subject to change without notice. Subscription rates for Japan include despatch by air and prices are available on request. Personal Subscription Rate for those whose library subscribes at the regular rate is available on request. Subscription enquiries from customers in North America should be sent to: Pergamon Press Inc., 660 White Plains Road, Tarrytown, NY 10591-5153, U.S.A., and for the remainder of the world to: Pergamon Press Ltd, Headington Hill Hall, Oxford OX3 0BW, U.K.

Second Class Postage Paid at RAHWAY, NJ. Postmaster send address corrections to Planetary and Space Science, c/o Pergamon Press Inc., 660 White Plains Road, Tarrytown, NY 10591-5153, U.S.A.

Whilst every effort is made by the publishers and editorial board to see that no inaccurate or misleading data, opinion or statement appear in this journal, they wish to make it clear that the data and opinions appearing in the articles and advertisements herein are the sole responsibility of the contributor or advertiser concerned. Accordingly, the publishers, the editorial board and editors and their respective employees, officers and agents accept no responsibility or liability whatsoever for the consequences of any such inaccurate or misleading data, opinion or statement.

Published Monthly.

Copyright © 1993 Pergamon Press Ltd

PLANETARY AND SPACE SCIENCE

Editor-in-Chief: D. R. Bates (Belfast)
Honorary Editor: F. L. Whipple (Cambridge, Mass.)

Regional Editors:

Europe
M. Ackerman (Brussels)
M. I. Pudovkin (St Petersburg)

North America
M. H. Rees (Fairbanks, Alaska)
C. T. Russell (Los Angeles, Calif.)

Asia
H. Fukunishi (Sendai)

Southern Hemisphere
K. D. Cole (Victoria)

Cumulative Subject Index prepared by R. G. H. Greer (Belfast)

PERGAMON PRESS OXFORD NEW YORK SEOUL TOKYO

Publishing and Advertising Offices

Pergamon Press Ltd, Headington Hill Hall, Oxford, OX3 0BW, U.K.; and Pergamon Press Inc., 660 White Plains Road, Tarrytown, NY 10591-5153, U.S.A.

Back Issues

Back Issues of all previously published volumes, in both hard copy and on microform, are available direct from Pergamon Press offices.

Published Monthly. Copyright © 1993 Pergamon Press Ltd

It is a condition of publication that manuscripts submitted to this journal have not been published and will not be simultaneously submitted or published elsewhere. By submitting a manuscript, the authors agree that the copyright for their article is transferred to the Publisher if and when the article is accepted for publication. However, assignment of copyright is not required from authors who work for organizations which do not permit such assignment. The copyright covers the exclusive rights to reproduce and distribute the article, including reprints, photographic reproductions, microform or any other reproductions of similar nature and translations. No part of this publication may be reproduced, stored in a retrieval system or transmitted in any form or by any means, electronic, electrostatic, magnetic tape, mechanical, photocopying, recording or otherwise, without permission in writing from the copyright holder.

Whilst every effort is made by the publishers and editorial board to see that no inaccurate or misleading data, opinion or statement appear in this journal, they wish to make it clear that the data and opinions appearing in the articles and advertisements herein are the sole responsibility of the contributor or advertiser concerned. Accordingly, the publishers, the editorial board and editors and their respective employees, officers and agents accept no responsibility or liability whatsoever for the consequences of any such inaccurate or misleading data, opinion or statement.

Photocopying information for users in the U.S.A.

The Item-Fee Code for this publication indicates that authorization to photocopy items for internal or personal use is granted by the copyright holder for libraries and other users registered with the Copyright Clearance Center (CCC) Transactional Reporting Service provided the stated fee for copying beyond that permitted by Section 107 or 108 of the United States Copyright Law, is paid. The appropriate remittance of $5.00 per copy per article is paid directly to the Copyright Clearance Center Inc., 27 Congress Street, Salem, MA 01970, U.S.A.

Permission for other use. The copyright owner's consent does not extend to copying for general distribution, for promotion, for creating new works, or for resale. Specific written permission must be obtained from the Publisher for such copying.

♾ The text paper used in this publication meets the minimum requirements of the American National Standard for Information Sciences—Permanence of Paper for Printed Library Materials, ANSI Z39.48–1984.

The Item-Fee Code for this publication is: 0032–0633/92 $5.00 + 0.00

CUMULATIVE SUBJECT INDEX, VOLUMES 1–40

AEROSOLS
atmospheric, *see also* SEEDING
extra-terrestrial, *see* METEORITICS
stratospheric,
evidence for unknown component, **30**,101
formations from volcanic H_2SO_4 and HSO_3, **32**,89
optical properties of volcanic dust, **32**,17

AIRGLOW, DAY
brightness increase at 1.25μm, **13**,457
far UV, atmospheric composition and temperature, **31**,967
far UV, N^{+*} from $N_2+h\nu$, **39**,1197
far UV, rocket data, **21**,879
fluorescence of solar ionizing radiation, **13**,947
Fraunhofer fill-in brightness, polarization, **37**,627
helium, 58.4nm, contamination by OII emission, **25**,193
hydrogen,
L_α, diurnal variations, satellite data, **18**,803
L_α, geocoronal emission, H concentrations, **15**,1531; **16**,929; **17**,769; **18**,803; **20**,297; **21**,309
L_α, variability with solar activity, **29**,907
hydroxyl,
excitation, effects of sunlight, **17**,1629
(8-6) band, balloon data, **21**,1945
infra-red, weak emissions observed, **17**,975
nitric oxide fluorescence in backscatter, **30**,137
nitrogen bands,
first positive, resonant scattering, **20**,549
second positive, 337.1nm, implication for photoelectron fluxes, **31**,221,1223
oxygen bands,
Herzberg, in backscattered spectrum, **30**,575
$O_2(^1\Delta_g)$ emission, global study, **30**,545
O_2 atmospheric, 761.9nm, altitude-intensity profile, **33**,17
O_2 atmospheric, simulation, **34**,1031
1.58μm IR, correlations, also twilight, **14**,1
O_2^+, vibrational distribution, ionosphere, **34**,1241
oxygen lines,
far UV, **12**,1021; **21**,879
53.7nm and 58.1nm, OII intensities, **25**,193
83.4nm, OII, excitation rate and intensity, **33**,1179,1303,1309
98.9 and 117.2nm multiplets, rocket measurements, **36**,987
117.2-6nm multiplet, electron impact excitation, **34**,1155; **36**,987
130.0nm, emission holes detected, **35**,1297
130.4nm, excitation, **18**,661
130.4nm, intensity ratio, assuming LTE, **30**,39
130.4nm, radiative transfer, **13**,871; **18**,661
130.4nm, resonant scattering model, **30**,439
130.4nm, rocket measurement, **13**,1273; **16**,929
130.4, 135.6, 164.1nm, satellite measurements, thermospheric oxygen densities, **36**,963
557.7nm, effect of solar UV and corpuscular radiation, **17**,1322
557.7nm, rocket, equatorial, **17**,1609
630.0nm, high resolution (PEPSIOS) observations, **25**,185
630.0nm, interferometric line width analysis, **12**,1139; **13**,551,1163; **14**,1035
630.0nm, rocket measurement, **13**,1273
63μm infrared emission, atmospheric heat balance, **18**,271
sodium, doublet, rocket data, **18**,1666
spectrophotometry during solar eclipse, **12**,875
visual, **14**,677

AIRGLOW, NIGHT
aeronomy, deactivation and charge transfer, **37**,363
atlas of spectrum, 300-1240nm, **9**,883
CO_2, infrared emission, excitation, **24**,749
contamination from aurorae, **16**,1418
continuum,
correlation with green line, **12**,97
gravity wave association, **31**,331; **38**,1105
green and near infra-red wavelengths, **34**,801
intensity profiles, **15**,1857; **16**,821, **34**,771
near infra-red, **25**,787; **26**,191; **34**,801
radiative association mechanisms, **40**,243
theory of excitation, **34**,1373
effects of high-altitude nuclear explosion, **10**,47
gravity wave effects on emission heights, **23**,896
hydrogen,
H_α, **12**,149; **15**,407,1223,1757; **17**,1320
H_β, intensity, radial velocity data, **17**,561
H_β, with N and OI emissions, ground spectrometry during magnetic storm, **36**,371
L_α, geocoronal emission, H concentrations, **1**,3,63; **9**,455,459; **10**,65; **12**,650; **17**,769; **18**,803; **21**,309; **24**,303; **26**,431
hydroxyl,
altitude-intensity profiles, **27**,341,1421; **34**,771; **35**,1029; **36**,897; **37**,49; **39**,1049
associated atmospheric motions, **25**,200,265; **26**,893; **27**,801; **33**,381,1013; **35**,413; **36**,975; **37**,649; **38**,1105,1421
band intensities, vibrational populations, **5**,158; **11**,149; **17**,173; **20**,624; **21**,1011,1731,1945; **22**,344,1058,1323; **23**,1211; **26**,525; **29**,1241; **31**,423; **33**,381; **35**,1029; **37**,649; **39**,1049
atomic oxygen densities, **24**,389; **36**,897; **37**,49
characteristic differences, **25**,509
contamination of line emission measurements, **20**,2198
correlation with Na(D-lines), **27**,801; **37**,649
correlation with oxygen bands, **19**,795; **27**,341; **34**,301; **37**,649
correlation with oxygen lines, **27**,341,801; **37**,649
emission altitude, ground, triangulation, **23**,1346
excitation mechanism, **8**,197; **10**,7; **18**,1271; **20**,624; **26**,933; **35**,1137; **36**,897; **40**,235

$H+O_3 \rightarrow OH^*+O_2$, $\Delta v=1$ sequence, **13**,1005
high latitude summer observations, **39**,1263
linked to geomagnetic disturbances, **20**,1363
meteoritic, noctilucent cloud correlations, **16**,134
polar region intensities, **32**,263
quenching of OH*, **28**,559
scanning spectrophotometric measurements, **27**,1221
temperatures, rotational, **5**,153; **9**,167; **15**,1515; **17**,173; **20**,261; **22**,1323; **23**,1211; **24**,665; **25**,595,596; **29**,1241; **31**,923; **32**,852; **37**,649; **39**,1171,1263,1397; **40**,235
transition probabilities, **37**,723
variations, diurnal, **18**,887; **19**,129; **21**,1011,1731; **22**,1059; **31**,423; **33**,381; **37**,649
variations, seasonal, solar cycle, geomagnetic effects, **17**,797; **21**,1011, 1731; **32**,897; **35**,977
NO, infrared emission, excition, **24**,749; **30**,1043
NO, δ and γ bands, satellite observations, **40**,481
NO γ bands, antarctic NO profile, **28**,867
nitrogen,
dissociation by extreme UV, **26**,449
N_2^+, global mapping, ISIS-II, **21**,819
N_2^+, middle latitudes, **14**,709
337.1nm, 520.0nm, magnetic ordering, **26**,339
391.4nm, with OI and H_β emissions, ground spectrometry during magnetic storm, **36**,371
520.0nm, contamination by OH, **25**,985
520.0nm, excitation, temporal behaviour, **17**,675; **26**,897
520.0nm, scanning spectrophotometer, **27**,1221
oxygen bands,
excitation and quenching, **36**,875; **37**,881
Herzberg, 373-474nm, rotationally resolved in oxygen afterglow, **34**,971
Herzberg, measured (ground) and modelled spectra, **39**,595
Herzberg, intensity profiles, **27**,925,1507; **34**,771; **40**,913
Herzberg, satellite measurements, **23**,1681; **40**,481
Herzberg , $O_2(A^3\Sigma_u^+)$ vibrational analysis, **30**,1133; **34**,811; **38**,1399; **40**,913
infra-red atmospheric system, Franck-Condon factors, **19**,1009
microwave emission at 2.53mm, **19**,777
O_2 photodissociation, aeronomic problems and related parameters, **36**,963
$O_2(a^1\Delta_g)$ chemical production mechanisms, **38**,529
$O_2(b^1\Sigma)$, excitation mechanism, **29**,383
$O_2(b^1\Sigma)$, quenching parameters for precursors, **34**,789; **38**,43
$O_2(b^1\Sigma)$, retrieval of green line profiles, **38**,43
oxygen atom concentrations, **37**,49,1333
oxygen UV high resolution spectroscopy, **36**,927
ozone abundance, O_2 1.27μm system, **40**,1391
ozone infrared band emission, **24**,748; **38**,1121
transition probabilities, **36**,869; **37**,881
twilight decay characteristics, **37**,61
761.9nm, altitude-intensity profile, rocket, **27**,341; **34**,771; **40**,783
864.5nm, intensity profile, rocket, **11**,437
864.5nm, correlation with hydroxyl, **19**,795; **33**,381; **34**,301; **37**,649
864.5nm, rotational temperatures, **34**,301; **39**,1363,1397
864.5nm, variability during polar winter, **35**,1275
1.27μm, intensity profile, **34**,771; **35**,1541; **36**,459; **37**,49; **40**,1391
1.27μm, balloon, diurnal variations, **17**,933
1.27μm, depletions and mesospheric ionization, **35**,1087
1.27μm, enhancement during auroral break-up, **26**,619
1.27μm, excitation mechanism, **26**,533; **35**,1541; **38**,529
oxygen concentration,
airglow inversion, **24**,389; **25**,79; **27**,341,925; **33**,571; **34**,771; **36**,897,963,987; **38**,221; **39**,627; **40**,775,929,1269
resonance fluorescence, **25**,79; **27**,925; **34**,771
oxygen excitation mechanisms,
association of atomic oxygen, **26**,897; **30**,251
most species, terrestrial planets, **29**,925; **34**,511
oxygen green line,
altitude-intensity profiles, **15**,1857; **16**,821; **20**,1781; **27**,801,1409; **34**,771; **35**,1389; **38**,547; **40**,783,1269
anomalous intensity increase, **9**,993
associated atmospheric motions, **10**,103; **25**,711; **27**,801,1409; **32**,897; **33**,381; **35**,413,1389; **36**,975; **37**,649; **38**,1105
continuum correlation, **12**,97
correlation with atmospheric bands, **34**,301; **38**,43
correlation with OH bands, **25**,541
correlation with OH and Na D-lines, **27**,801; **33**,381; **37**,649
correlation with solar activity, **12**,867; **15**,863; **16**,1311
covariance with the red line, **19**,1087; **37**,649; **38**,547,889,1161
Doppler temperatures, winds, **13**,901; **14**,383, 1331; **16**,211,431; **19**,467; **38**,1161
emission,equatorial enhancement, **19**,672
emission, hemisphere comparison, **38**,1161
excitation, lower thermosphere, **10**,19; **14**,113; **15**,1091; **25**,79; **26**,897; **27**,341,717,925,1409; **29**,1061; **34**,511,771; **36**,883,1077; **38**,43; **40**,211,1269
excitation, by O_2^++e, **36**,621; **38**,547,889
global mapping, ISIS-II data, **21**,819
Lord Rayleigh's data, re-examination, **12**,97
lunar time intensity variations, **11**,1133

nitrogen afterglow production, **3**,169
$O(^1S)$, precursor quenching, **34**,1101
$O(^1S)$, production from O_2^+, **34**,1101
$O(^1S)$, quantum yield from O_2^+, **28**,1081; **40**,607,893
oxygen concentration from intensity measurements, **20**,1781
polar cap, **25**,23; **30**,865
polarized component, zodiacal light, **16**,1291
seasonal variation, **15**,1091
simultaneous with red line and OH measurements, **18**,887
temperature dependence, **39**,1397
transition probability, measurement, **17**,1297
variations, diurnal, **12**,247; **18**,641,887; **25**,711; **33**,381
oxygen OI infrared limb emission, thermospheric temperature and oxygen density, **37**,1333; **38**,221
oxygen red line,
covariance with the green line and OH, **18**,887; **19**,1087; **37**,649; **38**,547,889,1161
covariance with OI(777.4), N and H_β emissions during magnetic storm, **36**,371
emission, hemisphere comparison, **38**,1161
enhancement, equatorial, **19**,672; **32**,1605
enhancement, latitude wide, **18**,1829
equatorial depletions, **29**,1251; **31**,355
excitation, deactivation, **9**,499; **11**,45; **14**,1225; **15**,427; **17**,1725; **22**,709; **23**,1013; **25**,155; **26**,93,161,897; **29**,589,595; **34**,1134; **36**,89; **38**,889,1243; **40**,211,607,699,893,1269
Doppler temperatures, winds, **12**,591; **16**,431, 1109; **17**,957; **31**,53,303; **33**,201; **36**,225; **38**,1161
F-layer dependence, **9**,133; **10**,29; **20**,11; **26**,93,161
geomagnetic activity dependence, **16**,140,1201; **20**,1363; **24**,629
global mapping, ISIS-II data, **21**,819
ground-based, OH contamination, **25**,985
intensity behaviour at Sacramento Peak, **14**,407
intensity profile, **15**,1857, **38**,547, **40**,1269
ionospheric model parameters, **38**,1243
ionospheric scintillations, **20**,41,1982; **22**,495
$O(^1D)$, quenching rate by $O(^3P)$, **34**,1143
SAR arcs, intensity during storms, **24**,629
temperature dependence, **39**,1397
variations, diurnal, **18**,887
wave-like intensity irregularities, **24**,521
oxygen UV lines,
130.4nm, atomic densities, global, OGO, **24**,313
130.4nm, intensity ratio, assuming LTE, **30**,39
excitation, radiative decay of $3s^3D^0$ and $3d^3D^0$ levels, **27**,719
O^+, equatorial ionosphere, **24**,945
O^+, radiative recombination, **27**,719
ozone chemistry and green line excitation, **36**,1077
ozone infrared emission, excitation, **24**,749; **38**,1121
patchiness, green and red emissions, **12**,725
photometry,
calibration, **12**,189; **14**,921
Hadamard coding, **20**,1351
profile analysis, statistical inference method, **37**,1327
review, IGY and IGC measurements, **8**,125
shadow height of Earth, **16**,1071
simultaneous measurements, mesosphere and F-region, **37**,649
sodium,
associated atmospheric motions, **32**,897; **33**,381; **36**,975
chemistry review, sudden sodium layers, **40**,247
correlation with OH and OI(557.7nm), **27**,801; **33**,381; **37**,649
correlation with rf absorption, **25**,45
excitation mechanism, **10**,19
implications for observations of Jupiter from Earth, **25**,603
intensities, diurnal, seasonal, solar cycle variations, **21**,1011; **22**,344; **29**,765; **32**,897; **33**,381; **37**,649
temperature dependence, **39**,1397
volume emission profile, **15**,1857; **26**,65
van Rhijn height determinations, **13**,855
variability, survey of research, **35**,1449
vibrationally excited molecules, **10**,19
Visible Airglow Experiment, a review, **36**,21
zodiacal light, *see* ZODIACAL LIGHT

AIRGLOW, TWILIGHT

anomalous brightness in near infra-red, **14**,445
Ca^+ emission,
excited in meteor trails, **15**,503
spatial extent, **15**,589
helium,
concentration, magnetic correlations, **16**,1103
excitation, **10**,73; **15**,1219; **16**,91; **17**,715
hydroxyl,
deduced mesospheric temperatures, **35**,1149
excitation, effect of sunlight, **17**,1629
variation, temporal, evening, **18**,637
metallic emissions, atmospheric dynamics, **10**,117
N_2^+ emission,
possible excitation from $He^+ + N_2$ reaction, **15**,19
Rayleigh scattering in troposphere, **16**,693
resonance scattering, **15**,1801
seasonal variation, height, excitation, **14**,1303
oxygen bands,
1.27μm, global study, **30**,545
1.27μm, ground based photometer, **18**,1065
1.27μm, ozone concentrations, **25**,165
1.58μm, excitation, seasonal variation, **11**,961; **14**,1
oxygen lines,
557.7nm, high energy electron flux, **16**,1418
630nm, conjugate effect, **22**,1297; **24**,327

630nm, excitation mechanisms, **21**,1937
630nm, O_2 abundance, thermospheric, **20**,2125
630nm, predawn enhanced, **17**,879,1677,1857; **18**,1011,1335,1367; **23**,305,1565; **24**,327,1141; **26**,211
777.4nm, excitation by conjugate electrons, **23**,305
line shapes, temperatures, **16**,431
$O^+(^2P)$, thermospheric, spectrophotometer, **27**,1221
radiation field available for photolysis, **39**,671
sodium content, doublet emission, **18**,623; **26**,65
solar ionizing radiation, **14**,1321

ALBEDO
Earth, outward thermal radiation, characteristics, **11**,663, 681; **13**,353
infra-red reflectance of ground terrains, **13**,1004
infra-red satellite data, cloud heights, **13**,377
lunar, radiance of surface objects, **13**,271
neutron, origin of trapped protons, **11**,1151
polarization of atmospheric reflections, **17**,1307

ANOMALY, RADIATION
see CORPUSCULAR RADIATION

ANTENNAS
see INSTRUMENTATION

ANTIMATTER
search for, in cosmic rays and outer space, **9**,875

ARGON
atmospheric, Earth, diurnal variations, **11**,1379
detector, Martian atmospheric abundance,**12**,726

ASTROPHYSICS
Amateur Astronomy in the Space Age, a review lecture, **36**,1125
astronomical unit, radar echo determination from Venus, **12**,1129
celestial mechanics, self-gravitating compressible fluids, **12**,1211
chemistry of CH^+, **40**,1683
cosmic plasma, shocks, discontinuities, **24**,617
cosmic radio waves, origin, **13**,861
galactic civilizations, space flight, **11**,485
galactic magnetic fields, forms and activity, **15**,1625
galactic L_α, atmospheric diffusion, **12**,650
galactic X-ray ionization, **22**,1583
interstellar hydrogen distributions, **38**,1487
interstellar hydrogen, resonance scattering, **20**,829,1784
nebulae, gaseous, UV emission spectrum, **11**,621
neutral gases in interplanetary space, **23**,93; **40**,439
planets, giant, formation, **30**,755
range and velocity in space, rf measurements, effect of Earth's motion, **11**,561
rf astronomy, from rockets and satellites, **9**,109
sky brightness, rf field temperature, **8**,68
sky colour, irradiance during eclipse, **16**,647
stellar occultation, atmospheric oxygen, **21**,339
X-rays, balloon experiments, **20**,331
X-rays, galactic, E-region effects, **20**,61

ATMOSPHERE, PLANETARY
see also individual planets
accretion, rare gas retention, **30**,765
composition yields surface temperature, **27**,1095
curve of growth, **16**,729
cyclones and anticyclones, mechanics, **17**,1149
escape mechanisms, **30**,773; **34**,279
evolution, climate and biosphere on ancient Earth, **36**,1391
evolution implications of surface-atmosphere interactions, **30**,803
GAIA or geochemistry, regulation of CO_2 and climate, **30**,795
heating imbalance, chemically induced, greenhouse effect, **28**,1011
heating, non-linear conductance and convection, **17**,1850
ionosphere, Jupiter and Saturn, Voyager, **39**,1715
latitudinal and longitudinal variations, occultation data, **18**,1769
magnetic fields, **21**,1475,1497
magnetospheric changes in the geological past, **26**,413
micrometeorite capture and precipitation, **21**,1605
non-rotating, density variations, **21**,2123
non-rotation, temperature distribution, **21**,2123
occultation studies, properties from inversion, **16**,1197
origin and evolution, **21**,1467,1605; **30**,741
outer, ionospheres and thermospheres, **39**,1591
outgassing from satellites, distribution of gas clouds, **24**,577; **27**,1163
Planetary Patrol Program, **21**,1511
primitive types, radiative-photochemical model, **30**,785
radiative association, continuum airglow, **40**,243
radiative transfer in planetary coronae, **25**,563
rotation rates, satellite orbit analysis, **34**,1263
satellite exospheres, **27**,1163
solar wind flow-past effects, **18**,1281; **21**,1647; **27**,243
thermal escape of gases, **27**,739; **28**,159
thermospheric, solar radiation, diurnal variations, **16**,1303,1531

ATMOSPHERE, TERRESTRIAL
composition,
atoms or molecules, *see also* individual species
accretion of meteoritic dust, rate data, **2**,121
acetonitrile, stratosphere, tropopause, **35**,259, 685,715

aerodynamic effects on measurements from rockets, **36**,921
aerosols in stratosphere, **30**,101
biological influences, **31**,1065
bromoform, stratospheric, UV absorption, **37**,1127
CO, influence on atmospheric temperatures, **33**,1187
carbon, production, **5**,164
CFC's, stratospheric, **35**,657; **37**,105
chemical budget in stratosphere, **31**,1009
chemical changes induce heat balance changes, **28**,1011
chemical fluctuations, ionosphere, **34**,979
chemical response to 11 year solar cycle, **32**,411
chemistry of photolysis at twilight, **39**,671
condensable species, tropospheric cold trap, **37**,151
D-region formation, **33**,1169 dayglow UV intensity interpretation, **31**,967
escape, atmospheric loss, **11**,901; **13**,1185; **15**,1219; **18**,449
evidence for nearby supernova, **28**,639
exospheric, **22**,209,1375; **27**,1163
F-region seasonal anomaly, **19**,1014
F-region structure, photochemical processes, **9**,149
gases, seeded, dispersal of, **26**,605
HCl, stratospheric, **34**,655; **35**,665
HF, stratospheric, **35**,665
HNO_3 vapour, troposphere and stratosphere, **33**,983
H_2SO_4, negative ions, stratosphere, **35**,685,693
ion and neutral, changes, magnetic storms, **19**,491
ion composition, spacecraft measurements, **5**,81,82
ions, stratosphere, **31**,813,1459; **33**,1363; **34**,245; **37**,315
ions, negative, troposphere, **34**,1229
ions, positive, troposphere, **32**,1567
mean molecular weight, night, mass spectrometry, **11**,297; **18**,929
mean molecular weight, thermospheric conservation equation, **31**,1209
metals, atoms and ions, mesopause, **32**,307
metallic emissions, information from, **10**,117
negative ions and H_2SO_4 in stratosphere, **31**,1459
neutral, auroral ion ratios, **31**,49
neutral cloud evolution, model, **40**,1139
neutral, magnetic activity effects, **24**,61; **33**,1283
neutral, mesosphere, **29**,747; **34**,723
neutral, regulator of red-arcs, **20**,461
neutral, thermospheric, **20**,379; **35**,807; **38**,67
neutral, variability in diurnal cycle, **39**,803
nucleation of H_2O, ion-induced, **28**,681,827,1003
odd nitrogen, theoretical considerations, **35**,637
organic compounds, simulated early atmospheric photochemistry, **2**,79
origin and evolution, **21**,1467
scale height, **11**,633; **12**,661; **13**,851; **16**,409; **20**,891,1213; **23**,1369; **27**,1131,1247; **29**,35,989; **34**,979; **35**,161; **40**,223
semi-annual variation, **18**,1051; **19**,723
stratospheric, HOCl, **27**,1047
structural parameters at night, **11**,441
thermospheric, **11**,1379; **13**,325; **27**,653,1469; **33**,617,1169,1283; **38**,67; **40**,271
topside, absorption of solar L_γ by N_2, **12**,656
total mixing ratios of atoms, **22**,175
trace gases, H_2 and HNO_3, analysis from ions, **28**,681
trace gases, troposphere-stratosphere study, **31**,1517; **32**,89; **35**,525
trace gases, absorption spectroscopy on Spacelab, **36**,291
trace gases, wavelike disturbances, **35**,673

density,
accelerometer measurements, **25**,499
annual, seasonal, diurnal, variations, **15**,627; **16**,509,675,937,1161; **18**,741,1051,1573; **19**,723; **38**,637
barometric law, thermosphere, **22**,183,186
chemical releases, *see* SEEDING
comparison of models for thermosphere, **36**,1121
correlation with geomagnetic, solar activity, **15**,1067; **16**,675,1161, 1427; **17**,181; **18**,1051; **19**,39; **21**,2049; **24**,61
dependence on viscous forces, **24**,349
diffusion of chemical releases, **12**,317; **19**,1193
diurnal variations, **11**,1273,1379; **16**,509; **17**,725; **18**,1021; **20**,289
E-region, comparison of measurements, **11**,513
exospheric, **14**,1149; **15**,627,1933; **18**,387; **20**,473; **22**,209,1375; **25**,59; **27**,403; **35**,199
foil cloud measurements, **21**,1131
kinetic theory and surface interactions, **17**,917
laser range data, thermospheric, **37**,1409
mass spectrometry in thermosphere, **36**,281
model, empirical, polar region, **21**,883
planetary ocultation data, **20**,1727
probe measurements, ionosphere, **22**,41
related to radiation belts, **2**,165
rocket experiments, **1**,259; **2**,33; **22**,41
satellite experiments, **13**,599,617,647,693; **14**,849; **15**,1329; **22**,209
satellite orbit analysis, **1**,115,136,184,259; **5**,79,314; **9**,529; **11**,261,1273; **12**,1111,1179; **14**,291,455,863,1023,1065,1149; **15**,627,1067, 1883,1933; **16**,937,581; **17**,49,107,197,985,1539, 2027; **18**,309,1573; **19**,297,316,685,1637; **20**,473, 1077,2165; **21**,1705; **22**,391,403; **23**,323,1003, 1301,1399,1405,1659; **25**,1011; **26**,291,913; **27**, 1247,1361; **30**,909; **31**,1501; **32**,1; **33**,721,735, 965,1417; **35**,1039,1127; **38**,637; **40**,223

dynamics,
ambipolar diffusion, height relationship, **1**,125; **5**,109; **18**,1836
antarctic upper atmosphere, **37**,943,955
circulation and tides, **10**,79
circulation, during proton events, **23**,1035
circulation, influence of IMF, **32**,1541
circulation, thermospheric, model, **26**,387; **31**,1479; **32**,469
circulation, tropospheric, increased upper-level heating, **12**,219
comparison of methods, radar, FP spectroscopy, **39**,1511
coriolis force, upper atmosphere heating, **22**,1031
coupling, protonosphere with F-region, **21**,43
diffusion coefficients, E-region, vapour trails, **8**,35; **10**,89
diffusion, F-region, **11**,879; **20**,103; **21**,1073; **22**,189; **25**,907; **26**,189; **31**,671
diffusive equilibrium, thermospheric, **35**,1157
dispersal of seeded gases, **26**,605
disturbance, by Lorentz coupling of electrojets, **18**,583
eddy mixing and circulation in ionosphere, **18**,1707
escape, Jean's, exospheric, **11**,901; **13**,1185; **15**,1219; **18**,449; **19**,275,675,791
expansion through Joule heating, **21**,2073
gravity waves, *see* WAVES
ionized irregularities, 3-dimensional drift, **12**,1
ions in topside ionosphere, **27**,1075; **31**,671; **32**,47
lateral flow of hydrogen in exosphere, **12**,1045; **20**,103
mesosphere, model, **27**,385
mesosphere, partial reflection drift technique, **25**,441
middle atmosphere response to 11 year solar cycle, **32**,411; **34**,1037
morphology characteristics, particle precipitation, **25**,991
motions in high shear regions, **22**,504,505
neutral atmosphere, ionospheric drift data, **23**,389
neutral gas acceleration, Pedersen conductivity, **13**,737
oscillations, pressure, theory, influences, **18**,1393,1719; **21**,1691
rotation, **12**,835; **13**,169; **14**,657,1339; **15**,1913; **16**,557; **17**,217; **18**,1433,1585; **19**,357,1201; **20**,891,1213; **22**,559,1565; **23**,1003,1369,1573; **24**,355,727,975,1151; **27**,1247; **28**,549; **29**,989; **32**,1
superrotation, global deposition of meteoroids, **23**,379,891,892
thermosphere, model, **27**,385
thermosphere, B_y changes in IMF, **34**,1
tides, *see* TIDES
translationally excited N atoms, implications for NO production, **31**,135
transport of thermospheric NO, **32**,399
transport of thermospheric nitrogen, **30**,1091; **32**,1407
transport of thermospheric oxygen, **21**,1001; **32**,1407
turbulence, E-region, **10**,89; **15**,811; **17**,1891
turbulence, F-region, **38**,79
viscosity of atomic oxygen, **9**,1
volcanic material into stratosphere, **32**,17
vorticity, 500mb level, auroral precipitation, **28**,419
waves, gravity, see WAVES
winds, *see* WINDS
electric fields, ground level measurements, **24**,801
energy budget, compared to radiation budget, **40**,1237
exosphere,
conditions, from satellite drag data, **14**,291
density, temperature, magnetic disturbances, **27**,403; **35**,199
escape, **11**,901; **13**,1185; **15**,1219; **18**,449
H content, **5**,257; **11**,1035; **12**,1045; **14**,425; **15**,599; **18**,803; **20**,1147; **27**,795
He content, **15**,599; **18**,803; **20**,1147
model, geocoronal applications, **39**,885
O (63μm) emission, cooling effect, **27**,795
protonosphere, F-region coupling, **21**,43
satellite particle content, **27**,1163
transport phenomena, **18**,823; **20**,103
mesosphere structure, OH emissions, **29**,1241
meteorology, *see* METEOROLOGY
models,
antarctic stratospheric chemistry, **36**,73,213
ARDC 1959 model atmosphere, **7**,454
energy budget, **40**,1237
exosphere, geocoronal applications, **39**,885
global, laser soundings of Na, **25**,1093
global, thermospheric , ionospheric, **35**,1167
interim model to 400 km from rocket and satellite data, **1**,20
Jacchia, thermosphere, **22**,955
polar densities, **21**,883
solar-terrestrial, applications software, **40**,541
thermospheric densities, **36**,1121
optical opacity,
absorption of grazing rays, **17**,1683
blue sky light, polarization of H_β line, **23**,557
colour of sky during solar eclipse, **16**,647
density, solar X-ray measurements, **15**,681
depth, large zenith angle, computations, **12**,761
distribution function, **22**,413
polarization of atmospheric Ring effect, **37**,627
polarization of reflections, **17**,1307; **23**,557
refraction measurements from satellite, **9**,351
scattering, non-spherical, **15**,1641; **23**,1011
shadow of Earth, effective height, **16**,1071

remote sensing, investigatory methods, **37**,943,955
stratopause, hemispheric similarities, tides, **16**,1011
stratosphere,
abundance of HOCl, **27**,1047
antarctic chemistry, implications for O_3, **36**,73
antarctic OClO chemistry, implications for Br, **36**,213
aeronomy, **20**,1671
chemical budget, **31**,1009
chemical composition, *see* composition
Cl-ClO-Cl cycle, **24**,1187
climate and biospheric environment on ancient Earth, **36**,1391
excited ozone precursors, **27**,411
ion chemistry review, **40**,255
ions, negative, **31**,813,1459
NO transportation from thermosphere, **32**,399
ozone changes in the polar regions, **40**,373,403
temperature,
auroral activities, response to, **33**,617,841
chemical releases, **5**,185; **9**,521; **15**,199; **17**,261; **19**,233,669,1625
CO content and solar constant, **33**,1389
Doppler line widths, *see* INTERFEROMETRY
effect on charged particles, **17**,737,815,841
electron, thermospheric model, **24**,739
exosphere, **5**,328; **22**,209; **25**,59
foil cloud measurements, **21**,1131
geomagnetic disturbances, **27**,403, **29**,249
H_2O variability , middle atmosphere, **33**,761
ionospheric, **11**,463,1297; **13**,143; **15**,944; **19**,15, 827,1313; **22**,41; **23**,1013; **29**,171,1319,1333, 1367; **30**,1025; **36**,553,1295
mean global, solar flux data, **31**,597
mesopause, oxygen rotational spectra, **39**,1363
mesopause, polar, OH spectrophotometer, **32**,249,263; **34**,1023
mesosphere, airglow and Rayleigh scattering, **35**,1149
mesosphere, geomagnetic activity, **21**,1447
mesosphere, MAX/EPSILON campaign, **37**,1303
mesosphere, Nimbus CO_2 15μm data, **29**,673
mesosphere, response to solar activity, **35**,959
profiles, radiative-convective modelling, **32**,803,1307
rotational, N_2^+ and O_2 emissions, **31**,1137
rotational, OH bands, **5**,153; **20**,261; **22**,1323; **24**,665; **29**,1241; **31**,923; **32**,249,263,852
rotational, OH bands, survey, **5**,153
rotational, O_2 atmospheric bands, **34**,301
O_2 microwave rotation line, 2.53mm, **19**,777
polar wind interpretation, **22**,1193
SAR arc observations, **35**,1077
satellite experiments, **7**,423,434; **13**,599,647; **22**,209
thermosphere, **35**,241,1255,1317; **36**,281,531, 677; **37**,1303,1333; **38**,221; **39**,1155,1363; **40**,1545
UV airglow interpretation, **31**,967
variation, diurnal, surface, **20**,1941
variation, diurnal, thermospheric, **11**,1379; **18**,1021; **20**,289; **21**,1457; **31**,1479
variation, semi-annual, **18**,741,1051
variation, solar cycle, mesospheric, **33**,795
variation, solar-maximum conditions, **29**,47
variation, zonal-winds, **20**,2099; **29**,1367
variation, 27 day, **17**,1737
vibrational, molecular oxygen, **18**,1255
thermodynamics,
accommodation coefficient, from orbit analysis, **29**,1089
cooling by greenhouse gases, **40**,1011,1535
cooling, CO_2 15μm, solar-cycle, **36**,177
cooling, electrons, attenuation by H_2, **29**,1333
cooling, electrons, D-region, **9**,439; **19**,313; **36**,65
cooling, NO, heat loss from thermosphere, **30**,515; **34**,131; **36**,271
cooling, oxygen 63μm emission, **18**,271; **27**,795
distribution function for hot $O(^3P)$, **27**,1321
energetics, thermal structure, **28**,585
energy budget models, **40**,1237,1585
energy sources of the upper atmosphere, **1**,14
greenhouse effect, heat changes through chemical changes, **28**,1011
heating, conjugate photoelectrons, **27**,583
heating, electromagnetic, **16**,231,1201; **20**,2205
heating, electron deposition in CO_2, **27**,491
heating, equinox tides, **32**,447
heating, ionosphere, by neutral winds, **19**,731
heating, ionosphere, dissipation of electric currents, **19**,59; **26**,201
heating, ionosphere, thermal domains, **27**,159
heating, Joule, corpuscular, **9**,939, **11**,1297; **15**, 1821; **16**,1201; **21**,559,1681,2073; **22**,925,1031; **24**,561,727; **29**,26,1319,1333; **30**,463,1083; **33**,279; **38**,207
heating, Joule, effect of Coriolis force, **22**,1031
heating, Joule, wind effects, **36**,851
heating, photons at F-region height, **18**,1745
heating, solar radiation, **16**,231,1531; **20**,1745, 1761; **29**,601; **33**,1451
heating, solar tides, **33**,283
heating, top-side, tropospheric response, **12**,219; **25**,907; **26**,189
heating, twilight, available radiation field, **39**,671
heating within auroral red arc, **18**,1489
greenhouse effect, CO_2, **29**,935
properties, rocket measurements, **5**,81
radiation balance, satellite data, **11**,839
radiation field, troposphere and stratosphere, **30**,923,935; **40**,1585
radiative thermal flux, **11**,987,983
role of atomic oxygen, **9**,1; **17**,1247
role of ion flows, **25**,1085
solar irradiance, UV, **30**,67,147
stratospheric warming, (OH), **32**,852

thermal balance, ionosphere, **27**,1063,1075,1175
thermal emission, spectral fine structure, **13**,353
thermal structure, over solar cycle, **35**,21
thermosphere,
composition changes from twilightglow, **27**,652
composition, chemistry and dynamics, **40**,271
composition, influence of gravity waves, **27**,1469
composition, neutral, from ion ratios, **31**,49
composition, temperature, **28**,225
conductance and convection, **17**,1850
emissions and tides, **25**,711
heat budget, **21**,575,1457,1633,2238
hydrogen atoms and ions, **5**,257
model, behavioural, **36**,1
model, dynamical, **27**,385
model for electron temperature, **24**,739
neutral, properties, **20**,761
temperature observations at 23° N, **40**,1545
transportation of constituents, **21**,1001; **30**,1091; **32**,399,1407
structure, **5**,1,85; **13**,325,1313
variations, composition, diurnal, pressure, **11**,1379; **21**,1457,1825
variations, diurnal and solar cycle, **17**,1581
variations, geomagnetic, 27 day, **17**,1709
transmission, *see* RADIATIVE TRANSFER
troposphere,
direct effects of increased solar activity, **12**,219,327,333
photochemistry, **20**,919; **21**,575
Rayleigh scattering, **16**,693
turbopause, nocturnal altitude variation, **25**,723

ATOMIC PROCESSES

see REACTION DYNAMICS

AURORAE

activity correlations,
airglow, ISIS-II, **21**,819
annual, secular variations, Wilson Bentley's data, **31**,1131
artificial beam injection, *see* SEEDING
break-up, D-region ionization, **12**,195; **16**,567,329
break-up, helium emission, **17**,1927
break-up, Poynting flux, **35**,1287
break-up, proton precipitation, **22**,735
break-up, ring current exchange instability, **15**,1287; **16**,329
conjugate observations, **17**,1459,1485,1919; **20**,1337
cosmic noise absorption, **11**,371; **17**,1565; **19**,891
cross-tail current disruption, Θ-aurora, **38**,1361
current systems, **16**,129,329,703; **21**,179
dayside, effect of IMF and magnetospheric substorms, **31**,1345; **37**,1347
electric and magnetic field variations, **38**,97
emission intensity, geomagnetic index, **16**,981; **19**,877
magnetic pulsations, **40**,1303
magnetic storms, **11**,371; **17**,1565; **19**,891; **20**,1363; **22**,1511
magnetosphere, **16**,567,891; **22**,885; **34**,293,1169
magnetospheric flare activity, **34**,1169
occurrence, Yule sunspot analysis, **36**,99
optical and radio, **12**,29; **15**,301,693,893; **20**,803
oval and substorm, **12**,273; **14**,121,587; **16**,47, 1365; **20**,313,821,1116,1391; **34**,293
particle and magnetic data, **22**,25
prediction scheme, **34**,77
radio star visibility fades, **16**,1155
solar flare effects, **32**,925
spectroscopic studies, thermospheric composition, **38**,67
thermospheric response, **33**,841
trapped ions, **11**,451
X-rays, **10**,165; **12**,1093; **16**,815,1419
arcs,
activity, electric field oscillations, **26**,555
altitude and position, iterative method, **35**,245
array, electron acceleration, **26**,81
associated field-aligned current, **28**,351
associated E-region neutral winds, **33**,869
characterisation, rocket, ground, **39**,1677
classification, associated electric fields, **32**,193
dayside, boundary layer plasma, **33**,1389
dayside, fine structure, **35**,759
deformation, imaging at substorm onset, **36**,715
discrete, formation , **37**,783
discrete, latitudinal structure, **35**,1009
dynamics, **30**,179
formation, by magnetospheric instability, **32**,119; **39**,395
hook-shaped, relationship to IMF, **34**,489
horn brightening, mapping into magnetotail, **38**,1179
O(557.7) and N_2(391.4), high resolution, **25**,405
polar cap, characteristics, mechanisms, **30**,319; **31**,193
polar cap, optical emissions, particle precipitation, **31**,161
polar cap, northward IMF, **36**,1317
pulsating, coordinated measurements, **37**,545
red, distortion, small scale, **18**,1735
red, excitation, **8**,49,59,198; **16**,525,915; **20**,591
red, heating, atmospheric response, **18**,1489
red, ionization troughs in F region, **17**,777,1867
red, orientation, **15**,277; **17**,1657
red, new mechanism, **19**,1393
red, position in southern zone, **17**,421
red, regulating atmospheric influence, **20**,461
red, spectroscopic studies, **20**,1309
red, stable, electric field excitation, **20**,591
red, stable, electron temperatures and densities, **16**,459; **21**,165,683,1957

rocket tomography measurement, 391.4nm emission, **39**,895
SAR, bi-Maxwellian transport equation, **34**,1335
SAR, electrojet activity, **34**,363
SAR, photometric, interferometric data, **18**,431
SAR, precipitation, hydromagnetic waves, **24**,105,629; **26**,245,777; **28**,69,375
SAR, storm associated, **35**,475
SAR, temperatures and meridional winds, **35**,1077
SAR, undetected, **16**,140
solitary, generation of, **30**,1
sun-aligned, convection, magnetic, **38**,1
artificial, region conjugate to Starfish, **18**,731
Austral oval, spherical harmonic analysis, **26**,691
beam-plasmas, ion-acoustic waves, **40**,1055
borealis, outer radiation belt, **9**,829
chemistry during PCA events, **13**,339
colour variations, **19**,399
cosmic noise absorption, **11**,371
cosmic rays, 557.7nm/391.4nm ratio, **12**,665
cusp, mid-day, OII(^2D-^4S) emissions, **39**,777
cusp region dynamics, **40**,879
cusp width, AE index and B_z, **36**,157
dayside,
cleft, topside optical view, **24**,937
possible observation, **15**,591
particle precipitation, VLF emission, **20**,803
related geophysical phenomena, **40**,621
dynamics,
absorption peak motions during substorm, **22**,1427
auroral belt and geomagnetic disturbances, **15**,209; **16**,881
break-up event, O_2 1.27μm enhancement, **26**,619
break-up event, magnetic associations, **29**,431
break-up event, Poynting flux, **35**,1287
break-up event, proton precipitation, **22**,735
break-up event, rocket and ground study, **31**,207
bulge expansion, **20**,821; **27**,1429
cusp region, **40**,879
IMF effects, **27**,665,699
substorm dynamics, **20**,821; **23**,269
expansion poleward during substorm, **20**,1391
large scale, IMF related, **23**,1349
radio-aurora, ionospheric currents, **10**,129
transport of N(^2D) in high latitude thermosphere, **30**,1091
westward travelling surge, spectral hardening, **29**,1011
wind decrease precedes 630.0nm intensification, **36**,851
echoes, ionization study, **5**,33,105
emission parameters and electron excitation, **20**,2081
emissions, argon, 104.8nm and 106.7nm, **24**,405
emissions, dayside cleft aurora, **29**,321
emissions, far ir, rocket interferometer, **36**,543
emissions, helium,
587.6nm transient during break-up, **17**,1927; **30**,695
1083nm intensity, **5**,75; **16**,91; **17**,1213
emissions, hydrogen,
charge separation in magnetosphere, **9**,711
H_α, line width, **15**,1599
H_α, magnetic activity correlations, **1**,57
H_α, polar cleft, and OI emissions, **23**,1053
H_α, refraction measurements, **9**,351
H_α, spectral line shape, **2**,130; **11**,1223
H_β, height-luminosity distribution, **14**,812; **22**,725; **27**,307
H_β, absent from westward surge, **17**,1409
proton bombardment, **10**,187,195
quenching by collisional ionization, **14**,1367
systematic behaviour, **5**,87,99
emissions, hydroxyl,
intensity, branch ratio at 1083 nm, **5**,75
precipitated by geomagnetic disturbances, **20**,1363
emissions, nitrogen,
band emissions and limits on electron fluxes, **20**,905
far ultraviolet, auroral properties, **33**,175
N, N_2, O, O_2 emissions and number densities, coordinated measurements, **26**,319
N^+, 108.4nm, **24**,405
$N^+(^5S)$, lifetime, and 214.5nm emission, **29**,263
N(^2D) and $N_2(C^6\pi)$ excitation, magnetic ordering, **26**,339
NI 520nm doublet, FP interferometry, **9**,811
NI 520nm doublet, horizontal transport effects, **32**,1407
N_2, excitation by extreme UV, **26**,449
N_2 Gaydon-Herman system, **31**,1525
N_2, vibrational distribution, theory, **19**,1457; **27**,901
N_2, 417.6nm, type-B, **16**,1115; **17**,1680
$N_2(c^1\Sigma$ and $a^1\Pi)$, branching ratio and expected intensities, **34**,399
$N_2 A^3\Sigma_u^+$ deactivation, **19**,1669
N_2^+, 391.4 nm, **10**,37,195; **13**,1008; **14**,651; **15**,689, 899,1801; **17**,1257; **19**,536,693; **23**,935; **25**,405; **27**,307; **33**,141; **35**,1061,1317
N_2^+ Meinel IR bands, excitation cross-section, **17**,1941
N_2^+, rotational temperatures, stepped filter band profile, **31**,1137
N_2^+, O_2^+, concurrent measurements, **37**,131
NO, γ and δ bands, possible source, **25**,1021
scattering spectrum of electrons, **17**,1527
emissions, oxygen,
excitation of forbidden lines, **15**,1097
130.4nm, excitation, radiative transport, **18**,691
130.4nm, 135.6nm, emission profiles, **22**,465
557.7nm, 391.4nm related, **12**,665; **15**,938; **19**, 693; **20**,53; **23**,935; **24**,893,896; **27**,307; **35**,1317

557.7nm, 427.8nm related, **16**,1259; **19**,49; **36**,893
557.7nm, 630.0nm related, **17**,1429; **19**,267; **33**,207,1225
557.7nm, 1083nm He emission, sunlit, **17**,1680
557.7nm, altitude-intensity profile, **27**,307
557.7nm, Doppler line widths, **5**,299; **14**,383; **16**,539; **21**,605
557.7nm excitation, **10**,159; **16**,737,1259,1418; **17**,1961; **19**,119,251; **20**,53,1569; **21**,863; **25**, 405; **27**,473,481; **32**,373,1195,1199; **33**,183,207, 1225
557.7nm, impulse response analysis, **32**,515
557.7nm, post-storm conditions, **29**,405
630.0nm, enhancement, post-sunset, conjugate effect, **22**,1297
630.0nm, horizontal transport effects, **32**,1407
630.0nm, intensification preceded by decreased wind, **36**,851
630.0nm, line widths, **21**,605, **34**,483, **36**,851
630.0nm, precipitated by geomagnetic disturbances, **20**,1363
630.0nm, SAR arcs, **24**,105,629
630.0nm, solar event, **27**,973
630.0nm, storm time electron fluxes, **19**,540
630.0nm, thermospheric winds, **19**,1225
630.0nm, 391.4nm related, **23**,935
630.0nm, 427.8nm related, **37**,341,1117
732.0nm O^+ doublet, F-P, **22**,636; **35**,845
844.6nm, FP interferometry, **9**,383
OII(^2P), polar cap, **38**,1367
O, O_2, N, N_2 emissions and number densities, coordinated measurements, **26**,319
O(^1S) excitation, **18**,187,895; **19**,119; **38**,161
O(^1S) quenching, **21**,1757
$O_2(b^1\Sigma_g^+)$, excitation, **2**,60; **38**,835
$O_2(b^1\Sigma_g^+)$, ground observations, **33**,119
$O_2(b^1\Sigma_g^+)$, rotational temperatures, stepped filter, **31**,1137
$O_2(^1\Delta_g)$, and NO^+ concentrations, **23**,1341
$O_2(^1\Delta_g)$, break-up event, **26**,619
$O_2(^1\Delta_g)$, electric field excitation, **18**,1031
O_2^+, absolute spectrometry, **35**,1317
O_2^+, spectral synthesis, **24**,999
O_2^+, type-B, **16**,1115
O_2^+, N_2^+ band enhancements, **37**,131
red, green line, concurrent photometric observations, **16**,297
red arc, *see* **arcs,**
red line, polarization, **1**,112; **2**,73
red line, delay relative to violet band, **2**,246
emissions, ultra violet, OGO observations, **24**,1059
energy source, solar neutral hydrogen, **12**,801
ionization from bremsstrahlung, **12**,1093
occurrence frequency, solar rf bursts, **1**,325
mid-day, during storm, **21**,696
mid-latitude, at solar maximum, **18**,1850
morphology,
boundary variation with IMF, **32**,25
brightening phase, Pi-2 pulsations, **22**,735
Chapman-Ferraro theory, **10**,233
characteristics, following solar flare, **18**,525
circular symmetry, **8**,142
dayside cleft, topside view, **24**,937
diffuse, electric field effects, **25**,859
diffuse equatorial edge, **36**,1031
diffuse, plasmapause behaviour, **24**,299
diffuse, polar cap features, **29**,1143
diffuse, temporal behaviour, **21**,799,857
discrete, continuous and diffuse, **22**,1723
displays correlated with particle, magnetic data, **22**,25
distribution in space, **9**,503
features in dark sector, substorm association, **22**,1511
features in south polar cap region, **36**,429
flickering in bright aurorae, **16**,1525
geomagnetic effects, **19**,477,525; **20**,1116; **24**, 223,375,573,717,955
global distribution, **32**,107
imaging instrumentation, rockets, **22**,1003
imaging, TV, whistler duct dimensions, **37**,979
lower borders, emission ratios, **37**,1117
luminosity, spatial variation, **15**,475,1695; **16**,815
mantle, midday sector, electron precipitation, **31**,889
mapping, ISIS-II, correlated with airglow, **21**,819,873
oval, afternoon sector, **23**,225
oval, Austral, harmonic analysis, **26**,691
oval, boundary of closed field lines, **18**,501
oval, location at night, **35**,241
oval, magnetospheric, IMF connections, **14**,587; **16**,129; **29**,731; **32**,561
oval, photograpy, **27**,541
oval, substorm development, **24**,955
particle and optical data in noon sector, **23**,1597
precipitation characteristics, **13**,565; **24**,487
pulsations, **17**,289,1141,1599; **24**,896
quiet, magnetospheric convection, **32**,127
quiet, configuration, electron precipitation, **36**,791
quiet, growth, expansive and recovery phases, **20**,1369
radio excitation, visual effects, **24**,375,425
review, **12**,783
spatial extent of O(^1S) and N_2^+ emissions, **19**,49
spatially discrete character, **16**,1297
spectroscopic, **21**,1213
structural thickness, TV measurement, **16**,205
substorms, visual effects, **20**,1116; **24**,223,955
surges in southern hemisphere, **24**,611
surges, westward, absence of H_β, **17**,1409

surges, westward, spectral hardening, **29**,1011
transients at magnetic noon, **38**,973
unusual, **14**,524
zone locations from magnetic and geographic equator, **30**,1073
particle,
configuration, spatial, energetic influx, **13**,63
electron acceleration mechanism, **28**,459,703
electron balance during PCA events, **13**,339; **15**,1049
electron energy, emission ratio and altitude electron flux, arc associations, **21**,165,683,1957
electron flux, excitation of 391.4nm, **13**,1008; **17**,255,617,1051, 1257,1997
electron flux isotropy, **21**,2042,2043
electron flux, nitrogen band intensities, **20**,905
electron flux, related to radio absorption, **14**,65; **16**,567; **17**,83
electron flux, wave generation, low frequency, **17**,61,1391
electron heating and excitation processes, **16**,1265; **17**,1709; **19**,313
electron ionization, **11**,1209; **12**,722
electron spectrum, rf absorption, **32**,391
electron spectrum, energy dependent mechanisms, **22**,1279; **24**,131
electron spectrum, inverted-V event, origin, **26**,673; **32**,379
electron spectrum, oxygen and ozone densities, **16**,371; **21**,605
electron spectrum, photometer and riometer, **13**,225; **14**,597
electrom transport, angular dependence, **37**,109
energy deposition rate, **37**,239, **40**,299
heating, temperatures, **10**,215; **15**,873,1049; **21**,559
ions, composition, correlation with NO, **25**,103
ions, energetic, anisotropy, **19**,279; **21**,537,1115
ions, from outer zone ring current, **25**,149
ions, outflowing on field lines, **30**,715
ions, velocity distribution, **25**,243
precipitation, and geomagnetic variations, **14**,807; **15**,277,1287; **25**,5,89,149
precipitation and ULF electric fields, **26**,833
precipitation, from Alfvén waves, **37**,749
precipitation, model, time-dependent, **25**,991
precipitation, see also PRECIPITATION
proton, atmospheric interactions, **30**,463
proton, lateral dispersion, **22**,341
proton, optical studies, **10**,187,195; **23**,787
related optical measurements, **23**,1597
sources and sinks, **10**,219: **18**,1821
pulsations,
arcs, photometer, incoherent scatter, **37**,545
day-sector, **26**,635
causes, characteristics, **14**,207,217
cosmic noise absorption, correlation, **19**,891,959
electron fluxes, **40**,1043
energy transfer, $N_2(A^3\Sigma_u^+)$ to $O(^1S)$, **21**,698
frequency, **20**,285
mid-latitude, **22**,1315
optical, correlation with magnetic pulsations, **32**,735; **37**,1477; **38**,149
optical, correlation with VLF hiss, **32**,809
optical, correlation with X-rays, **18**,495; **32**,31
optical, detection of ion-cyclotron waves, **25**,643
optical, observations, **15**,347; **17**,289,1141,1599; **19**,536,693; **24**,896
optical, lifetime and heights of $O(^1S)$, **19**,119; **20**,53
optical, phase and amplitude study, **19**,251
radio frequency, **15**,1075
spatial coherence, **20**,1843
waves, fast, **20**,437
radiation, generation theory, **27**,915
radio,
absorption, and magnetic bays, **18**,1301; **23**,905
absorption, conjugate and closely spaced observations, **18**,1691; **19**, 513
absorption, electron energy distribution, **32**,391
absorption events, height, **12**,579,1035; **17**,61,1565; **27**,445
beam-plasmas double layers and solitons, **40**,1055
characteristics and conjugacy, **15**,1571,1585; **17**,1459,1485,1919
conjugate effects, riometer absorption, **38**,127
distribution in southern polar cap, IMF, **34**,307
electron precipitation effects, **13**,1171; **14**,65; **17**,83,389
frequency dependence, interpretation, **14**,269, 1231; **16**,449
geomagnetic activity effects, **14**,991; **15**,917; **17**,869; **40**,1371
ionization trough association, **17**,777
kilometric radiation through particle acceleration, **28**,703
LHR noise, rocket observations, **35**,127
local scatterers, interferometric evidence, **38**,933
morphology, southern auroral zone, **17**,403
optical associations, **12**,29
polar cap absorption, see RADIO WAVES
polarization of auroral echoes, **18**,655
position dependence on IMF and geomagnetic activity, **36**,441
radar echoes, drift of, **26**,519; **35**,153
reflection mechanisms, **10**,179
reviews,
IGY and IGC measurements, **8**,125
spectral types, magneto-correlations, **16**,47
theories, observations and experiments, **10**,247
spectral class,
class-1, ion composition, **18**,379
class-B, **16**,1115; **17**,1680; **24**,893; **27**,169
storm association, hydromagnetic theory, **9**,947
temperature, corpuscular heating, **10**,215

TV imaging, whistler duct dimensions, **37**,979
wave, auroral generation, **16**,993,1453; **18**,565, 591,599; **19**,437; **37**,749
X-rays,
atmospheric transit, **19**,1069
bremsstrahlung ionizing radiation, **12**,1093
electron bombardment, **10**,165
luminosity form changing, rapid, **16**,815
luminosity, VLF hiss correlation, **16**,1419; **35**,1231
spectra, bremsstrahlung, interpretation, **37**,1053

BALLOON-BORNE EXPERIMENTS
ion conductivity in stratosphere, **35**439
NO profiles, chemiluminescent sondes, **35**,609
ozone measurements, **35**,587,595,603
whole air cryogenic samplers, **35**,647

BATES, DAVID ROBERT
an appreciation, **40**,1583

BIOCHEMISTRY
biological influence on atmospheric composition, **31**,1065
ozone, impact on human activity, **37**,1653
peroxyacetyl, influence on odd nitrogen in atmosphere, **31**,1075

BREMSSTRAHLUNG
auroral, interpretation of X-ray spectra, **37**,1053
ionization in the atmosphere, **12**,1093

CARBON DIOXIDE
Earth, 15μm emission, mesospheric cooling, **29**,673; **36**,177
Earth, above troposphere, and CO, **18**,1729
heavy, stratospheric enhancement, **39**,945
influence on climate, *see* GREENHOUSE EFFECT
Mars, photopysis, **19**,1701
Venus, atmospheric abundance, **8**,23; **11**,1303

CERENKOV RADIATION
see also COSMIC RAYS
from magnetospheric electrons, **22**,1597; **23**,843
VLF wave generation, **22**,333

CFC's
UV absorption, effects on ozone layer, **37**,105; **38**,617
MAP/GLOBUS data, **35**,657

CHAFF
see SEEDING

CHAPMAN MEMORIAL LECTURE
The aurora and the magnetosphere, **22**,885

CHEMICAL RELEASES
see SEEDING

CHLORINE
stratospheric, removal through HOCl, **23**,1567; **26**,1017

CHORUS
see RADIO WAVES

CIVILIZATIONS
galactic, relativistic space flight, **11**,485

COMETS
acceleration of local particles, **34**,1061
bow shock, Alfvén wave generation, **39**,1045
charged particle motions, **16**,395
cometary plasma production, physics and critical ionization velocity, **15**,1407, **30**,491
cooling of electrons by water vapour, **34**,961
currents in cometary atmospheres, **27**,121
emission, continuum and CO_2, comet Burnham, **19**,1229,1259
double scattering of plasma streams in bi-thermal ionosphere, **16**,845
dust, chemical analysis by SIMS, **32**,187
dust collection and analysis, laboratory simulation, **31**,11
foreshock region, positive ion energization, **33**,1243
fountain model for plasma envelopes, **16**,1221
Giacobini-Zinner, magnetosonic and whistler waves, **37**,167
Giacobini-Zinner, pick-up ions in vicinity, **37**,1169
Giacobini-Zinner, water ions, **35**,1323; **36**,1429; **39**,479
Halley and Giacobini, ion structure comparison, **35**,299
Halley, bow shock structure, **38**,1355
Halley, detection of up-stream ions, **37**,517
Halley, impact ionization and spacecraft potential during encounter, **33**,667
Halley, impacts on probes, **34**,1089
Halley, plasma tail observations, **39**,697
head, neutral particle distribution, **19**,143
ice, dirty, solar heating of encased particles, **37**,193
ice, simulated vapour pressure, temperature, **40**,1311
ice sublimation below crust, simulation, **39**,515
ice, thermal conductivity at low pressure, **39**,507
interaction with solar wind, **12**,719; **17**,1413; **21**,1647; **24**,287
ions and em waves, resonant interactions, **35**,1501
Kohoutek, **24**,287
packing effect in fluffy particles, **31**,655
optical scattering from non-spherical particles, **15**,1641
search for comets near Earth, **37**,1185
simulation, temperatures and vapour pressures, **40**,1311
snows, cometary environment, experiment, **18**,709
snows, of nucleus, gas adsorption in, **18**,717

tail,
creation of ionized rays, **34**,819
helical waves, Morehouse, **27**,1239
Kelvin-Helmholtz instability, **30**,245
radiation force on small particles, **29**,127
streamers in solar wind, **15**,137
type 1, theory, **14**,303; **21**,663
X-ray emission from comet Bradfield, **29**,1373

COMMUNICATIONS
direct contact, galactic civilizations, **11**,485
radio frequency,
belts of needle satellites, **9**,153
range and velocity in space, effect of Earth's motion, **11**,561

COORDINATE TRANSFORMATIONS
a user guide, **40**,711

CORPUSCULAR RADIATION
see PRECIPITATION or RADIATION BELTS

COSMIC RAYS
albedo, satellite data, **15**,1169
anisotropy, functions of time and direction, **1**,155,187; **12**,973; **15**,547; **16**,29,1131; **18**,509; **20**,533,721,1799; **22**,1185; **27**,355,730; **30**,879; **31**,1259,1269; **33**,191,395,1057,1069; **34**,99,453; **36**,1451; **38**,1267,1387; **39**,1233,1637; **40**,1227
antimatter search, **9**,875
anomalies, maxima, above south atlantic, **9**,513
asymmetry, N-S, sector position of IMF, **27**,39
Cerenkov radiation, **1**,105; **19**,813; **21**,1076; **38**,373
Compton-Getting effect for particles and photons, **18**,25
cosmic noise, see RADIO WAVES
deceleration, adiabatic, in solar system, effect on spectrum, **14**,371
dependence on solar cycle and heliomagnetic polarity, **39**,1617
diffusion and energy loss, **15**,1723
distribution, latitudinal cut-offs, magnetospheric tail effect, **13**,753
dust, increased twilight luminosity, **23**,1011
electron energy and galactic rf noise spectra, **17**,1
electrons and positrons, **14**,652
electrons, charge composition, **15**,398
energy modulations due to IMF, **15**,257,1375
energy modulations, solar effects, **15**,727
energy spectra, different groups of nuclei, **11**,193
equator position, satellite data, **9**,867; **11**,87
flares, geomagnetic sudden commencement, **14**,871
fluctuations,
diurnal variations, **9**,195; **12**,735; **15**,1723; **16**,15,1209; **17**,31,1121,1173,1749,1781,1879; **19**,1169; **20**,533,1799: **22**,1185; **25**,39; **34**,468; **35**,39,1111,1117; **37**,1421; **38**,1267
heliospheric radius determination from, **16**,783
heliospheric transport parameters, **35**,45
magnetic cloud passage, **40**,979
modulation, long term, **28**,177
modulation, residual, solar minimum, **20**,2196
modulation, coronal green line, **21**,1661
modulation, solar cycle periods, **19**,981; **28**,195; **40**,811,1227
period, siderial time, **19**,1025; **21**,133
secular variation, erosion of meteorites, **29**,1109
short period, interplanetary field, **16**,818
27-day variation, **21**,1141
flux gradient, ecliptic plane, **20**,791
Forbush decrease,
center-limb solar flare effect, **13**,435
geomagnetic storm fields, **14**,979
ground level event, interplanetary acceleration, **36**,539
recovery phase, transient anisotropy, **14**,791
rigidity dependence, 11 year variation, **19**,981; **24**,835
shock effects, **40**,1109
transient anisotropic increase, **17**,1913
transit time of modulating cloud, **16**,1095
VLF, SC and solar flare effects, **16**,1081; **20**,81
galactic anisotropy, interplanetary space, **12**,1055; **13**,115; **18**,81; **20**,791; **24**,281; **25**,681; **27**,39
gamma rays, **15**,881; **18**,939,1607; **20**,1961; **39**,23,67
ionization, stratospheric, **26**,513
ionization, upper atmosphere, Pioneer II, **1**,343
modulation, heliospheric radius determination, **16**,783
muons, underground, sidereal anisotropy, **33**,1069; **40**,1167
NO production in atmosphere, **23**,637
nuclear component,
heavy, detection, satellite measurements, **5**,83; **11**,209
hydrogen and helium flux, **14**,503; **15**,619,715
intensity variations, solar activity, **9**,41,195,511; **11**,427; **13**,867
neutrons, during magnetic storm, **27**,577
neutrons, generation in upper atmosphere, **11**,1151, **22**,177; **23**,115
particles with $Z \geq 3$, **18**,265
photon component,
barometric effect at sea level, **16**,7
solar diurnal effect, sea level, **16**,15
power spectra, pressure oscillations, **18**,1719
power spectrum, ground level, **23**,1603
primary composition, **11**,183; **15**,1169,1787; **16**,253
primary, long-term intensity modulation, **14**,177
propagation,
direct mode, **19**,1419
interplanetary space, **12**,735; **13**,9; **14**,371; **16**,818; **17**,31,1121
perpendicular, solar equatorial plane, **19**,549
reflections by rotational discontinuities, **22**,1571
radioactivity induced in spacecraft, **11**,167

rf emissions, *see* RADIO WAVES
rocket measurements, **8**,165
satellite measurements, **5**,79
soft component, Soviet satellites, **1**,87; **5**,82
solar, *see* SUN
Störmer theory and Euler potentials, **15**,1525
transient, possible observable effects, **17**,1619

CURRENT SYSTEMS
atmospheric, correlations, **20**,1443
auroral associations, **16**,129,329,703; **21**,179
B_y dependent, during positive B_z, **36**,523
Birkeland, geomagnetic modelling, **39**,641
cause of positive bay in low latitudes, **22**,1219
cleft, and interplanetary electric field, **32**,1551
continuity at the Harang discontinuity, **26**,237
cross-tail disruption, auroral effects, **38**,1361
current sheet, *see* MAGNETOSPHERE
drift components, mid, low latitudes, **34**,645
dynamo, effect of ionospheric emf's and winds, **25**,1075; **26**,705
dynamo, geomagnetic L-variations, **32**,629
electric field, *see*, IONOSPHERE
electrojet,
auroral, atmospheric disturbances, **17**,1107, 1817; **18**,565,591,599; **24**,203; **28**,763; **39**,907, 919,1189
auroral, conductivity ratios, **30**,525
auroral, influence of IMF, **28**,29,803
auroral, total current estimations, **30**,621
counter equatorial, **21**,1355; **29**,1091
eastward, and Pi2 pulsations, **33**,351
eastward, in dawn sector, **23**,1377
equatorial, abnormal S_q(H) variations, **29**,1091
equatorial, conductivity, electrostatic field, **20**,47
equatorial, integrated current density, **30**,93
equatorial, ionospheric dynamics, **18**,583; **19**,1497
equatorial, longitudinal variations, **29**,703
equatorial, lunar tides, H-field, **18**,367
equatorial, magnetic variations. **21**,1,1251,1339
equatorial, properties, **17**,1375; **28**,1125
equatorial, sporadic-E variations, **14**,529
equatorial, theory-data inconsistencies, **14**,519
Lorentz coupling, ionospheric disturbance, **18**,583
MHD pulsations, **23**,1129; **26**,473; **33**,351
westward, **26**,473; **31**,435; **32**,1291; **33**,1317
estimations from geomagnetic data, **31**,1199
field-aligned,
above auroral arc, **28**,351
adiabatic potential transitions, **26**,925
auroral, Alfvén wave approach, **31**,579; **32**,1497
Birkeland, geomagnetic modelling, **39**,641
coincident electron beam and plasma data, **32**,561
conductivity gradient, ionospheric, **35**,1405
conductivity ratio with electrojet, **30**,525
current reversals, auroral fine structure, **35**,759
erosion of magnetosphere, **23**,1257
generation, magnetosphere-ionosphere coupling, **35**,903
ionospheric, **23**,1355; **27**,99,351,1027; **39**,1107
ions, thermal flows at high latitudes, **38**,1187
magnetic disturbances, associated, **27**,1451; **29**,1315; **30**,1033; **33**,1037
plasma pressure inhomogeneities, **33**,1037
polar cap arc relationship, **36**,1317
polar cusp variations, **30**,635; **32**,99
radio aurora, particle interaction, **28**,847
Radler effect in magnetotail plasma, **30**,875
short-wave drift instabilities, **30**,581
thin layered, in solar wind, **26**,1027
Hall, *DPY* system at high latitudes, B_y IMF effect, **34**,41
Hall, generated by hydromagnetic waves, **18**,749; **30**,389
hydromagnetic waves, associated, **17**,247
incoherent scatter measurements, **24**,479
interplanetary interaction region, **32**,1541
ionospheric,
auroral dynamics, **10**,129
automatic evaluation, **17**,491
directional, nocturnal E-region, **31**,1177
disturbance morphology, **22**,1611
during solar eclipse, **32**,1013
dynamo, **19**,263
equivalence of Pc3 pulsations, **36**,641
from radar and magnetic perturbations, **24**,193
geomagnetic daily variations, effect, **29**,703
geomagnetic sudden commencement, **33**,11
heating through dissipation, **19**,59
ion flows, substorm associated, **38**,1251
ion flows, thermal, field-aligned, **38**,1187
planetary ionospheres, MHD approach, **38**,1061,1327
polar, model, **21**,1287
related to radio and visual aurora, **24**,717
solar wind induced, **21**,463,2089
magnetopause, geomagnetic variations, **18**,1471
magnetospheric models, **24**,215; **30**,985
magnetotail, **22**,609
oceanic, and around islands, **21**,97
polar,
arc related, **25**,53; **36**,1317
cap boundary, IMF changes, **35**,1301
dynamics, **17**,1395; **20**,1773; **33**,11,407
flow patterns in quiet conditions, **22**,427
magnetospheric association, **22**,1101
ring current association, **20**,183
three dimensional, during substorms, **22**,1219,1231,1403,1471
ring,
anisotropy, ion cyclotron instability, **23**,123
auroral activity connection, **12**,945; **15**,835, 1225,1287; **16**,129,329,703,891; **17**,707; **28**,69

composition and sources, **29**,1195
connection with polar electrojet, **20**,183
decay of, **21**,983; **33**,1097; **36**,765
drift instabilities and precipitation, **26**,985
effect on magnetosphere topology, **18**,699
effect on VLF propagation, **20**,731
electrons and VLF emissions, **29**,825
energy injection rate, **31**,901
growth, IMF association, **27**,1039; **32**,975; **33**,1097
hydromagnetic waves, compressional. **25**,549
induced electric field, **20**,2039
interaction with plasmasphere, **40**,859
ion lifetime, pitch angle dependence, **25**,385; **37**,1433
ion precipitation, magnetospheric turbulence, **25**,149
lifetime of particles, **30**,733
loss-cone instability, gradients, thermals, **24**,609
models, **17**,375,999; **27**,285
protons, dynamics, **23**,1045,1337; **24**,783
quiet time, electron temperatures, **27**,1175
radii, cosmic ray neutron data, **27**,577
simulation, geomagnetic variations, **39**,821
solar wind-magnetosphere coupling, **30**,627
storm-time simulations, **38**,1133
time-dependent, inductive electric field, **23**,1205
S_q, chemical seeding, thermosphere, **21**,1237
S_q, geomagnetic variations, **14**,163; **17**,471
S_q, tidal dynamics, **17**,889; **18**,121,367,423,1075, 1091
S_q^p variations, **21**,329
S_q(H), abnormal, equatorial electrojet, **29**,741
three-dimensional, magnetosphere-ionosphere region, **28**,475

DOBSON G.M.B.
spectrometers for O_3 measurements, historical, **37**,1601
the man and his work, **37**,1485

DUST
see METEORITIC MATERIAL

EARTH
charge, surface, positive, **12**,652
electric field, ground level, **24**,801
electric field, stratospheric, **30**,1013
orbital motion, rf communications into space, **11**,561
reflection of radiation, angular, spectral, **11**,681
shape, oblateness, satellite orbit analysis, **29**,35

ELECTRIC FIELD
see IONOSPHERE

ENERGY TRANSFER
see REACTION DYNAMICS

ESCAPE
see ATMOSPHERE, TERRESTRIAL

EROSION
lunar, intrinsic and extrinsic causes, **5**,321; **11**,1257,1335
rates for bodies in Earth orbit, solar-wind bombardment, **11**,885,1257

EXPLOSION
grenade, *see* CHEMICAL RELEASES
nuclear, *see* NUCLEAR EXPLOSION

GEGENSHEIN
cause, lunar ejecta theory, **19**,841
pertubations in counterglow, **21**,1185
photometric study from space, **21**,1179

GEOMAGNETIC FIELD
abnormally quiet day occurrence, **24**,567
activity correlations,
airglow, **16**,140,211,297,1103,1201; **17**,797,1677, 1867; **18**,1011,1335,1367; **20**,1363
atmospheric density, **17**,1539,1709; **18**,387; **24**,61
atmospheric dynamics, **18**,1793; **33**,461
atmospheric explosions, **10**,47; **15**,1419; **34**,395
atmospheric temperature, **21**,1447
auroral absorption, **18**,1005,1691
auroral dynamics, **15**,209; **16**,881; **71**,433,1599
auroral echoes, **18**,655
auroral electrojet activity, **34**,363,1285
auroral emissions, **15**,1075; **16**,47,981; **19**,540,877; **20**,1363; **33**,841
auroral morphology, **15**,277; **18**,501,1735; **24**,375
auroral plasma, **28**,135
convection at high latitude, northward IMF, **29**,687
effect on meteor train diffusion, **29**,415
electrojet, equatorial, **21**,1,197,1251,1339,1355
equatorial, conductivity and current dependencies, **30**,93,97
Forbush decrease and VLF emissions, **16**,1081
forecasting, and proton showers, **35**,487; **36**,205
forecasting, 27-day recurrent activity, **36**,1133
Hale sector boundary, **29**,167; **30**,519
IMF characteristics, **17**,1183; **20**,1033; **22**,193, 1173, 1413,1611; **23**,929,945; **25**,15; **27**,699,1033; **28**,545; **32**,605; **33**,415; **37**,385
indices, air density variations, **15**,1067; **16**,675; **17**,181
indices, Aschen light on Venus, **16**,1417
indices, auroral emission, **16**,981
indices, electron concentrations, **15**,295
indices, micropulsations, **20**,637,849
indices, variations at Hale sector boundaries, **29**,167
interplanetary and solar causes, **38**,109

ionization, night time E-region, **20**,61; **25**,651
ionospheric charge, currents, **17**,617,777,1977; **18**,259,749; **24**,193
ionospheric irregularity height variations, **19**,1588
ionospheric spread-F, **22**,1579; **23**,899
location of southern radio aurora, **36**,441
low latitude, sector boundary passage, **25**,161
magnetic cloud passage, **40**,979
magnetodynamic noise, **17**,1497
magnetosphere, electron precipitation, **18**,65; **23**,913; **27**,867
magnetosphere, flare activity, **34**,1169
magnetosphere, proton precipitation, **23**,1141
magnetosphere, viscosity, **18**,349
magnetospheric alignment, extended auroral intensity contours, **33**,183
magnetotail currents, **22**,609
models, comparison based on laser range data, **37**,685
patterns and coronal structure, **24**,381
penetration of solar wind plasmoids, **40**,193
polar ion-exosphere model, **18**,41,103
radio VLF emissions, **24**,375; **34**,1361
solar coronal 530.3nm emission, **21**,703; **24**,381
solar eclipses, long term effect, **30**,587
solar plasma effects, **12**,87; **15**,1677; **21**,1475,1923; **22**,841; **28**,495
thermospheric temperatures and winds, **36**,677
annihilation in current pinch (neutral sheet), **15**,733
anomaly,
Brazilian, particle precipitation , **21**,169
South Atlantic, **23**,15,671; **32**,1513; **38**,633
antenna impedance, hf interaction, **14**,1227
bays,
auroral absorption, **18**,1301
development of, model, **17**,1795
Harang discontinuity, associated thermospheric winds, **36**,225
Harang discontinuity, electric current continuity, **26**,237
Harang discontinuity, IMF B_y component, **32**,1021
Harang discontinuity, substorm injection boundary, **25**,1119
low latitude, IMF sector boundary, **25**,161
positive, caused by polar currents, **22**,1219
positive, observational test for origin, **36**,1149
trapped plasma, **17**,2017
calculations and local models, **11**,1263
cavity, and van Allen belts, **14**,641: **15**,495
cavity, resonance excitation by MHD waves, **16**,831
charged particle dynamics, **13**,469; **14**,483
conjugate studies, **13**,303; **15**,1585; **16**,1357; **17**, 1459,1485,1677,1867,2025; **18**,731,1005,1011,1691, 1225,1275,1335,1367
coordinates, invariant, **25**,411
cosmic ray cut-off control, **17**,1173
currents, *see* CURRENT SYSTEMS
depressions, sporadic-E disappearance, **20**,371
diffusion of meteor trains, **15**,1131
dipole, eccentric, algorithm for spherical harmonics, **16**,1341
dipole interaction with moving plasma, **15**,515, 1479,1847
dipole inclination, **22**,595; **23**,889; **38**,1203
displaced poles, thermospheric winds, **22**,623
disturbances,
DP_2, interpretation and comment, **20**,1259; **21**,1255,1260,2232
DP_2, ionosphere and magnetosphere, **29**,495
DP_2, polar cap, **21**,691,692
D_{st}, equatorward shift of aurora, **27**,997
disturbance vectors, computed distribution, **19**,543
effect on cosmic ray flux, **15**,1169; **16**,818,1081
exospheric propagation, **27**,403
high-altitude nuclear explosion, **10**,47
horizontal, in auroral ionosphere, **31**,641
influence of interplanetary interaction regions, **32**,1541
influence on PCA events, **13**,1075; **14**,991; **20**,1163
infrasonic pressure wave, **20**,313
morphology, ionospheric storms, **11**,31
non-recurrent, solar wind streaming, **31**,865
polar, **11**,1395; **14**,807; **19**,643; **27**,1451
polar cap convection, sun-aligned arcs, **38**,1
solar wind pressure changes, **20**,1909
dynamics of ionospheric irregularities, **16**,273
dynamo action, plasma motions, **12**,1147; **19**,1016
electric field from plasma interactions, **19**,749
electrostatic potential along field lines, **21**,1691
field features at equatorial electrojet, **28**,1125
field, fluctuations
annual and semi-annual, **20**,423; **21**,1455,1456
annual, Ci characteristic figures, **20**,225
annual, heliographic independent, **33**,577
asymmetry, dawn-dusk, storm-time, **39**,821
daily, ionospheric currents, **29**,703
daily, nature of, **18**,1834
daily, nighttime, low latitudes, **35**,1523
daily, sector boundary passage, **25**,1183
daily, surface equatorial, **20**,1113
F-region drifts, **32**,1327
generated by sea tides, **18**,1597
ground level, ionospheric currents, **24**,193
intensity measurements, soviet satellite, **5**,244
intensity, minimum, middle latitudes, **19**,1319
interplanetary sector and season effects, **21**,839; **22**,193,1173,1413,1611
linearly varying, rays and foci, **28**,837
neutral sheet association, **21**,2013
oceanic and island effects, **21**,97
pertubations, magnetopause, **31**,1237
pulsations, associated auroral forms, **37**,1477

secular, morphological aspects, **13**,1097
SI type, **22**,1117
SID events, **20**,871
siderial-day variations, **21**,145
substorm effects, **20**,1455
total field, **22**,1413
troughs, **24**,1177
field, H-component,
27-day oscillation **18**,287
asymmetry, N-S, IMF-B_y effect, **34**,639; **39**,751
at MAGSAT altitude, **38**,883
coastal effects at equatorial latitudes, **32**,845
distribution of B_y in tail, **27**,769
galactic X-ray ionization effects, **22**,1583
ground data and ionospheric E_s, **36**,1165
intense, small scale, high-latitude ionosphere, **33**,1383
lunar tidal effects, in electrojet, **18**,367,1075
oscillations, 27 day, equatorial, **18**,287
periodic fluctuations, during storms, **12**,855
variations, spectral analysis, **20**,1613
field, lines,
auroral, electron trapping and scattering, **28**,1073
eigenfrequencies, and Pc4 pulsations, **33**,1369
inclination angle at geosynchronous orbit, **32**,1283
in Earth's tail, **21**,528
in space, **1**,285
L-variations, represented by dynamo current, **32**,629
model of distant field, **9**,305
model, OGO 3 and 5 observations, **21**,1763
model, quantitative, Birkeland current data, **39**,641
model, Williams and Mead, **19**,1016
motion due to solar flare-substorm coupling, **30**,1183
open geometry, dependence of IMF, **29**,803,809; **32**,107,113; **40**,1513
oscillations, artificial, **27**,463
polar cap boundary defining features, **28**,1019
topology in dayside cusp region, **28**,525
transmission of electrostatic potential, **21**,1691
tubes of force of unit flux, **19**,521
tubes, propagation of MHD wave, **29**,609
graphical display, **19**,643
heating in upper atmosphere, **16**,231,1201
historical survey of solar-terrestrial studies, **17**,295
indices,
A_a and A_p, semiannual variation, **32**,297
A_p, IMF sector structure, **26**,767; **27**,1033
AE, global Joule heating, **33**,279
AE, polar cap potentials, **38**,1207
AE_{12}, correlation with polar cusp width, **36**,157
K_p, M-region storms, **11**,505
K_p, solar cycle dependence, **22**,537
K_p, solar wind dependence, **21**,2139
PC, new index of DP_2 in polar cap, **36**,1095
related to neutral density variations, **21**,2049
solar interaction region, influence of, **30**,1079
variations at Hale sector boundaries, **29**,167
infrasonic pressure disturbance, **20**,313
ion cloud motion, ambipolar diffusion, **17**,519
L-shell configurations, **19**,1583
lunar induced variations,
effect of sea, **17**,487
solar cycle influence, **21**,1923
magnetometers, *see* INSTRUMENTATION
origin, theories
Chapman-Ferraro theory, **10**,233; **12**,573; **16**,1023; **37**,1037
dynamo action, ionospheric, magnetospheric effects, **13**,729,737; **18**, 1075,1091
Earth and other planets, **14**,579
magnetospheric injection mechanism, **12**,209
simulated, laboratory experiment, **12**,1189
pulsations, *see* MAGNETOHYDRODYNAMICS
quiet conditions,
effect of IMF, **26**,403
ionospheric conductivities, **16**,353
plasma convection patterns, **25**,303
scaling for magnetospheric experiments, **15**,1479
S_D field, asymmetry of main phase, **15**,205
S_D field, origin, auroral filtering, **2**,49
S_R variations, induced effects, **24**,1049
Störmer theory and Euler potentials, **15**,1525
storms,
airglow, line width variations, **18**,784
Atlantic, S, anomaly, VLF disturbances, **38**,633
Brazilian anomaly, particle precipitation, **21**,1699
causes, IMF significance, **35**,1101
composition changes in thermosphere, **35**,807
cosmic rf noise attenuation, **2**,99; **11**,371
DS axis, observed shift, **15**,937
DS variations, equatorial latitudes, **22**,991
D_{st}, equatorward auroral shift, **27**,997
D_{st}, phenomenological study, **40**,731
dayside polar region, **30**,1033
development, asymmetric, **12**,607
development, controlling factors defined, **39**,1163
development, expansive phase, **22**,1403,1511; **35**,1199
development, growth phase, **20**,1095,1521
development, mechanism, **20**,1245; **23**,1279
development, negative phase, **24**,607
development, negative sudden commencement, **12**,573
development, prediction of, **29**,1151
development, pre-plasma enhancement, **13**,297
development, pre-substorm phase, **30**,371
effect on energetic trapped protons, **33**,39
electron enhancement, **15**,1603; **16**,951; **17**,1949; **19**,503, 761; **20**,511,1299; **40**,1409
energy source, magnetospheric dynamics, **40**,581

energy source, solar hydrogen, **12**,801,905
equatorial electrojet, **39**,907,919
field effect on Forbush decrease, **14**,979
global fluctuations, statistics, **18**,1381
IMF relationships, **20**,1033; **21**,2003
ionospheric efects, **11**,31; **15**,1157; **16**,653; **17**,841, 1993; **18**,917; **20**,627,1299; **21**,349; **22**,223,237; **24**,69,607,867,1031; **39**,907,919
ionospheric E_s-p layer, **21**,197
origin, hydromagnetic theory, **9**,947; **12**,660; **13**,281; **28**,449
magnetospheric time variations, **33**,81
magnetotail field, currents, **39**,833
mainphase, theories, **11**,1277; **15**,205
plasmasphere response, **22**,223; **39**,1069
post phase, green aurora and electron precipitation, **29**,405
prediction schemes, **34**,77; **40**,457
protonosphere depletion and recovery, **28**,453
recovery phase, effect of field-aligned currents, **29**,1315
recovery phase, proton precipitation, **25**,1186
recurrent, M-region, solar wind, interaction theories, **11**,505; **12**,113; **23**,143; **25**,2085
ring current effects, **21**,983; **38**,765,1133
satellite, effect on, **19**,1339
solar coronal features, **17**,1039; **21**,703
solar cycle distribution, **38**,181
solar flare effects, **13**,435; **15**,39
solar radio bursts, **1**,325; **2**,223
solar wind effects, **16**,309; **21**,2139; **28**,933; **30**,669; **38**,765
sudden commencement, auroral precipitation, **24**,487; **25**,823
sudden commencement, equatorial enhancement, **32**,599
sudden commencement, following cosmic ray flares, **14**,871
sudden commencement, global structure, **25**,373
sudden commencement, ionospheric currents, **33**,11,711; **38**,365
sudden commencement, negative impulse, interplanetary shock wave, **13**,675; **21**,1931
sudden commencement, pulsations and impulses, **15**,573; **21**,1713
sudden commencement, SSC(-+), **19**,371
thermospheric relationships, **19**,491; **20**,379,511; **24**,1031; **25**,607; **33**,1283
trough development, correlation with, **19**,821
viscous interaction, solar wind and magnetosphere, **12**,45
VLF emissions, **1**,253; **15**,799; **17**,13,869,1565; **18**,944; **38**,633; **40**,1409
winds and electric fields, **40**,595

substorm,
active region location changes, **22**,1341
associated ion flows, **38**,1251
asymmetric field, auroral bulge, **30**,389
auroral absorption, conjugate studies, **18**,1005; **22**,1427; **23**,269,619,867,905; **31**,1415; **38**,127
auroral, associated TID's, **35**,785; **38**,913
auroral, field, electron density, temperature, **29**,249
auroral emissions, **18**,525; **20**,1116,1443; **22**,1511; **27**,453
auroral, infrasonic waves, **24**,1155; **29**,57
auroral, onset studies, **29**,1287
auroral oval, morphology, **24**,955; **27**,453
auroral precipitation, **14**,807; **20**,1433; **24**,365; **25**,931
bay-like disturbances, **24**,1133
characteristics, associated VLF emissionn, **34**,225
critical issues, **34**,563
current systems, effect of, **22**,1231,1403; **24**,215,717; **30**,389
cusp shift equatorwards, **29**,317
development, **11**,1395; **12**,273,945; **15**,1287; **16**,891,1365; **17**,707; **27**,217
distinction between storm and DP-2 event, **19**,205
dynamics, from conjugate auroral studies, **38**,127
electric field variations, **20**,1475
energy dissipation in atmosphere, **23**,1589; **24**,223
energy flow at satellite altitude, **38**,241
energization, impulsive, ions in magnetotail, **38**,491
global study, **38**,1495
IMF relationship, **19**,697; **22**,111; **25**,895; **28**,381; **34**,1109
injection boundary, Harang discontinuity, **25**,1119
isolated, SAR arc observation, **35**,475
magnetic signature, statistical, **26**,269
magnetospheric electron islands, **16**,1441
magnetospheric model, **23**,575; **24**,269; **28**,749
magnetospheric plasma sheet effects, **19**,1275,1413
mechanism, MHD wave propagation, **29**,695
model for mechanism, **29**,271,1069
morphologies, auroral infrasonic waves, **22**,151
observations from ground, **28**,763
observations from sounding rockets, **23**,1321
onset, initial ionospheric conductivity, **30**,1315
onset, related to auroral absorption, **22**,1427
polar, electrojet relationship, **21**,1
polar, time sequence, **23**,1483; **24**,1133
polar cap, signature of development, **27**,217
precipitation, *see* PRECIPITATION
precursary phase, magnetosphere, **23**,1257
propagation, radially antisunward, **38**,771
pulsations, simultaneous with aurorae, **24**,573; **29**,539; **37**,1477

reconnections of field lines, **23**,813; **24**,269; **35**,227,405,451,727,813,1199
simulation, associated thermospheric vortex, **32**,71
solar wind, importance of, **23**,75
triggering conditions, **38**,211
VLF emissions, **25**,261; **34**,225
weak, and intense, **23**,579
westward surge, absence of H_β, **17**,1409
westward surge, auroral rf absorption, **31**,1373; **35**,145
winds, **18**,1623
transition region field between magnetosphere and bow shock, **15**,239
trapped particles,
auroral electrons, **17**,1051; **28**,1073
diffusion of meteoritic ionization, **28**,997
distribution of, and geomagnetic effects, **11**,869,1219
ions, related activity, **11**,451
protons, origin, albedo neutron theory, **11**,1151
wind-shear theory of sporadic-E layer, **14**,909

GRAVITATIONAL FIELD
Earth-Moon system, classification of lunar satellite orbits, **16**,285
Earth models, intercomparison, **30**,215; **32**,151
geo-field models, accuracy of, **26**,1081
geo-field models, comparison by lumped coefficients, **29**,653
geo-field model, Goddard TOPEX, **35**,997
geo-potential harmonics, orbit analysis, **8**,43; **11**,789; **13**,1151,1213; **14**,49; **15**,53,741,1549,1829; **16**,195; **17**,629; **20**,1213; **22**,391,509,645,1045,1269,1349; **23**,229,541,1239; **24**,711; **26**,611; **27**,1,1247; **30**,5,73,411; **31**,829; **32**,717; **33**,97,223,1145; **34**,47,58,183,1307,1319; **35**,79,921,937,997; **37**,220,236,351,693,795,805; **38**,407,1147,1409,1469; **39**,685,961,1549
inner radiation belt, position dependence, **9**,841
moon, *see* MOON
pertubation of satellite orbits,
eccentricity variations, **40**,847
extra-terrestrial effects, **9**,659
geostationary, longitude dependent field terms, **11**,1325
lunar effects, **18**,1137,1499
model for Earth's field, **7**,154
near-circular, **14**,433
oblateness of Earth, **5**,84
planetary influence on orbital elements, **33**,1359
resonant or near-resonant, **17**,1505
solar effects, **18**,1499
surface gravity from harmonic coefficients, **12**,1027
tesseral harmonics, **11**,797

GREENHOUSE EFFECT
atmospheric cooling, enhanced gases, **40**,1011,1535
atmospheric heating and photodissociation rates, **38**,807
GAIA or geochemistry, regulation of CO_2 and climate, **30**,795
ionospheric, electron densities and heights, **38**,945
review of the effects of atmospheric CO_2, **28**,1011; **29**,935

HELIUM
atmospheric abundance, diurnal variations, **11**,1379; **16**,1103
atmospheric abundance, winter bulge, **33**,23
atmospheric, excitation, emission, **10**,73; **12**,91; **13**,403; **15**,1219; **16**,1103; **17**,715
atmospheric, loss processes, **13**,925; **15**,1219; **18**,449; **40**,1639
emission, solar, rocket measurement, **11**,73
interstellar, interaction with solar wind, **28**,799; **34**,387
ion content of magnetosphere, **14**,1273
ions, atmospheric, production, loss mechanisms, **9**,599; **12**,1169; **13**,1125; **26**,255; **32**,791
global distribution during solar minimum, **32**,1523
metastable concentrations, **9**,701
transport in plasmasphere, **27**,1441
turbopause level, **18**,1051

HISS
see RADIO WAVES

HYDROGEN
atoms, ions, thermosphere and exosphere, **5**,257; **10**,65; **14**,417,425; **19**,1441; **20**,521,581,1147; **21**,309,686; **22**,1375; **27**,795
cooling effect of O(63μm) emission, exosphere, **27**,795
escape, exospheric, **18**,449; **26**,855
geocorona, abundance-emission relationship, **12**,149; **17**769; **18**,803; **24**,303; **33**,499
geocorona, Lyman-α emission, **20**,297; **24**,303; **26**,431; **29**,907
global density distribution, **26**,863
interplanetary distribution, **11**,767
interstellar, resonance scattering, **20**,829,1784
latitude variations, polar wind, **26**,873
molecular, sources, sinks, anthropogenic activity, **25**,521
molecular, thermospheric, **11**,1035,1379; **12**,1045; **13**,905; **14**,417
velocity distribution, **26**,431

HYDROXYL
see also AIRGLOW
transition probabilities, airglow relevance, **37**,723
tropospheric production rates, **23**,1507

HYPERSONICS
diffusion effects on shock structure in plasma jet, **4**,358
cratering, planetary, hypervelocity projectiles, **28**,567,599, **617**,625
eject parameters, **26**,469
electrode contamination of air-arc plasmas, **4**,374
electron concentrations,
high temperature air, with additives, **6**,79
plasma sheath, errors in rate constants, **6**,74
electrostatic contamination of insulated current detectors, **5**,85
heating and vaporisation of impacts, **26**,463
heat transfer coefficient, measuring technique, **4**,352
high temperature air, collisions, scattering cross-sections, **6**,24
impact, high velocity, associated light flash, **23**,1519; **24**,771; **26**,463
plasma production by fast dust particles, **25**,135
puncture at cosmic speeds, **5**,84
re-entry, *see* SATELLITES
shock layers,
composition, plasma sheath data, **6**,47
configurations about blunt shapes, **4**,337; **6**,10
ionization rate, **6**,94
signal transmission, *see* SATELLITES

INCOHERENT SCATTER
see RADAR

INDICES, MAGNETIC
see GEOMAGNETIC FIELD

INSTRUMENTATION
antennas,
dipoles, electric and magnetic, rf field noise, **8**,68
dipole, impedance in ionosphere, **9**,445,639; **13**,723,979; **20**,1185
dipole, micrometeoroid detection, **37**,1291; **38**,949,951
impedance in ionosphere, **14**,631,1007,1227; **17**,1437; **18**,1357
impedance in warm magnetoplasma, **20**,997
impedance, orientational dependence, **21**,1262
impedance, satellite wake structure, **18**,901
loop, VLF input impedance, **21**,1810
plasma flow-past, effects, **15**,155,463,1479,1489, 1847
power-handling, coronal breakdown, **6**,142
radomes, microwave breakdown, **6**,155
resonance rectification in plasma probes, **13**,725,969
satellite, effective area, **11**,817
slotted-sphere, transmission characteristics in plasma sheath, **6**,116
telecommunications during re-entry, **6**,207
transmitter for whistler excitation, **21**,2113
auroral scanner, dual-λ, ground based, **20**,1935
auroral scanner, imaging, **22**,1003
capacitor effect of satellite surface, **22**,321
CCD images of Mars, telescope, **39**,273
charged particle trap, three-electrode, satellite, **12**,175
chemiluminescent sampler for NO, O_3, balloons, **22**,19
density measurements in air, gas-surface interactions, **17**,917
deployment system, pneumatic, rocket magnetometers, **13**,89
discharge source for O_2(0-0) and $O(^1S)$ emissions, **27**,1209
dust collecting remotely, avoiding contamination, **17**,575
electric field, dc, **18**,1551
electron flux analyser for rocket, **24**,115
electrostatic contamination of current detector in plasma, **5**,85
electrostatic flux-meter, **22**,1131
energy from space plasma for instrumentation, **25**,615
filters for solar short-wave studies, **9**,987
goniometer for VLF observations, **21**,899; **27**,1371
image intensifier, spectroscopy, **15**,1211
imager gives oxygen rotational temperature, **39**,1363
ionosonde, directional, **19**,1387
Langmuir probe, *see* probe, electrons,
light flash detection, from particle impact, **23**,1519
optics for atmospheric investigations, **9**,675
optics, telescope, meteorite impact damage, **12**,77
oxygen sensor, silver film, rockets, **18**,1527
magnetometer,
balloon-borne, **20**,331
ground array for pulsation studies, **30**,1199; **34**,863
limitations of spectral analysis, **40**,707
proton, operation in moving vehicle, **13**,521
micrometeorites, electronic detection, **12**,627; **19**,195
neural networks for solar-terrestrial effects, **40**,457
neutron monitors, **22**,177; **23**,115; **24**,683
phosphor, thermo-luminescent, X-ray and UV detection, **11**,1489; **12**,167
photocathodes for solar far UV emission, **9**,869
photo-electric, telescope satellite tracking, **12**,261
photometer,
airglow, portable, **17**,1073
airglow, rocket borne, **11**,419; **15**,1857; **18**,835
auroral imaging scanner, **22**,1003
calibrations, **12**,189; **14**,921; **25**,173
contamination corrections, **22**,725
Hadamard, **20**,1351
scanning, airglow, **27**,1221
tilting filter, ground based OH observations, **23**,1211

plasma gun, rocket borne, **26**,367
pressure guage, orbiting, effects of adsorption on measurements, **15**,1329
probe,
composition measurements, **17**,693,1641
electric field, ionospheric, rocket, **20**,1281; **22**,1145
electron density, ionosphere, from rockets, **9**,247; **14**,731; **19**,827; **22**,41,1585; **24**,87,115,183
electron temperature, ionospheric, **16**,257; **19**, 827; **20**,899,1717; **21**,993,1983; **22**,41,180,873
Faraday rotation, two-frequency, **17**,1045
interactions with local plasma, **37**,21,873,1001; **39**,1325
ionospheric, impedance, low frequency, **22**,583
ionospheric, impedance, swept-frequency, **22**,1017
ionospheric, performance evaluation, **21**,1049; **23**,1085
Langmuir, characteristics in different ionospheric conditions, **32**,1427; **39**,1217
pressure on plasma due to probe field, **40**,1063
resonance, plasma signal rectification, rockets, **13**,725,969; **16**,845
rocket skin, ionospheric currents, **27**,99
perturbed by spacecraft environment, **21**,1625; **22**,1145
spherical, **22**,41,873
surface contamination effects, **24**,87,183
triple, plasma parameter measurement, **25**,973
whistler excitation in ionosphere, **21**,2113
potential of metal sphere in space, **9**,259
radar auroragraph, drift echoes, **26**,519
radiometer, actinometric, solar flux, **11**,1085
retarding potential trap, contamination, **23**,1309
space plasma as energy source for instrumentation, **25**,615
spectrograph, extreme UV, rocket, **11**,335
spectrometer,
Ebert, rocket, dayglow, **16**,929
mass, spacecraft, **5**,85; **9**,269; **11**,173,297; **23**,1621; **27**,1213; **37**,315; **37**,315
planetary atmospheres, **15**,1211
solar UV, **11**,81; **15**,1211
stepped filter masks for band profile measurement, **31**,1137
spectrophotometer, scanning, airglow, **27**,1221; **36**,1269
telephotometric systems, **11**,833
television cinematography,
auroral displays, **17**,75
rocket trajectory determination at night, **17**,579
time recording of satellite photography, **11**,161
topside optical station, **11**,1235
tracking head, solar, **11**,977
wave guide, 'chemical' low frequency, **38**,1075
weightlessness, emptying and filling vessels, **11**,1343
X-ray equipment, solar studies, **11**,1493

INTERFEROMETRY

Doppler imaging system for the auroral thermosphere, **32**,273
Fabry-Perot,
airglow OI 557.7nm, **13**,901; **14**,383,1331; **16**,211,431; **19**,467; **33**,373,869; **38**,1161; **39**,1511; **40**,1599
airglow OI 630.0nm, **12**,591,1139; **13**,551,1163; **16**,431,1109; **17**,957; **30**,1025; **31**,53,303; **33**,201,817,841; **35**,1255; **36**,197,225,677,851; **38**,1161; **39**,1511
airglow, O_2 atmospheric bands, **39**,1363
airglow NI 520nm, nocturnal excitation, **17**,675
airglow Na D-lines, twilight and night, **26**,65
auroral NI 520nm doublet, **9**,811
auroral OI 557.7nm, **5**,299; **9**,295
auroral OI 630.0nm, **9**,295; **18**,431; **32**,273; **34**,483
auroral OI 844.6nm, **9**,383
auroral OII 731.9nm doublet, **22**,636
wind determinations by inversion, accounting for scattered light, **33**,1049; **40**,1599
Michelson
airglow OI 557.7nm, WAMI, **14**,483
auroral OI 557.7nm, WAMI, **21**,605
auroral OI 630.0nm, WAMI, **21**,605
PEPSIOS, OI 630.0nm dayglow, **25**,185
rf 21 cm, position of Jupiter's magnetic axis, **16**,445
rf, investigation of cosmic plasma, **24**,617
rf, study of localized auroral scatterers, **38**,933
VHF, ionospheric electron concentrations, **5**,50

INTERPLANETARY SPACE

magnetic field,
auroral dynamics, large scale, **23**,1349; **27**,665,699; **29**,731;**32**,25
B_x,B_y, polarity effects on electron precipitation, **31**,489
B_y, auroral arc shapes, **34**,489
B_y, electrojet influence, **28**,29
B_y, Harang discontinuity, **32**,1021
B_y, induced field-aligned currents, **31**,363; **36**,523
B_y, magnetospheric asymmetries, **29**,79; **33**, 1327; **34**,639
B_y, sector effect in geostationary orbit, **31**,73
B_y, thermospheric effects, high latitude, **34**,1
B_z, AE index variations, **36**,829: **37**,609
B_z, convection in polar cap, **28**,595; **38**,1077
B_z, effect on polar electric field, **29**,205
B_z, ionospheric flow characteristics, **36**,471,1415
B_z, polarity reversals, equatorial electric fields, **36**,785
configuration at 1AU, solar flare effect, **35**,793
conjugate auroral absorption effects, **17**,1919
cosmic ray anisotropy, **15**,547,975,1723; **16**,1131; **33**,395; **38**,1387; **39**,1233

cosmic ray asymmetry, sector polarity, **27**,39
cosmic ray diurnal variations, **16**,15,1209; **17**, 1121,1749,1879
cosmic ray transit, **15**,1375,1723; **16**,29,783
discontinuity, effect on polar cap geometry and arc formation, **32**,113,119
disturbance, event models, **38**,575
disturbance, solar flare association, **36**,669
disturbance tracking by scintillations, **37**,73
effect on dayside aurora, **31**,1345
effect on electric and potential fields, **32**,907
flux decrease, solar protons, **23**,1445
flux dependence on direction, **28**,545
geoelectric field responses, **37**,1404
geomagnetic field association, **17**,1183,1803; **20**, 1033; **21**,703,839,1743,2003; **22**,111,1117; **23**, 945; **24**,518; **25**,15,161,465,895; **26**,195,229,403; **27**,47,255,425,699,1033,1055; **30**,635,641; **31**, 559; **32**,113,605; **34**,987; **35**,405,1301; **36**,1485, 1489,1495
heliomagnetic polarity reversals, **33**,395
heliospheric configuration model, **28**,609; **29**,313
influence of neutral hydrogen, **22**,1719
interaction between solar wind and large obstacle, **16**,145
irregularities, small-scale, temporal independence, **14**,649
lunar magnetic tail and wake, **16**,142
magnetic clouds, geomagnetic response, **36**,1485,1489,1495; **37**,385; **40**,519
magneto-electric parameters, storm criteria, **35**,1101,1301
magnetotail structure effects, plasmasheet changes, **28**,757
model compatibility with cosmic ray modulation data, **15**,257; **16**,818; **17**,31
model, vicinity of Earth, **9**,305; **12**,961
momentum transfer across magnetopause, **37**,1347
orientation, polar cusp extension, **24**,518
planetary magnetic fields, influence on, **14**,579; **30**,1061
plasma observations, VEGA spacecraft, **39**,697
plasma sheet effect, **34**,683
polarity, related to cosmic rays, **27**,39; **33**,395
polarity, related to geomagnetic field, **23**,929; **24**,55
probed, cosmic ray observations, **12**,1055
propagation of solar protons, **13**,745; **23**,1445
pulsations, MHD, effect on frequency, **33**,387
radio aurorae, location in polar region, **36**,441
scintillations, MHD model, **36**,1155
sector boundary, Hale, activity effects, **29**,167; **30**,519
sector boundary, Jovian rf bursts, **31**,129
sector polarity and structure, **21**,703,839, 2003; **22**,193,1173,1413,1611; **24**,55; **25**,161,465; **26**,767; **28**,1155
sector polarity, effect on geomagnetic N-S asymmetry, **32**,605
shock event, distribution of energetic protons, **31**,1388
shock wave at magnetosphere, **13**,675,1111; **16**,1483; **18**,319; **24**,459,951; **28**,381; **34**,825; **37**,385,1347
solar wind effect for solar rotation, **16**,1
solar wind temperature anisotropy, **17**,1009; **18**,321
strength relative to magnetosheath field, **17**,1803; **24**,147

medium,
cold meteoroids, Pioneer measurements, **39**,1573
corotation interaction region at 1AU, ion content, **32**,1179
corotating streams at high latitude, **32**,1273
corpuscular radiation, solar, **9**,103; **13**,435
cosmic plasma, rf interference investigation, **24**,617
cosmic ray continuity and momentum equations, **17**,31
cosmic ray modulation, **12**,1055; **13**,115; **19**,1169
disturbance, large scale, observed effects on Earth, **31**,1171
dust, collection from remote sites, **17**,575
dust, degradation by solar wind, **15**,593; **27**, 1283; **29**,127
dust, density above ecliptic plane, **29**,137
dust, lifetime, planetary and drag effects, **36**,747
dust, space probe detector calibration, **37**,1197
dust, zodiacal, concentration, **11**,311,387; **15**, 1081; **17**,949; **27**,1269; **28**,657; **31**,373,871
electric field, cleft currents and plasma convection, **32**,1551
electric fields, unbalanced, **21**,187
electron, ion flux variability, **9**,21,103; **28**,803; **32**,779; **39**,47
energetic particle composition, **39**,47,57
feasibility of metal vapour release studies, **13**,95
fluctuations behind bow shock, **35**,1419
flux through magnetopause, **34**,1349
gas particles, diffusion and orbital pertubations, stochastic impulses, **31**,1
gas scattering of solar emission, **37**,369
gas temperature changes, **26**,111
gases, neutral, of interstellar origin, **23**,93
grains, electrostatic charge on, **17**,155
H atom flux, detection possibilities, **40**,1525
He^+, backscatter of solar HeII radiation, **21**,1795
He, interstellar, solar wind, **28**,799
heating by solar wind, **31**,1157
heliosphere, current sheet, **33**,915,925
heliosphere, enhances ion fluxes, **35**,1359
heliosphere, neutral flux anisotropy, **40**,439
heliosphere, radius estimation, particle density, **16**,783; **28**,815

hydrocarbons, airglow evidence from meteoritic activity, **16**,134
hydrogen, helium, ionization, emission lines, **2**,86
hydrogen, resonance scattering of solar L_α, **20**,829
ions in corotating regions at 1AU, **33**,147,557
ions, pick-up, ISM captures, model, **37**,555
ions, pick-up, vicinity of comet, **37**,1169
kinetic and transport properties, **9**,461
outgassing from the satellites of outer planets, **24**,577
parameter variability, long term, **39**,411
particle anisotropies, **20**,1051,2113; **25**,799; **29**,127
passage of energetic charged particles, **13**,9
plasma irregularities, **15**,953; **16**,749; **19**,1615; **35**,487; **40**,1063
radiation force on particle motion, **29**,127
radio investigations, **9**,391; **16**,749
scattering centres, phase function, polarisation, **21**,2149
scintillations, dispersion analysis, **18**,95
scintillations, disturbance modelling, **35**,271
scintillations, latitude dependence, **21**,1617
scintillations, plasma density, **22**,1041; **24**,951; **38**,955
shock waves, **14**,901; **18**,319; **19**,1121; **24**,459,951; **25**,657,947; **38**,343
solar wind, kinetics, structure, **18**,321; **19**,1121

IONOSPHERE
absorption,
attenuated hydromagnetic waves, **9**,771; **16**,567
cosmic noise at sunrise and sunset, **11**,371
cosmic noise, time lag from pulsations, **19**,959
electron density profile equation, **16**,529
PCA, associative detachment in mesosphere, **17**,731
PCA, conjugate twilight observations, **13**,583
PCA, electron densities, **13**,339,1171; **35**,947
PCA, geomagnetic activity, **13**,1075; **18**,1005
PCA, height, characteristics, **12**,579,1035
PCA, incoherent scatter data, **35**,947
PCA, mesospheric oxygen and ozone decrease, **21**,1969
PCA, model for, in D-region, **15**,1111
PCA, proton energy deposition in O and O_2, **23**,787,935
PCA, recovery, midday, **15**,1667
PCA, review of characteristics, **12**,495
rf, critical survey of models, **8**,151
rf, during auroral disturbance, **1**,102; **13**,1171
rf, IMF sector structure, **24**,55
rf, power spectrum, **24**,17
rf, satellite beacon signal, **16**,1415
rf, westward travelling surge, **31**,1373
sudden storm commencement, **38**,365
anomalies and disturbances, theories, **12**,553
anomaly, equatorial, effect on VLF reception, **28**,17
auroral, *see also* AURORA
C-region, rf absorption after solar flare, **1**,193
conductivity,
auroral break-up associations, **16**,329; **36**,1359
comparison E and F-regions, nocturnal, **25**,197
gradients, **35**,1405
initial magnitude at substorm onset, **30**,1315
ion mobility spectra, **36**,163
tides and dynamo model, **16**,353
variations, and micropulsations, **28**,475
coupling fluxes to magnetosphere, **28**,245,407
currents, *see* CURRENT SYSTEMS
D-region,
anomalous characteristics in winter, **27**,1333
chemical fluctuations, scale times and lengths, **34**,979
chemistry, hemispheric differences, **17**,1459
chemistry, negative ion, **20**,295
disturbance phenomena, and VLF, **13**,175
electron and ion densities during auroral absorption, **12**,543; **33**,583; **35**,947
electron concentrations, **13**,1013; **15**,1717; **17**,609,1855
electron cooling, **9**,439
electron heating, electric field, **14**,987
ion chemistry and winter anomaly, **25**,1135
ions, negative and positive, chemistry, **29**,735; **30**,1065
ions, positive, during solar eclipse, **15**,1035
ionization by auroral electrons, **23**,1321
ionization correlated with PCA events, **12**,195; **15**,1111
NO formation, related parameters, **33**,1169
origin of, **5**,76; **8**,200
positive ion composition, **23**,1621
properties, chaff-cloud observations, **20**,877
radio absorption events, magnetotail electrons, **16**,567
recombination during solar flare, **21**,367
solar precipitation effects, **38**,1479
SPE disturbed, model, **26**,883
water-cluster ions, quiet daytime, **25**,275
disturbances,
double scattering of plasma streams, **16**,845; **18**,1843
due to auroral particle precipitation, **33**,591,597
due to solar particles, **5**,59; **11**,599; **15**,1677
due to travelling material body, **9**,321; **15**,1499
electromagnetic, amplification, **14**,1077
geomagnetic pulsation effects, **31**,569
geomagnetic storm associations, **21**,349
large-scale, universal time effects, **40**,1093
oscillations, Doppler, ULF pulsations, **38**,1581
Perkins instability, **40**,1615
Rayleigh-Taylor instability, **39**,1667
satellite wake, **18**,793,901

TID, associated gravity waves, **37**,967
TID, conjugate effects, **31**,1409
TID, and MED waves, radiotelescope data, **40**,447
TID, polar origin, **23**,381; **35**,785
TID, propagation and pattern, **39**,583,1189
TID, review, **40**,829
TID, sourced in electrojet, **18**,583
TID, substorm onset, **38**,913
dynamics,
coupling between neutral and plasma motions, **15**,671; **16**,1019
damping of geomagnetic pulsations, **26**,201
diffusion, ambipolar, height variation, **18**,1836
diffusion, ambipolar, ion cloud motion, **17**,519; **18**,1319; **21**,526,1073
diffusion, electron-ion collisions, **22**,833
diffusion, thermal, **15**,1151; **16**,1019; **17**,853; **18**,535; **25**,907
diffusion, transequatorial, **15**,1261
drift of ionized irregularities, **1**,205; **11**, 639,759,823; **12**,1; **13**,959; **14**,459: **17**,433,519,1693; **21**,1109,1237; **23**,560; **24**,69; **28**,407; **35**,785,1489; **40**,663
flow, ions, **25**,967; **36**,693
flow, heat, **25**,907
flow, protons, **25**,291
general transport properties of electron gas, **18**,1535; **19**,1593
low auroral fringe during disturbance, **40**,1101
plasma motions and *em*-emissive power, **40**,509
response to magnetic cloud transit, **40**,519
turbulence, plasma, spectral form, **29**,931
vertical F-region movements during storm, **21**,1805
vortex structures, **39**,1025
winds, *see* WINDS
dynamo action, plasma motions, **12**,1147; **13**,729,737; **19**,263; **25**,587,1075; **38**,301
dynamo region, heat input, **18**,423
dynamo theory, **22**,821
E-region,
absorption, geomagnetic and current control, **2**,1
directional currents, **30**,209; **31**,1177
drift velocities, **23**,389
drifts, electron density irregularities, **11**,639,759, 823
electrical coupling to F-region, **22**,743; **23**,557; **25**,197
electrons and ions, densities, temperatures, **17**,737; **28**,207
electron temperatures, density, dynamics, **22**,961; **35**,1
formation, nocturnal, mid-latitudes, **24**,131
incoherent scatter observations, **40**,355
influence of galactic X-rays, **20**,61
ion chemistry, in-situ experiment, **19**,15
ion composition and NO, auroral, **25**,103
ion distribution function, **32**,1061
ion layers, linear attachment law, **15**,1055
ion layers, wind shear, **15**,27
ionization sources, **23**,1321; **28**,1027
magnetic activity effects, **25**,651
nocturnal, equatorial, irregularities, **18**,1307
nocturnal, mid-latitude, particle influx, **19**,270
thermal balance, **19**,15
E, layer,
blanketing type, empirical approach, **21**,889
characteristics, **2**,195; **18**,1417
disappearance, magnetic field depressions, **20**,371,2205
distribution frequency over solar cycles, **33**,457
drift profiles, vertical, metallic ions, **31**,253
echo signature on VHF backscatter radar, **32**,1455
electric fields and neutral winds, **24**,475
electron density, rf measurements, **20**,809
electrons, ions, temperatures, **15**,123
equatorial, auroral, temperate zones, **11**,639
equatorial electrojet variations, **14**,529
equatorial spread-F, **12**,127; **16**,21; **19**,1131
formation at low magnetic latitudes, **34**,1081
formation by horizontal wind shear, **21**,811
ground-based H-component data, **36**,1165
height, rocket observations, **19**,1319
horizontal motions, ionosonde array, **39**,1007
ionization and drift characteristics, **1**,205
ionization and winds, **12**,1173; **13**,1161; **17**,1207; **26**,705
irregularities, **14**,759; **16**,1475
Joule heating of electrons, magnetic equator, **11**,1297
magnetic field and wind-shear theory of origin, **14**,909; **15**,123
meteoritic influx, ionization and loss processes, **17**,1233; **18**,1659; **38**,145
parameters and seasonal structure, **32**,1533
radar observations, **31**,1397; **33**,1407
scintillations, associated, **16**,21,1475
spread-E_s, related to spread-F, **33**,1081
tracers for atmospheric waves, **39**,1421
two types, geomagnetically controlled particle precipitation, **2**,49,56
vertical profile measurement, **9**,765
electric field,
auroral, dependence on IMF B_z component, **29**,205
auroral, detector design, **18**,1551
auroral, diffuse, **25**,859
auroral, effects of horizontal magnetic disturbances, **31**,641
auroral, substorm, **29**,249; **36**,1359
Chapman-Ferraro problem, **37**,1037
conductivity gradient, **34**,59,713,1213; **36**,163,1359

convection, effect on radiation belt electrons, **34**,271
convection, effect on ring current protons, **23**,1045; **27**,603
convection, magnetospheric implications, **34**,315,319,353
correlated with magnetic pulsations, **23**,311
disturbances, substorm related, **40**,95,595
divergence around westward travelling surge, **35**,1489
E and F-regions, artificial ion cloud, **19**,1; **23**,973
electric-magnetic correlations, **35**,1287
equatorial, IMF effects, **36**,785: **37**,1403: **40**,941
fluctuations, **20**,141,483,1475
generated by atmospheric tides, **22**,569
generated by field-aligned currents, **27**,223
generated by ring current, **20**,2039; **23**,1205
ground level, **24**,801
high latitude, **20**,1281; **34**,59
horizontal, stratospheric, **23**,825
inhomogenities, **21**,1897,2089
magnetospheric, a review, **37**,899
magnetospheric, field for particle entry, **27**,1523
magnetospheric, from whistler signals, **26**,171
magnetospheric, penetration to low latitudes, **38**,1051
magnetospheric plasma interaction, **19**,749; **27**,1351,1383
magnetotail, potential and vortex parts, **39**,563
mapping, auroral ionosphere, **35**,1513
mapping, equatorial plane, **18**,259
measurements, **20**,135,571,859,1281
oscillations near auroral arc, **26**,555
parallel, effect on particle precipitation, **26**,581; **29**,915
particle acceleration, **18**,1821
patterns associated with auroral arcs, **32**,193
patterns of intensity, IMF activity, **32**,193
patterns, thermospheric charge distribution, **36**,1005
plasmaspheric, geomagnetically disturbed conditions, **39**,1305
potentials, mapped from ionosphere to magnetosphere, **31**,1329
power spectra, post-sunset F-region, **40**,655
probe measurements, GEOS, **35**,61
properties from electron measurements at plasma sheet, **30**,261; **35**,991
source of auroral arc formation, **20**,591; **21**,179,741
space charge distributions, polar thermosphere, **36**,1005
Volland model, current distributions, **36**,631
waves, characteristics, **18**,155,847

electrons,
ambient and photoelectron interaction, **21**,523
anisotropic distribution, F-region, **37**,1207
beams, propagation, front structure, **22**,1597
content, anomalous nighttime increase, VHF satellite data, **18**,1163
content, altitude profile, **18**,159; **19**,15; **20**.11,1061; **21**,1581; **23**,107,523; **24**,247
content, effects of winds, **31**,377
content, equatorial region, **21**,713
content, model, **29**,869
cooling, **9**,439; **16**,125,1079,1371
density, airglow line shapes, **16**,1109; **17**,1725
density, conjugate points, **20**,141,1061,2045; **33**,321
density, distribution function, **24**,33
density, ion-transition heights, **24**,229
density, incoherent scatter, **18**,1225; **24**,479,541
density, model, U.T.effect, **26**,1179
density, nightside auroral oval, **38**,1031
density, radar measurements, **13**,1031
density, rocket measurements, **11**,59,321; **13**,1013; **16**,529,1349; **17**,617; **18**,945; **19**,827; **20**,809; **21**,119; **24**,87
density, satellite data, **13**,829; **14**,313,1123; **18**,901; **19**,1505
density, satellite wake depletion, **21**,993,1049
density, VLF propagation, **26**,219
distribution function, B-F-P theory, **25**,743
distribution, global, intensity maps, **38**,483
energy distribution, **11**,45,1209; **24**,409,900
energy transfer rates, **20**,1121
enhancements, magnetic storm effects, **16**,951; **17**,1949,1993; **19**,503,761
equatorial anomaly, **20**,2093; **21**,409,421; **22**,1309
equatorial, VLF interaction, auroral X-rays, **35**,1231
Faraday rotation, **5**,169,213; **11**,1431; **14**,1057, 1123; **15**,295,1313,1603; **17**,1045,1667,2030; **18**,129; **19**,1533; **20**,353,395; **23**,107
flow properties, **27**,753
heating, **11**,1297; **14**,987; **16**,321,525; **22**,1343; **23**,337, 589,599; **40**,901
high energy (10kev), detection, **9**,27
influence on radio wave propagation, **5**,80; **13**,1171; **16**,1277
lunar-solar tide effects, **19**,1349
photoelectron flux, **26**,1161
photoelectrons, from magnetic conjugate points, **18**,1011,1335,1367; **27**,31
power spectrum data analysis, **21**,153
power spectrum of fluctuations, all dynamic causes, **19**,1593; **23**,133; **24**,17
production and loss rate, **13**,507,839; **18**,945
rf probe measurements, **20**,809,997
rocket VHF dispersion interferometer, **5**,80
slab thickness, scintillations, **16**,1277; **19**,1313
sources, inner radiation belt, **35**,1281
storm effects, **20**,511

temperatures, **11**,463,1297; **13**,143,647,1031; **15**,95,123,1049,1557; **16**,257,1109; **17**,815,1247, 1763; **18**,1225,1489; **19**,827,1313; **20**,997; **21**, 1301; **22**,180,961; **24**,247; **29**,171,1367; **32**,1513; **33**,875; **34**,609,689; **35**,887; **37**,211,1453
temperatures, low, origin of, **26**,571
thermal, cooling rates, **36**,65
thermal, distribution at S_q current vortex, **27**,183
thermal, heating at boundary layer, **32**,657
thermal, quenching of N(^2D), **34**,689
Thompson scatter data, **21**,763
transport properties, **18**,1535; **23**,337,533
variations, seasonal and solar, **16**,385,1073; **19**,723
velocity distribution, **22**,1201
F-region,
airglow OI 630.0nm associations, **26**,93,161
auroral, ion velocity distribution, **35**,1429
auroral region, *in situ* study, **23**,1669
anomalies and disturbances, theories, **12**,553; **19**,1014; **20**,2093
anomaly, equatorial, VLF reception at ground, **28**,17
asymmetry, transequatorial winds, **17**,97
conjugacy, latitudinal variations, **17**,2025; **18**,1275
coupling with protonosphere, **21**,43; **26**,281,727,753
daytime valley, dynamical explanation, **26**,1007
decay of ionization, theory, **9**,815
densities, temperatures, radar backscatter, **15**,1387
diffusion, ambipolar, and drift motions, **13**,959; **21**,526
diffusion, thermal. **18**,535
diffusion, upper boundary conditions, **11**,879; **15**,701,825
dissipative structures, Rayleigh-Taylor instability, **39**,1667
diurnal variations, model, **23**,1017; **32**,47
drift waves and field-aligned currents, **30**,581
drifts, fluctuations, D-component, **32**,1327
dynamics of neutral and plasma motions, **15**,671; **17**,97,1097,1269, 1691; **19**,263,1327; **22**,743
effects of E-region electric field, **21**,2227
electrical coupling to E-region, **22**,743; **23**,557; **25**,197
electrons, ions, density, temperature, **11**,587; **12**,915; **13**,1031; **15**,95,1049; **17**,841; **18**,1225, 1489; **19**, 1313; **20**,11,616,1287; **23**,523,935; **29**,171,1367; **35**,887; **37**,1207
electron content, lunar effects, **17**,923; **19**,1349
electron content, satellite signals, **1**,130
electron density, correlation with solar wind, **18**,1832
electron density, O(^1S), O(^1D) yields, **40**,607
equatorial, lattice model, **19**,1185
F-lacuna events, **26**,785; **27**,1293
h'F, correlation with winds, **17**,957; **19**, 1087
h'F, electron density, semi-annual variation, **19**,723
heating, particle effects, **14**,717; **40**,901
heating, photon effects, **18**,1745
high-latitude changes to ULF penetration, **39**,1657
incoherent scatter observations, **40**,355
instability, E×B, **38**,273
ion chemistry, in-situ experiment, **19**,1087; **20**,616
ion transport, **31**,671
ionization troughs, **17**,777,1867
lunar tide effects, theory, **23**,1071
maintenance at night, vertical drifts, **12**,979
median height changes, sunspot cycle, **39**,1607
model, empirical, low magnetic activity, **33**,909
morphology, **20**,233
neutral winds, **23**,401,973; **31**,53
O^+ loss, increased, effects, **40**,1631
pertubations by Pi2 pulsations, **40**,1461
photo-ionization, day, high latitudes, **14**,891
polar, during substorm, **21**,399; **24**,25
polar, model, **26**,559
polarization fields, by neutral winds, **19**,357
production and loss processes, **9**,149; **18**,1181
propagation of MHD waves, **21**,2157
recombination, nightglow 630nm intensity, **9**,133; **10**,29; **11**,45; **16**,1177
scintillations, drift velocities, **23**,560
scintillations, satellite, synopic study, **13**,51
source of metallic ions, **33**,807
spread-F, geomagnetic, solar activity, **2**,133, 150,214; **12**,127; **23**,899; **27**,127,593
spread-F, related to spread-E_s, —bf 33,1081
storm conditions, **9**,95; **22**,237; **24**,69,293; **36**,371; **40**,595
swept-F, sunspot, geomagnetic activity, **22**,1579
thermal balance, **19**,15; **21**,159; **27**,1063; **31**,53
thermal coupling with magnetosphere, **18**,1447
transport, heating, in auroral plasma, **27**,203; **31**,671
triple splitting, ionograms data, **2**,214
Faraday effect, *see* **electrons,**
Faraday factor, changes with K_p, **23**,107
greenhouse effect on electron densities and heights, **38**,945
heating,
ambient electrons by charged particle streams, **15**,873; **40**,901
atmospheric expansion, **22**,925
coriolis force effect, **22**,1031
night-time, **15**,95
parameters in auroral region, **29**,455
polar wind, **22**,1193
thermal structure, relative ion flows, **25**,1085
turbulence, effective conditions, **35**,345

incoherent scatter, see RADAR
ionogram production and analysis, **20**,2029
ions,
auroral, anisotropy, **19**,279
auroral, velocity distribution, **25**,243; **29**,1353
chemistry in D-region, **25**,1135; **29**,735; **30**,1065
chemistry in E and F-regions, experiment, **19**,15
chemistry in stratosphere, **40**,255
clouds, artificial, neutral winds, **19**,1
clouds, artificial, striations in, **18**,1105
clouds, diffusion, **17**,519; **18**,1319; **21**,526,1073
collision frequencies, **37**,211
composition measurements, **5**,81; **8**,179; **9**,175, 179,845; **11**,169; **13**,1,647,1031; **18**,145,559,741, 965; **19**,77,491; **21**,227; **23**,1621
concentrations, altitude profile, **19**,15; **29**,185,195,895
concentrations, B-F-P theory, **25**,743
density, theoretical, **21**,1875
diffusion of H^+, He^+ and O^+, topside, **29**,851
distribution function in auroral E-region, **32**,1061
energetic flux in inverted-V events, **26**,673
exchange, non-magnetic, with solar wind, **27**,242
extra-terrestrial origin, **11**,173
field-aligned flows of H^+ and He^+, **40**,751
H^+, cooling by He collisions, **16**,911
H^+, density, **20**,581; **25**,967
H^+, velocity distributions, **16**,759
H^+, He^+, N^+, O^+, diurnal, seasonal variations, **29**,775
He^+ ion loss processes, **12**,1169; **13**,1125; **26**,255
heating effect in auroral conic generation, **32**,1115
heavy, synchronously trapped, **29**,1045,1169, 1205
ion chemistry, see REACTION DYNAMICS
Joule heating at magnetic equator, **11**,1297
Mg^+, stratospheric chemistry, **29**,479
mass densities from ULF pulsations, **32**,1069
metallic, vertical drift profiles and E_s, **31**,253
N_2^+, twilight production, **13**,529
N^+, atomic, **20**,616
negative, lower stratosphere, **32**,1223
O^+, density, **20**,581; **25**,967; **40**,1631
O_2^+, vibrational distribution, **34**,1241
outflowing on auroral field lines, **30**,715
positive and negative, lower ionosphere, **30**,1295,1307
positive, F-region, night, **13**,1; **21**,43
positive, stratospheric, **30**,101; **32**,1567
ratios yield thermospheric composition, **31**,49
recombination, **21**,367; **30**,1275
ring current deposition, **25**,385; **37**,1432
S^+, ionization by elecron impact, **30**,1269
Si^+, mesospheric chemistry, **29**,895; **30**,499
sifting, **11**,779
stratospheric, composition and height profile, **31**,813,1459; **35**,439; **40**,255
subauroral, drift evolution and signatures, **40**,663
temperatures, **15**,77,123,200,1557; **18**,417,1225; **36**,553; **37**,211
thermal, flow characteristics, **30**,595; **36**,693; **38**,1187
transport, charge exchange and loss, **29**,1215
transport, F-region, **31**,671
transport, turbulent flowing plasma, **32**,949
trapped, geomagnetic and auroral connections, **11**,31,451; **29**,1045,1169,1205
trough, high latitude, location and source, **31**,99; **33**,1375
trough, ion temperature, neutral wind effect, **28**,895
trough, number density, **20**,1593
trough, mid latitude, temperature structure, **37**,1453
trough, supersonic wind, **20**,1923
velocity distribution, model, **22**,1; **30**,1137; **31**,889
water-cluster, quiet daytime, **25**,275
ionization mechanisms,
auroral, enhancement during substorm, **23**,619,1321
bremsstrahlung from auroral X-rays, **12**,1093
critical ionization velocity, **35**,345
effect on characteristics of meteor train echoes, **23**,1261; **24**,605,606
electron impact, sulphur ions, **30**,1269
general processes, **11**,1359,1459; **23**,1261
neutralization rates, **24**,697
nitrogen, **2**,157; **20**,616
oxygen, **9**,175
troughs, F-region, **17**,777,1867
irregularities,
airglow (OI 630.0nm) interpretation, **22**,494
amplification, spatial resonance, **21**,297
associated radio aurora, due to ion-acoustic waves, **16**,449
associated scintillations, **16**,1475; **17**,585,1557; **18**,1785; **19**,1588
diurnal, seasonal and magnetic dependence, **20**,957,965
generated by gravity waves, **16**,273; **17**,749
global morphology, **24**,873
magnetospheric, consequences, **12**,127; **13**,1255
plasma mixing by large-scale drifts, **38**,961
spectral characteristics, **38**,79
structure, associated with plasmapause, **22**,1289
VHF signal fluctuations, **22**,1331
lens effect on radio waves to moon, **16**,999
model for boundary regions, **21**,507
model, related airglow red line emission, **38**,1243
model, relate delectric fields, currents, plasma, **24**,841

Pedersen conductivity, neutral gas acceleration, **13**,737
radio wave propagation, model, rocket data, **2**,110; **5**,80
reaction rates, laboratory and in-situ, **14**,33
scintillations, see RADIO WAVES
SIDs, characteristics and listed observations, **12**,419
slab thickness, mid-latitude, **21**,1775
solar eclipse effects, **21**,1799
soviet investigations, early, rockets and satellites, **5**,223; **8**,183; **9**,391
structure, vertical, measurements, **11**,281
temperatures,
diurnal variation, **15**,331,944
electrons, ions, *see above*
topside,
auroral absorption, substorm, **20**,1375
composition and temperature, **23**,1103
density of O^{2+} ions, **18**,559
diffusion and heat flow equations, processes, **25**,907; **26**,189
diffusion coefficients for H^+, He^+ and O^+ ions, **29**,851
depletion trough, location and source, **31**,99
enhancement and depletion during magnetic storm, **16**,653; **20**,627; **24**,1081
equivalent thickness, Faraday records, **11**,1057,1431
ion composition model, **16**,1405; **25**,967
ion flow characteristics, **30**,595; **39**,1209; **40**,751
ion transition heights, **24**,229
morphology, electron inhomogeneities, **14**,313; **20**,233; **24**,873
over Arecibo, **23**,315; **28**,47
proton cyclotron frequency phenomena, **22**,793
scale height variations, **18**,41; **20**,2015
supersonic plasma flow, **20**,73
transient response to precipitation, **25**,773; **38**,973
wave-particle interactions, **20**,409
winds, *see* WINDS
winter anomaly, absorption and ion chemistry, **25**,1135

JEAN'S ESCAPE RATE
see ATMOSPHERE, TERRESTRIAL, dynamics,

JUPITER
airglow, day, extreme UV, **19**,327; **29**,79
atmospheric abundances, intensified solar telescope, **15**,1211
atmospheric circulation, **14**,669; **20**,607
atmospheric colour changes, **28**,1055
atmospheric dynamics, review, **21**,623
atmosphere, structure, **21**,1587
atmospheric superrotation, **31**,1339
chorus related electrostatic bursts, **39**,721
continuous emission, 21.2cm, **14**,15
corotation lag, magnetospheric energetics, **37**,1393
decametric emission,
controlling factors, **14**,1291
excitation by cyclotron radiation, **14**,469; **22**,687
location of sources, **27**,963
modulation by satellites, **13**,997; **14**,173,347,741; **15**,1203; **19**,1297
passage through IMF sector boundary, **31**,129
polarization, **22**,1491
power-frequency spectrum, **14**,347
solar activity, possible correlation, **16**,1147; **20**,2051; **26**,1193
theory, **18**,217
turbulence in the IMF, **29**,783
dust,
origin of rings, **28**,1101
physical processes, **28**,1087
time variations, **28**,1111
dynamo region and equatorial electrojet, **31**,633
equatorial anomalous features, **34**,117
equatorial current features, **33**,987
equatorial jet, dynamics, **23**,1223; **32**,1053
heat source, thermospheric, soft electrons, **25**,817
Io,
decametric emission, controlled, **21**,1431
deposition of Jovian sodium, **27**,419
interaction with magnetosphere, **21**,1399
mass pick-up in plasma flow, **32**,1079
model for Na and H gas clouds, **25**,415
particle acceleration by Alfvén waves, **40**,1499
plasma-torus source, **28**,781; **38**,995
structure of torus, sulphur ions, **30**,855
visible spectrum, new features, **27**,215
wave propagation in flux tubes, **21**,1417
ionosphere,
proton collection, **22**,143
proton-methane reaction, **23**,377
structure and variations, **21**,751,1389
UVS occultation experiment, **30**,151
Voyager data modelled, **39**,1715
magnetic axis, determination, **16**,445
magnetosphere,
Birkeland currents, corotating, **28**,781
bow shock, theoretical model, **24**,661
current sheet, scale height, **32**,1531
diffusion, induced conductivity, **36**,145
electric field, dawn-to-dusk, **32**,179
energetics from corotation lag, **37**,1393
hydrogen bulge, co-rotating convection, **29**,215
interaction with solar wind, **22**,1501
model, effects of rotation, **26**,311
particle structure, **20**,1345; **21**,1389
particles, energetic, acceleration, **24**,657, 995,1207; **25**,887
plasma, radial outward flow, **35**,119
plasma sheet, theory, **25**,673
plasmasphere, thermal structure, **26**,745
radio emissions, **24**,657
rotation and toroidal field, **34**,575
radiation belt, source and structure, **21**,1593

rotation period, decametric emissions, **15**,1687; **19**,391
rotational effects on magnetospheric plasma, **15**,381
sodium emission, interpretation of data, **25**,603
solar wind characteristics near orbit, **17**,595
spectra, H_β profile, **13**,1164
spectral index, radiation 178 to 610 Hz, **13**,889
spots,
light, dark, equatorial, **26**,335; **27**,1127
north equatorial belt, measurements, **16**,1061
red, characteristic movements, **17**,1573; **23**,805
red, oscillation, Mercury coincidence, **25**,890
waves, Alfvén, along Io's flux tube, **21**,1417

LABORATORY EXPERIMENTS
afterglows,
nitrogen, electron-ion temperature dependence, **13**,667
N_2 and (N_2+O_2), far UV spectroscopy, **1**,7,40
oxygen-nitrogen ion-molecule reactions, **13**,219, 823,911; **17**,1759
$O^+ + O_2 \rightarrow O_2^+ + O$, reaction rate, **13**,579
beam experiments,
atomic, study of space-flight problems, **3**,162
electron, from spacecraft, *see* SEEDING
electron excitation of $N_2^+(A^2\pi_u)$, **17**,1941
electron paramagnetic resonance, atom concentrations, **3**,194
interaction of solar plasma stream and geomagnetic field, **12**,1187
Lozier electron impact apparatus, molecular studies, **3**,187
molecular, high temperature, **3**,253
plasma discharge, from rockets, **30**,347
proton, spreading by charge exchange in atmosphere, **20**,292
condensation and sublimation of CO_2 and H_2O, **16**,495
helium ion loss processes, **12**,1169
photochemistry, simulated early atmosphere, organic compounds, **2**,79
plasma sheath,
flame generation, em wave propagation, **6**,172
hypersonic projectiles, microwave investigation, **6**,186,196
telecommunications during re-entry, **6**,207
wind tunnel, em wave propagation, **6**,180
self absorption, transition probability for $O(^1S)$, **17**,1297
spectroscopy,
discharge lamp for oxygen emissions, **27**,1209
emission line widths, **35**,1471
excitation of $O(^1S)$, nitrogen afterglow, **3**,169
photolysis of NO in far UV, **1**,333
recombination of O, flash spectra of Schumann-Runge system, **3**,175
rotationally resolved O_2 UV afterglow, **34**,971
temperature of shock-heated oxygen, **3**,158

LIDAR
density, temperature, sodium, **26**,27,511
density, potassium, **26**,27
gravity waves, *see* WAVES
SEASAT laser range data, atmospheric density, **37**,1409
sodium, mesospheric, **30**,169; **37**,657
stratospheric gravity wave spectra, **39**,1541

LITHIUM
motion of test ions, AMPTE, **33**,685
origin in upper atmosphere, **9**,89

MAGNETOHYDRODYNAMICS
bi-Maxwellian transport equations for polar wind, **37**,85
bipolar magnetic flux model, **32**,213
Chapman-Ferraro model, **10**,233; **12**,573; **16**,1023; **37**,1037
convection, airglow connections, **26**,339
convection, changes in ionospheric electron content, **19**,503
convection, effect of finite parallel conductivity, **33**,493
convection, low level power, **30**,1057
convection, plasma flow, plasma sheet, **38**,355
convection, polar arcs, northward IMF, **36**,1317
convective amplification, hybrid waves, **33**,1331
coupling, solar wind to magnetosphere,
bounce resonance, trapped particles and pulsations, **17**,349
characterisation of geomagnetic storms, **12**,573; **28**,495,823
coupling function, **38**,627
discontinuity interaction, **38**,841
electric fields, currents and plasma, **24**,841; **29**,425,915,1151; **35**,903
energy transfer through reconnections, **33**,1091
field variations in IMF, **22**,1117; **34**,987
flare activity, auroral magnetic effects, **34**,1169
flux transfer events, **36**,503; **37**,1461
ionization irregularities, radio propagation pecularities, **13**,1255; **16**,999
injection mechanism for plasma, **12**,209; **16**,971; **20**,973
interconnection of field lines, magnetosphere to magnetosheath, **30**,331; **40**,879
interplanetary shock wave, storm commencement, **13**,675
ionospheric flows, IMF effect, **36**,471; **40**,1071
MHD filiaments, different to solar wind plasmoids, **29**,843
particle injection, **20**,1051,2113; **30**,331
particle-wave interactions in neutral sheet, **29**,399
penetration of discontinuity through bow shock, **21**,499
power transfer, storm effects, **38**,765

Primdahl-Spangslev hypothesis, **34**,745,753
scaling relations, **30**,359
solar protons, field fluctuations, **20**,1979; **21**,971
solar wind interaction theory, **22**,1075
storm theory, **13**,281,297,675
two-fluid model, **40**,131
viscous interaction, **12**,45; **15**,515
cyclotron radiation,
excitation by electron stream in plasma, **14**,335
forward sub-luminous mode, Jupiter's decametric emissions, **14**,469
instability and VLF emissions, **19**,567
spectra of solar noise storms, **14**,1139
decay of plane-stratified F_2 ionization, **9**,815
diffusion, pitch angle, Fokker-Planck equations, **18**,123
dynamics,
adiabatic motion, electron bunches, **31**,659
charged particle motion, **16**,395; **19**,1209; **24**,515; **34**,631
compression and expansion of field, **22**,939
convection patterns in plasmasphere, **25**,303
convection reversal, morning sector, **32**,837
convection stratification, ionospheric effects, **32**,127; **34**,315,353
drift of electromagnetic components, **34**,645
expansion of injected electron beam, **22**,633
filamentary elements, penetration of, **25**,887
flapping motion of tail plasma sheet, **24**,147
flow, collisionless, parameters, **25**,973
flow, hydrodynamic, with mass loading, **34**,403
flow, planar stagnation-point, velocity shear, **38**,411
flow topology in one-fluid plasma, **30**,701
flow towards Earth, from thinning plasma sheet, **25**,703
ion acceleration in current sheet, **38**,751
ion cloud motion, **20**,25
ion reflection at collisionless shock, **38**,419
open flux tube motion, dayside, **37**,1461
open flux tubes, particle trapping, **38**,1343
particle reflection from shock wave, **27**,193
particle motion, non-adiabatic, in current sheet, **33**,847
particle stream flow, kinematics, **33**,831
plasma motions, processes, detection, **12**,1147; **13**,921; **21**,187,1855; **25**,1027,1145; **26**,81
proton bursts in magnetotail, **32**,313
rotation, toroidal field, effect on magnetosphere, **34**,575
storm, energy output rate, **40**,581
temperature anisotropy instabilities, **28**,169
turbulence, spectral energy density, **25**,1027
velocity filter effect, **34**,197
vorticity, **22**,1703; **31**,1099,1117
waves, ionosphere, electrostatic, **17**,61
waves, magnetopause, reflection, refraction, **21**,2213
dynamo action, plasma motions, **12**,1147; **23**,817; **30**,367,371,537
eigenvalues, VLF, in Earth-ionosphere waveguide, **40**,1363
electron flux, effect of sudden compression, **21**,1345
electron plasma oscillations, detection, **13**,921
electron trapping, magnetic mirror, **20**,747
electrostatic waves in ionosphere, resonance noise, **17**,61
energization of magnetospheric plasma, **10**,239; **14**,223,1207
Faraday effect, *see* IONOSPHERE
fields, electric, parallel. **21**,741
field induction in rotating conductor, **17**,685
field lines, evolution and reconnection, **21**,1151; **40**,63
flux transfer event, the stastical cusp, **40**,1251
flux tube interchange, irregularities, **27**,1351
geomagnetic storms and aurora, **9**,947; **12**,660; **13**,281,297
hydromagnetic noise, field-line merging, **20**,1651,1786
instability,
cause of auroral arc, **39**,395
curvature-driven drift mirror, **36**,383
heat conducting solar wind plasma, **36**,775
ion-acoustic, dispersion relation, **19**,1188
ion-acoustic, double layer, **36**,1009
ion-acoustic, magnetotail noise, **37**,145
ion-acoustic, radio aurorae, **16**,449
ion-acoustic, scattering of em waves, **35**,295; **36**,1009
ion-cyclotron, **20**,1173; **23**,123; **25**,643; **27**,691; **32**,219,1371,1393; **35**,51; **37**,1,1157; **38**,507,709
Kelvin-Helmholtz, at boundary, **13**,131; **20**,1; **27**,881; **29**,359,1119; **30**,677; **31**,821; **32**,1169, 1335; **34**,1223; **36**,687; **38**,1577
low-frequency, neutral induced, **40**,1197
non-resonant, quasilinear theory, **40**,1479
proton-cyclotron, **36**,207
magnetic bottle and shock, solar flare, **22**,493
magnetic field interaction with cold plasma, **17**,333
magnetohydrodynamic generation process, **32**,757
oscillations, and stability of shell distributions, **25**,981
outflow of thermal protons from ionosphere, **25**,291
particle streaming in solar corona, **18**,1213
plasma, *see* PLASMA
pulsations,
absorption in cold plasmas, **38**,1017
amplitude and phase at ground, damping effect, **32**,619
associated storm commencements, **38**,603
asymmetric spectrum, **21**,2193
bounce resonance with trapped particles, **17**,349
CNA, waves at conjugate stations, **36**,1255
continuous, high resolution study, **27**,1371

correlation, in solar wind and on ground, **26**,547; **28**,535
correlation with auroral optical pulsations, **32**,735; **40**,1303
correlation with electric fields, **23**,311
damped, cause of hydromagnetic oscillations, **18**,407; **26**,201
data analysis technique, **30**,1249
dayside events near plasmapause, **34**,155
diminishing period, ground and satellite observations, **28**,387
disturbances in conjugate areas, onset time interval, **32**,819
giant, in plasmasphere, **33**,1155
IMF effects, ground based, solar wind data, **31**,559
indices, **20**,849
inferred from whistler-mode signals, **25**,957
IPDP events, radar electric fields, **36**,1103
IPDP events, simultaneous sectors, **35**,827
IPRP events, boundary layer effects, **30**,129
IPRP events, polar cusp variations, **30**,113
irregular, decreasing period, trapped particle flux, **15**,1239
latitude phase effect, **24**,612; **27**,617,679
long lived, in boundary layer, **32**,1205
low frequency, non-linear theory, **27**,249
low frequency, properties and quantitative data, **29**,1119; **33**,1251
micro-, and VLF emissions, **15**,1427; **16**,137,863
micro-, cyclotron amplification, **17**,2009
micro-, equatorial study, **18**,229
micro-, global events, conjugate study, **37**,253
micro-, hydromagnetic emissions, **18**,291; **23**,611
micro-, latitude-period relationship, **17**,1937; **19**,897; **37**,767,859
micro-, period depending on magnetospheric size, **17**,1432,1849,1937
micro-, polarization of, **15**,1361
micro-, propagation in magnetosphere, **16**,111,863
modulation 'pearls', evolution, **20**,1817; **31**,859
origin, trapped charged particles, **11**,869
orthogonal curvilinear coordinates, **27**,895
Pc1, **17**,2009; **18**,395; **19**,165; **20**,637, 1661,1786,1883; **22**,801; **23**,431,611,993; **25**,473,481,487; **26**,507; **27**,151,809; **28**,61,739; **29**,715; **31**,295,473,859,931; **32**,935; **33**,271; **34**,537; **35**,71,91,879,1381; **37**,39; **39**,709,1657; **40**,139,1081,1353
Pc1-2, **24**,673; **28**,1; **30**,1229; **33**,53,777, 993,1277; **39**,1473
Pc2-4, **23**,311
Pc3, **34**,519,1329; **35**,1437; **36**,641; **39**,1017; **40**,1399
Pc3-4, **19**,715; **24**,79; **25**,689; **33**,239,387,1073; **36**,733; **37**,1079; **39**,559; **40**,495
Pc3-5, **24**,465; **27**,79; **39**,975
Pc4, **26**,955; **27**,821; **33**,1369; **38**,269
Pc5, **23**,733; **24**,921; **26**,1,473,1077; **27**,131, 631,1123; **28**,213,713,727,1035; **29**,293,1159; **31**,459,473,573,931,1279; **32**,551; **33**,365; **34**,571; **35**,429; **38**,1315,1517; **39**,1239; **40**,797
Pc_L, new index of activity, **25**,15
Pg, auroral zone observations, **27**,63
Pg, magnetic and optical signatures, **38**,1443; **40**,953
Pi1, associated auroral pulsations, **38**,149
Pi1, geotail field-line merging, **20**,1651
Pi2, **17**,497; **19**,137; **21**,532,721,731,831,1273; **22**,1461,1519; **23**,693,1129,1581; **24**,573,1025; **25**,663; **28**,9,475,875,907; **29**,225; **30**,1239; **31**,143,435; **32**,1361; **33**,351; **34**,1259; **35**,799; **37**,1367; **38**,589; **39**,983,1271; **40**,495,1461
Pi3, associated with substorms, **29**,539
Ps6, characteristics, magnetotail convection, **34**,319; **39**,785
PP, pearl-type Pc1, **20**,1817; **22**,309; **27**,165
period, latitude-dependent, **12**,137; **38**,85
period, long, **22**,1157
power spectrum analysis in storm, **22**,1711 propagation mode in magnetosphere, **13**,761; **18**,299
propagation, poleward, near cusp, **37**,775
quasiperiodic, low altitude cusp, **35**,1553
source induced vertical components, **26**,715
spatial distribution from eigenmodes, **20**,1875
statistics of plasmapause relationship, **23**,1169,1195,1551
sudden commencement associations, **15**,573; **20**,1499
time lag to cosmic noise absorption, **19**,959
toroidal mode eigenfrequency, **17**,1281
vicinity of bow shock, **38**,1069
waveguide propagation in ducts, **35**,1093 whistler mode, magnetospheric plasma study, **13**,773; **15**,799,1427; **18**,1799

resonances,
absorption of fast waves in cold plasma, **38**,1017
bounce, growth phase of waves, **25**,573
cavity modes, **37**,407
coupled poloidal-toroidal modes, **19**,1012
cyclotron, amplification of micropulsations, **17**,13,2009
cyclotron, non-parallel propagation, **18**,395
electron instability, waves near plasmapause, **26**,195
field lines, **22**,483; **24**,561; **33**,253; **37**,407; **38**,1517,1573
interaction, Alfvén wave and trapped particles, **27**,503
interaction, electrostatic wave and current sheet electrons, **20**,1205
interaction of ion sound wave traps em wave, **18**,1813

plasma, magnetospheric radio emissions, **19**,813
source regions, ground magnetometer data, **30**,1199
structure for azimuthal asymmetry, **35**,1193
synchrotron radiation from trapped electrons, **17**,389
ULF,
amplitude modulation in signatures, **40**,965
correlation with particle precipitation, **26**,833
damping, joule dissipation, **32**,1463
decay rates of transients, **33**,607
diurnal period variations, **32**,727
eigenperiods in auroral plasma trough, **32**,1069; **36**,185
foreshock boundary, **40**,1203
generation by resonant electron instability, **26**,195
growth rate in magnetosphere, **25**,573
ion-cyclotron instability, **23**,123
ion-cyclotron, optical detection, **25**,643
ion-cyclotron, refractive index, attenuation, **20**,1173
ionosphere-magnetosphere coupling, **30**,285; **36**,801
ionospheric Doppler oscillations, **38**,1581
non-linear distortion, **39**,1119
phase variations, **30**,399
power measurements, **37**,1385
pulsation spectra correlated with sudden impulses, **34**,543
spatial and temporal structure, **33**,159; **40**,1215
thermal electron collision model, **38**,953
transients, associated ground magnetic effects, **34**,1073
waves,
Alfvén, anomalous resistivity region, **31**,267
Alfvén, auroral field-aligned currents, **31**,579; **32**,1387; **36**,417
Alfvén, auroral particle generation, **37**,749
Alfvén, axisymmetric model, **27**,79
Alfvén, cometary bow shock, **39**,1045
Alfvén, impulse and Pi2 pulsations, **22**,1519
Alfvén, induced in ionosphere and surface, **39**,529,547
Alfvén, interaction with trapped particles, **27**,503
Alfvén, magnetosonic, characteristics, observations, **13**,485; **30**,199; **32**,481; **36**,949; **37**,567,579; **38**,823; **39**,1097
Alfvén, oscilations, monochromatic, nonstationary, **37**,1095,1109
Alfvén, poloidal spatial structure, **38**,1231
Alfvén, propagation in ionosphere, magnetosphere, **33**,127,471, 1103
Alfvén, reflection by non-uniform ionosphere, **31**,107; **32**,1343
Alfvén, resonance effects, **36**,411
Alfvén, saturation in ring current region, **40**,477
Alfvén, scattering by drift waves in plasma, **36**,499
Alfvén, spectrum, plasma diagnostics, **37**,1011
Alfvén, standing wave structure, **38**,665
Alfvén, toroidal mode, **27**,939; **36**,1461
Alfvén, transmission at bow shock, **17**,1029; **30**,1127; **35**,405
Alfvén, turbulence, **21**,692; **37**,761
Alfvén, vortex turbulence spectrum, **40**,1235
Alfvén, waveguide mechanism above F-layer, **38**,1075; **40**,139
amplification in ionosphere, **14**,1077
amplification through bow shock, **18**,1,1143
attenuation in ionosphere, **9**,771
auroral generation, **16**,993,1297,1453
auroral kilometer radiation, **39**,1223
auroral LHR noise, **35**,127
cavity, Earth-ionosphere, excitation, **16**,831
coupled wave interaction in cold plasma, **21**,391; **34**,1189
coupling to magnetosphere, Poynting flux, **35**,1181
depolarization at rough surface, **14**,563; **15**,1337
electrostatic and electromagnetic, **24**,1097
electrostatic, dusty plasma, **38**,543,1143; **40**,1,973
electrostatic, model approximation, **36**,123
electrostatic, beam generated, **34**,851
electrostatic, dispersion relations, **32**,1135
electrostatic, electron interaction in current sheet, **20**,1205
electrostatic, excitation in cold current sheet, **31**,285
electrostatic ion loss-cone waves, **23**,1337
electrostatic, ion velocity distribution, **35**,867
electrostatic noise, **32**,1201; **37**,145; **38**,695
electrostatic shocks, paired in polar region, **38**,263
electrostatic, ULF modulated, **34**,845
equatorial activity at 5 to $8R_E$, **38**,1335
evolution of, in bow shock, **38**,1069
exact frequencies , **29**,1251
Farley-Buneman, unstable, parallel propagation effects, **30**,315
growth phase, bounce resonances, **25**,573
hybrid, convective amplification, **33**,1331; **40**,473,477
hydromagnetic noise, **20**,1651,1786
hydromagnetic waves, **12**,227; **14**,223; **18**,407; **24**,907,915,1065,1195; **25**,549,765; **26**,555,777; **27**,211; **28**,789; **30**,1209; **32**,1371,1393,1497; **34**,371
infrasonic, auroral, radar investigation, **24**,1155
interplanetary shock, **16**,1483
ion-acoustic, dispersion relation, **19**,1188
ion-acoustic, double layer, **36**,1009; **39**,1343; **40**,1055

ion-acoustic, dusty plasma, **38**,543; **40**,1,973
ion-acoustic, magnetotail noise, **37**,145
ion-acoustic, radio aurorae, **16**,449
ion-acoustic, scattering of em waves, **35**,295; **36**,1009
ion-cyclotron, auroral, optical detection, **25**,643
ion-cyclotron, bands in VLF saucers, **38**,507
ion-cyclotron instability, **23**,123; **27**,691; **32**,219; **35**,51; **37**,1
ion-cyclotron, interaction with energetic particles, **32**,1371,1393
ion-cyclotron, interaction with thermal electrons, **38**,709
ion-cyclotron, refractive index, attenuation, **20**,1173
ion trough supersonic shocks, **20**,1923
magnetosheath lion roars, stability analysis, **31**,1165
magnetosonic, excitation of, **23**,279; **25**,833; **33**,1029
magnetosonic, interaction with plasmasphere, **39**,859
mode coupling by Coriolis force, **24**,101
neutral sheet, **34**,1253
oscillation modes in current sheet, **23**,751; **26**,1141
oscillations, electric field, **26**,555
oscillations, forced, **34**,863
oscillations, long period, modulated particle fluxes, **26**,1149
oscillations, magnetosphere-solar wind interaction, **18**,407
oscillations, stability of shell distributions, **25**,981
plasma, non-linear interaction, **20**,711
propagation, generation of Pc1 events, **19**,165
propagation in magnetic field tubes, **29**,609; **30**,687
propagation in plasma, **1**,319; **5**,288,292; **6**,100,105; **9**,793; **17**,247
R-wave cut-off, relativistic theory, **40**,433
radiation damping in current sheet, **19**,635
radio, magnetospheric, plasma resonances, **19**,813
reflection and transmission at lower ionosphere, **17**,509
reflection from stratified magnetoplasma, **15**,1059
resonance interaction with trapped particles, **15**,557; **17**,349,389
scattering, induced, **22**,95
shock, associated with solar flare, **22**,493
shock, interplanetary, and transients, **36**,301
shock parameters, determination, **32**,641
short period, duct propagation, **35**,91
solar dependence, **39**,879
surface, on plasmasheet boundary, **33**,1313
toroidal, **16**,1305; **18**,315; **32**,1119
twisted, magnetosphere-ionosphere circuit, **18**,749
wave-particle interaction in ULF range, **30**,1219; **33**,385

MAGNETOSPHERE
anomalies and disturbances, theories, **12**,553
asymmetry, auroral and magnetic disturbance distribution, **14**,121; **16**,47; **29**,79
auroral oval and substorm correlation, **14**,587
Birkeland currents, geomagnetic modelling, **39**,641
boundary layer,
adjacent flows and fields, **16**,971
energy transfer processes, **33**,891
exploration, **40**,1431
heating of thermal electrons, **32**,657
influx of charged particles at cusps, **17**,339; **28**,487
Kelvin-Helmholtz instability, *see* MHD
location, period of micropulsations, **17**,1849
pertubations in magnetic field, **31**,1237
plasma as source of auroral arcs, **33**,1389
relationship to IPRP events, **30**,129
shape calculations, **32**,1029
signature from precipitation electrons, **36**,1219
signature within flux transfer events, **35**,871
size, effect on micropulsation periods, **17**,1432
stability, **13**,131; **15**,997; **16**,587,953
velocity shear instability, **28**,789
bow shock,
acceleration processes, ambient protons, **31**,689
amplification of hydromagnetic waves, **17**,1029; **18**,1,1143; **24**,261
comparison with Mars, Phobos mission, **39**,99
diffusion of solar protons, **21**,971
electrical conductivity, **17**,425
evolution of MHD waves, **38**,1069
IMF fluctuations, **35**,1419
origin of energetic protons, **27**,365
orientation and shape, **27**,1151
penetration by solar wind discontinuity, **21**,499; **25**,657
solar wind structure, **24**,617,621
structure, laboratory, satellite results, **31**,615
substorm onset for low mach numbers, **19**,1519
cavity, Pc1 pulsations, **35**,879
cleft, dayside, photometric observations, **28**,149; **29**,321
cleft, electron precipitation energy, **24**,937; **25**,1161
configuration change, current disruption, **38**,1361
cosmic ray cut-off, screening, **13**,753; **16**,1381; **17**,1173
coupling, thermal, with F region **18**,1447
current sheet,
adiabatic solutions, **27**,265
electromagnetic noise, **17**,1285
electrostatic wave, interaction with electrons, **20**,1205; **31**,285

equilibrium structure, pressure anisotropies, **26**,1037
heliospheric, no neutral line, **40**,105
heliospheric, solar wind interaction, **39**,1123
ion dynamics, in tail, **31**,235; **33**,773,847
model, magnetotail effects, **22**,1641; **37**,5
model, one dimensional, **26**,539
model, Speiser, **20**,1555
particle scattering, non-adiabatic, **33**,1433
quasi-neutral, ion acceleration, **38**,751
stress balance, asymmetric plasma, **35**,467
structure, **36**,105
tearing structure, non-linear, indications, **27**,351
wave damping by radiation, **17**,1291
wave energy ducting, **23**,751
cusp, dayside, location variations, **25**,1167; **29**,317; **30**,113
cusp, dayside, plasma properties, **26**,993; **27**,1479
dayside, disturbed, origin of hot ions, **31**,173
discontinuity, penetration through bow shock, **36**,499
discontinuity, tangential, particle trapping, **36**,1477
Earth's paleomagnetospheric past, **26**,413
electric fields, **37**,899
electron concentrations above auroral oval, **38**,1031
electron distributions, models, **40**,671
electron islands and auroral absorption, **15**,917
electron plasma oscillations, detection, **13**,921
erosion, due to field aligned currents, **23**,1257
disturbance, obstacle in plasma flow, **15**,155, 463,1479,1489,1847
dynamics, magnetic storm applications, **14**,947
geomagnetic cavity and van Allen belts, **15**,495
geomagnetic lobes, energetic ions, **39**,761
geometry, dependence on IMF, **29**,803,1809
Harang discontinuity, driving forces, **36**,225
Harang discontinuity, substorm injection boundary, **25**,1119
imaging of structure in solar EUV light, **37**,379
interaction with solar wind, see MHD
magnetic clouds, **36**,1485,1489,1495
magnetopause,
current system, surface geomagnetic variations, **18**,1471
dayside, open flux tube motion, **37**,1461
electrostatic field, magnetosphere-ionosphere circuit, **18**,749
interaction with hydromagnetic wave, **18**,1,349
interaction with solar wind, **26**,229
Kelvin-Helmholtz instability, **13**,131; **20**,1; **27**,881; **29**,359,1119
momentum transfer from IMF, **37**,1347
motions, pressure driven, ground response, **37**,589
particle bursts, spacecraft data, **28**,487
plasma flow at dawn, **28**,1163
position, dependence on IMF, **22**,1443; **25**,657
reconnections, **40**,879
rotational discontinuity, Alfven waves, **30**,1127
shape, magnetotail-neutral point height ratio, **30**,711
structure, **17**,333; **18**,239; **27**,1137; **38**,437
tangential discontinuity, electron trapping, **35**,483
waves at lunar distance, **18**,239
magnetosheath,
cold ions, measurements, **33**,675
magnetic field, steady state, **30**,473
penetration by solar plasma, **21**,499,1191,1497; **23**,945,1445; **25**,1111; **27**,867; **32**,745; **33**,1109; **37**,1227
surface shape, simulated tilted dipole, **21**,485
turbulence, solar wind fluctuations, **18**,1143
variations in fields, **17**,1803; **18**,1203; **33**,1327
magnetotail,
adiabatic plasma convection, **26**,1185
anomalous resistivity, **26**,1033
auroral acceleration phenomena, **28**,459
cislunar region, **35**,1347
configuration changes, plasma sheet thinning, **27**,103
conductivity theory, **18**,613
current configuration, substorm onset, **39**,833
current-free lobe model, **38**,255
current, interaction with ionosphere, **21**,329
current, near geomagnetic field, **22**,609
current sheet model, implications, **22**,1641; **23**,1,751; **37**,5
electric field, potential and vortex parts, **39**,563
electron bursts, radio absorption events, **16**,567; **24**,855
energy related to substorm intensity, **24**,223
field-line merging, **20**,1651,1786; **27**,1087
ISEE, review of results, **34**,931
length, from magnetospheric convection study, **31**,885
lobe characteristics, **35**,285,467
magnetic field and plasma, **20**,2057; **21**,528; **23**,1119
magnetic B_y field distribution, **27**,769
magnetic storm theory, **13**,281; **17**,1795
natural resonance eigen-periods, **18**,1381
near Earth and distant, simultaneous storm data, **35**,209
near the neutral sheet, **18**,1845; **20**,1651; **23**,723
neutral line signatures, **24**,855
pitch angle distribution of energetic ions, **38**,851
plasma sheet oscillations, **24**,147
plasma sheet, steady state, **40**,27
reconnection layer, structure, **38**,437
reconnections and substorms, **35**,227,405, 451,727,1199
shape and field , effect of neutral sheet currents, **17**,233; **32**,313

solar particle injection, **20**,1051; **23**,27
solar wind phenomena, structure and length, **39**,1039
structure , effect of IMF, **28**,757
supplementation, magnetospheric shrinkage, **23**,1257
theory of, self-consistent, **18**,1349
viscous drag, dynamic action, **27**,1087
models,
Choe-Beard, **25**,457
boundaries for particle loss and trapping, **30**,999
independent physical parameters, **29**,1
interpretation of satellite data, **30**,985
magnetosphere around planets, **29**,1101
magnetotail, current-free lobes, **38**,255
structural, **13**,363; **18**,699
neutral points, **15**,787
neutral sheet,
electron counts, **21**,2013
hydromagnetic waves, **34**,1253
model, **17**,233,665
particle motion and curents, **21**,2027
structure and disruption of field lines, **15**,733; **19**,525; **20**,1651; **23**,723
wave-particle interactions, **29**,399
particle influx pertubations, **13**,63; **20**,973, 1051,1979,2113
physics of the magnetosphere and aurora, **22**,885
plasmapause,
association with Pi2 power spectra, **23**,1581
associated geomagnetic pulsations, **23**,1169,1195,1551; **33**,777; **34**,155
associated ionospheric irregularities, **22**,1289
associated ionospheric troughs **24**,1177
diffuse aurora, **24**,299
discontinuity and injection events, **30**,483
effect on topside composition, **16**,1405: **17**,447
evidence for existence, **19**,897
formation, **22**,757; **29**,479
interaction with IMF, **25**,657; **26**,651
magnetosonic waves, excitation, **23**,279; **26**,195; **36**,733
motion, from whistler study, **22**,1139
non-thermal continuum radiation, **30**,399,657
plasma density profile, **30**,399
position and mid-latitude trough, **22**,1089
resonant electron instability, **26**,195
whistler-mode wave propagation, **39**,425
plasmasheet,
absence at lunar distance, **20**,429
boundary, surface waves, **32**,1547
convection, electric field properties, **30**,261
convection, formation of magnetotail, **30**,1007; **36**,353
coupling, magnetosphere-ionosphere, **40**,1071
drift instabilities, **26**,985
electrons, energetic, source region, **27**,1479; **30**,261; **35**,991
energization, non-adiabatic processes, **29**,1325
field aligned currents, **22**,1485; **35**,991
flux transfer events, **40**,1551
magnetic field fluctuations, **35**,289
magnetospheric radiation belt, **16**,703
particle acceleration, **37**,503
particle bursts, velocity dispersion, **36**,1181
steady-state, in distant magnetotail, **40**,27
structure, **19**,1275; **39**,1083
substorm onset, ion bursts at lunar distance, **19**,1413; **28**,363,757
temperature variations during substorms, **29**,837
thinning, **24**,849; **25**,703; **27**,103; **36**,1285
variations during geomagnetic storms, **19**,1339
plasmasphere,
cavity resonance, Pi2 pulsations, **37**,1367
contraction during storm, **22**,223
convection electric field, **23**,1045
convection patterns, ground observations, **27**,643
coupling with ionosphere, **32**,585
deformations, dynamical interpretation, **26**,661
density distributions for diffusion equilibrium, **31**,1315
electron density, whistler group delays, **39**,1059
electron-wave interactions, **38**,709
formation in rotating magnetic field, **32**,365
He^+ and H^+ distributions, **16**,899; **32**,611
ion flows, dayside, nightside, **36**,693
ionospheric coupling fluxes, **26**,171; **37**,283
magnetic storm effects, **39**,1069
photoelectrons, conjugate, field-tube distribution, **27**,557,567
plasma distribution, from pulsations and magnetic bays, **17**,2017
plasma enhancements in auroral oval, **32**,561
plasma, hot, interaction with cold ionosphere, **19**,749
plasma, magnetic field interaction, **37**,987
plasma streaming, **19**,107,651; **24**,689
plasma, tail-like extrusion, **19**,869; **20**,2057
plasma, thermal, **20**,707; **22**,79; **24**,765
proton precipitation, **23**,1045,1103,1337; **24**,783; **25**,385; **26**,281,727,753; **29**,1273,1281
response to quiet magnetic conditions, **25**,303
ring current interaction, **40**,859
shock waves, tangential discontinuities, **24**,617,621,1043
structure, detected by whistlers, **24**,987
statistical cusp, flux transfer event, **40**,1251
transition region, steady state field, **15**,239
wake, plasma characteristics in, **17**,321

MARS

see also ATMOSPHERE, PLANETARY
albedo and surface temperatures, **39**,267
accretion of ions from solar wind, **40**,121,131
atmospheric properties,
aerosol characteristics, photometers, **39**,199
composition, IR spectrometer, **39**,189

CO, mm waves, spatial variability, **39**,219
CO, mm waves, thermal structure, **39**,209
CO, IR spectrum emission lines, **39**,213
density, exospheric, escape of atomic isotopes, **26**,949
dust and ozone, vertical profiles, **39**,175
history and climate, **30**,819
ion wake in solar wind, **22**,967; **27**,1111
ionosphere below 80 km, **19**,243,971
mapping, reflected and emitted radiations, **39**,237
photochemistry, **27**,113
photolytic stability, **22**,878,879
satellite occultation data, **16**,1035
Schumann resonances, **39**,1673
thermal and dynamical structure, **16**,615
bow shock, comparison with Earth, **39**,99,153
bow wave, location, **20**,205
brightness temperature, radiometric, **14**,15,1017
CO Cameron band spectra, **31**,317
CO_2 photolysis, **19**,1701
CO_2^+ reaction with atomic oxygen, **18**,1267
condensation and sublimation of CO_2 and H_2O, **16**,495
dark areas, seasonal evolution, **9**,371
Deimos,
interaction with solar wind, **39**,123
plasma and magnetic field effects, **39**,113
diameter in UV and IR, photographic, **13**,261
electron flux distributions, **39**,139,147
He content, thermal loss effects, **22**,500
images, using CCD's and telescope, **39**,273
interaction with solar wind, **39**,75,123
interior, elastic properties, **20**,557
ion fluxes, **39**,131,139,153
ion-clustering reactions, effects on O_2 and CO_2, **21**,2039
ion-neutral reactions, **14**,969; **21**,881
ionosphere, solar control of, **38**,539
magnetic field and magnetosphere, **39**,73,83, 167,1493; **40**,707,719
nitrogen atoms, production and escape, **28**,41
nitrogen oxides, **13**,73,1003
oxygen isotopes, evolution of volatiles, **24**,1107
ozone distribution, global, **25**,839; **27**,113; **29**,21
ozone, effects of clouds and dust, **36**,125
Phobos,
dynamics and gravitational constant, **39**,349
imaging, TV experiments, **39**,281,297
interaction with solar wind, **39**,123; **40**,1033
plasma and magnetic field effects, **39**,113
small bodies in solar system, **39**,377
spectrophotometry, infrared, **39**,311
surface brightness, **39**,335,341
surface, analytic model, **39**,355
surface topography, **39**,225,327
photogrammetric interpretation of orbital photography, **30**,45
photolytic stability of atmosphere, **21**,1333
photometry, multicolor, **2**,26
plasmas and waves around planet, **39**,89
radiative heating, atmospheric equilibrium, **15**,1465
radiative relaxation times, **15**,247
radio waves,
ionospheric refraction, **21**,881
6.0cm, **14**,1017
21.2cm continuum, **14**,15
Rayleigh scattering, atmospheric, **12**,799
recombination rates, **23**,661
reflectivity of disk, violet layer, **9**,81
regolith-atmosphere H_2O and CO_2 exchange, **30**,819
solar wind flow past, **18**,1281
spectra, effects of anisotropic scattering, **24**,967
surface mapping, reflected and emitted radiations, **39**,237
temperature at surface, evolution of, **24**,41
water, surface, diurnal behaviour, **24**,161
water vapour, chemical equilibrium, **11**,355
wave of darkening, biological or dust?, **15**,817
winds and dust clouds, **21**,1549

MATHEMATICAL METHODS

Boltzmann-Fokker-Planck, electron distribution function, **25**,743
celestial mechanics, self-gravitating fluid, integral solution, **12**,1211
coupled equations, waves in plasma, **21**,391; **25**,209,217
Fokker-Planck equations, collisional heating, **23**,419
Fokker-Planck equations, plasma pitch angle, **18**,123
Fourier transforms, isolation of components, **26**,21
Laplace tidal equations, eigenvalue solutions, **29**,1339
Newton-Raphson, temperature profiles from radiative convective model, **32**,803
phase methods, non-stationary processes, **21**,187
running means, power spectrum analysis, **21**,153
Störmer theory and Euler potentials, **15**,1525
superposed epoch analysis of geophysical data, **34**,1133
wave mechanics, bound free continuum for C^-, **2**,10
WKB approximation, plasma, microwaves, interaction, **6**,105

MERCURY

albedo variations in surface, **22**,99
dayglow, UV argon lines, **21**,383
neutral and ion-exospheres in solar wind, **21**,2181

METEORITICS

impact phenomena,
cratering, resulting plasma enhances local magnetic field, **30**,395

impact, depth of penetration, **11**,1365; **28**,567
impact, heating and vaporisation, **26**,463; **28**,599
impact phenomena, **23**,1519; **24**,771; **28**,321,511
microcratering and accretion on lunar rocks, **28**,617,635
penetration limit of thin films, **28**,321
solar wind sputtering rates, **28**,511
meteorites,
ablation, residual dust, **17**,575; **33**,315; **34**,1201
aerosol influence on thermospheric O_3 measurements, **22**,1035
D-region deposits, hydroxyl nightglow, **16**,134
deposition in ionosphere, sporadic-E, **32**,1533
ejecta parameters, primary velocity, **26**,469
Fe, Mg, ionic, neutral, at mesopause, **32**,307
flux, impacts to 135 km, **2**,75
ionization and loss processes in E region, **17**,1233; **18**,1659
ions in mesosphere, chemistry, **30**,1117
iron particles, fall-out measurements, **2**,39
He^3 distribution, Grant meteorite, **1**,66
mechanical parameters, acoustic data, **5**,83
metallic dust and hydrocarbons, **16**,134; **33**,807
origin, review of hypotheses, **13**,243
spluttering in ionosphere, **18**,1653
Tunguska event, **37**,329; **38**,1351
meteoroids,
capture by solar radiation field, **9**,801
'cold', measurements on Pioneer, **39**,1573
detection by dipole antenna, **37**,1291; **38**,949,951
Earth-Moon system, anisotropies, **23**,981
electrostatic charge on interplanetary grains, **17**,155
erosion in space, by cosmic rays, **29**,1109
flux, solar system dust cloud, **20**,1949
global deposition, atmospheric superrotation, **22**,559; **23**,379
gravitational concentration near Earth, **9**,541; **11**,499
hyperbolic orbits, cause of, **23**,183
impact on Gemini windows, **18**,953
implications for lunar microcraters, **23**,151
mass, speed and direction, **23**,215
orbital influence of planets, **33**,1359
planetary precipitation and capture mechanism, **21**,1605
spatial, physical characteristics near Earth, **23**,205,1451; **27**,511; **28**,333
meteors,
Ca^+ twilight emission, **15**,503,589
excitation of ionic lines and molecular bands, **27**,59
ionization columns, initial radii , **28**,575
ionization diffusion, geomagnetic control, **28**,997
radio propagation, ionization effects on, **27**,533
shower, ETA Aquarid, radar detection, **37**,837
shower, Quadrantid, contamination of upper atmosphere, **19**,1585
showers, underdense trains, echoes from, **15**,1131; **24**,605,606
spectrum, Fe^{57} Mossbauer spectroscopy, **26**,289
spectrum, near infra-red, **5**,137
trains, ambipolar diffusion, height, motion, **1**,125; **5**,109; **17**,519; **18**,1153,1836; **21**,1671; **29**,415
trains, drift, atmospheric winds, **18**,1623; **22**,777; **23**,389,509; **39**,1283
trains, luminosity decay, **26**,697
trains, radio reflection and irregularities, **17**, 553,1519; **20**,301; **22**,777,1669; **23**,1261; **26**,969,979; **27**,533,905,1131; **38**,55,925; **39**,873,1289; **40**,1487
wind shears, gravity waves or turbulence, **16**,61; **17**,553; **20**,301
microparticles,
acceleration of, **11**,1485
detection technique and characterisation in space, **12**,627
dust cloud, origin and concentration, **11**,311,387; **15**,1081; **20**,1949; **36**,747
dust, cosmic origin, twilight luminosity, **23**,1011
dust, detector calibration for space probes, **37**,1197
dust, fast, ion production, **25**,135
dust, related to sporadic-E activity, **38**,145
impact damage on optical space telescopes, **12**,77
rocket, satellite measurements, **1**,27; **2**,121; **7**,417; **8**,82; **11**,305
radio emissions from trains in IQSY, **14**,1253

METEOROLOGY

biospheric environment on early oxygen-poor Earth, **36**,1391
circulation of artifically injected NO, **23**,247
climate, Earth, regulation of CO_2 and chemistry, **30**,795
climate, Earth, variability of solar radiation, **30**,147
climate on oxygen-poor ancient Earth, **36**,1391
climate, Mars, H_2 and CO_2 in atmosphere, **30**,819
clouds, distribution, satellite study, **9**,70
cloud heights, IR albedo measurements, **13**,377
cyclones and anticyclones, **17**,1149; **19**,907
electric currents in seas and around islands, **21**,97
greenhouse effect, *see* GREENHOUSE EFFECT
influence of solar activity, **12**,219,327,333
lightning, source of radio noise in space, **13**,1137; **17**,1310; **18**,1848
sea tides, lunar cause of geomagnetic variations, **18**,1597
thundercloud, ionospheric cavity formation, **38**,703
weather disturbances, by gravity waves, **23**,493

MICROWAVES

atmospheric emission, attenuation at 85-118 GHz, **23**,61
absorption, atmospheric, line shapes, **11**,1139

propagation in plasma, **6**,100,105,186,196
scattering from belts of needle satellites, **9**,153
solar, and PCA, **21**,707

MOON
albedo, photometry of Surveyor footprints, **16**,1465
atlas, orthographic, grid errors, **12**,318
atmosphere, interaction with solar wind, **9**,,211, **12**,1075
atmosphere, response to volcanic release, **20**,1849
cometary impact and magnetization, **24**,45
ejecta theory, cause of Gegenschein, **19**,841
exosphere, diffusion model, **20**,103
geology,
altitude estimations, photographic analysis, **9**,917
crater alignments, satellite photographs, **16**,501,809
craters, distortions, stresses, **9**,3,11
craters in lunar walled plain Ptolemaeus, **11**,125
contraction and expansion, **8**,1
erosion and acretion, **5**,321; **11**,1335
erosion, simulated solar wind sputtering, **11**,1257
gravitational field, **18**,1137
internal constitution, **9**,625
internal elasticity, **19**,929; **20**,557
interpretation, **2**,256; **9**,835
maria, origin and development, **5**,283; **16**,665
mascons, evidence from Apollo orbits, **18**,1137
material, simulated, **15**,1653
microcraters and micrometeors, **23**,151
outgassing, coronagraphic search, **16**,825; **20**,1849
regolith samples, packing state, **21**,113
ring structures, **16**,665
serpentines, excited fluorescence, **15**,633
soil, loose depth, Ranger photo, **15**,49
soil, first decimeter, radiant characteristics, **11**,135
soil, particle size distribution, **16**,101
Straight Wall, topography and tectonics, **11**,23
stress history, **2**, 249; **5**,286
volcanic releases, **20**,1849
influence in geomagnetic field, **17**,487
influence in ionospheric F region, **17**,923
ion bursts from terrestrial magnetosphere, **31**,235
libration clouds, scattering of sunlight, **23**,1313
magnetic field, **9**,305; **17**,685; **21**,1923
magnetic storms, **12**,649
magnetic tail and wake, model, **16**,142
modulation effects of electrojet, **29**,1091
photographic analysis, altitude estimations, **9**,917
remote side,
photoelectric study, **11**,549
photographic analysis, **9**,565,581,589,835,961
radiance of surface objects near opposition, **13**,271
radio reflection, depolarization effects, **15**,1337
radio wave lensing by ionosphere, **16**,999
satellite orbits, classification, **16**,285
satellite orbits, lifetimes, **15**,1549
temperature measurements at 3200 MHz **5**,307
thermal radiation at 1420 MHz, **1**,213
thermally stable, consequences, **22**,1691
tidal effects in F-region, **23**,1071
tidal vector calculation, **17**,483
tidal winds in ionosphere, **18**,1075
tides, sea, Earth, geomagnetic variations, **18**,1597
water, detection, **15**,771
X-rays, detection, **13**,1249

NEPTUNE
condensable species at cold trap, **37**,151
internal constitution, **15**,1609
magnetic dipole, inclination, eccentricity, **39**,1259
model atmosphere, **21**,1601

NEUTRINOS
spectrum, from model of solar interior, **12**,119

NEUTRONS
cosmic ray generated, origin of trapped protons, **11**,1151

NITROGEN
atomic,
auroral morphology, **27**,453
chemistry, density, thermospheric, **40**,337
'hot' atoms, atmospheric, neutral chemistry, **39**,929
N (^4s -^4P) multiplet, linewidth studies, **31**,1291
N_2^+, twilight production, **13**,529
recombination on surfaces, **3**,38
translationally excited, thermospheric aeronomy, **31**,135
chemistry, *see also* REACTION MECHANICS
molecular,
absorption of solar L_γ, atmospheric composition, **12**,656
concentration in Earth's atmosphere, **8**,9; **9**,877
diffusion in thermosphere, **22**,189
ionization in ionosphere, **2**,157; **25**,735
metastable, resonant electron scattering, **31**,843
new emission bands, vacuum UV, **35**,267

NITROGEN OXIDES
NO, aeronomic dissociation, **21**,925
NO, atmospheric concentration, rocket spectrometry, **1**,161; **14**,623
NO, auroral morphology, **27**,453
NO, 5.3μm, cooling effect in thermosphere, **34**,131
NO, correlation with E-region ion composition, **25**,103
NO, chromospheric processes, **21**,939
NO, fluorescence in Earth's backscattered spectrum, **30**,137
NO. influence of peroxyacetyl nitrate in lower atmosphere, **31**,1075

NO, infra-red radiation in upper atmosphere, **30**,1043
NO, Martian atmosphere, **13**,73
NO, origin of, **18**,1111
NO, photolysis in far UV, quantum yields, **1**,333
NO, stratospheric, chemiluminescent sampler, **22**,19; **35**,609
NO, stratospheric, non LTE effects, **37**,847
NO, stratospheric seeding and circulation, **23**,247
NO, thermospheric, γ-bands, rocket, **35**,191
NO, thermospheric cooling, 5.3μm, **30**,515; **36**,271
NO, thermospheric, diurnal variability, **25**,735
NO, thermospheric, photochemical model, **40**,315
NO, transport, E-region, longitudinal asymmetry, **36**,11
NO, transport, thermosphere to stratosphere, **32**,399
NO, vibrational relaxation, **3**,86
NO_2, stratospheric, **35**,615,631
NO_3, stratospheric, **35**,615
N_2O, atmospheric characteristics, **15**,189; **17**,1319
N_2O, UV absorption and temperature effects, **38**,617
N_2O_5, conversion to HNO_3 in stratosphere, **31**,185
odd nitrogen, theoretical considerations, **35**,637

NOCTILUCENT CLOUDS
meteoritic deposits, hydroxyl nightglow, **16**,134
nature and origin, **1**,146; **30**,1147; **33**,761
non-correlation with mesospheric radar echoes, **37**,1013
temperature effects, **33**,761
wave formations, **5**,92

NUCLEAR EXPLOSION
high altitude, Starfish, artificial aurorae, **18**,731
geophysical effects in upper atmosphere, **10**,47; **15**,1419; **34**,395

OPTICAL DEPTH
atmospheric, at large zenith angles, **12**,761

OXYGEN
airglow, *see* AIRGLOW
atomic,
absorption of energetic electron energy, **19**,1653
atmospheric abundance determinations, **16**,371; **18**,379,1527; **19**,801; **23**,1413; **24**,313,389; **25**,79; **27**,341,925; **32**,771; **34**,391,393,771; **36**,893,897,963,987; **37**,49; **38**,221; **39**,617,627,1155; **40**,775,1153
atmospheric, distribution function, **25**,117
ionized, five times, atomic properties, **11**,1001
odd oxygen, photodissociation products, **35**,769
photoionization cross sections, **12**,235
thermal conductivity and viscosity, **9**,1
transport in thermosphere, **21**,1001
aurora, *see* AURORAE
chemistry, *see also* REACTION MECHANICS
interaction with metal vapours in atmosphere, **21**,89
mesospheric decrease during PCA event, **21**,1969
molecular,
absorption in the millimetre region, **11**,1139
atmospheric content, measured, **1**,161; **18**,379,1255; **21**,339; **24**,589
ionization mechanism, **9**,175

OZONE
aerosol effect on thermospheric measurements, **22**,1035
airglow identification, recombination spectra, **38**,1121
AROSA 60 year total ozone record, **37**,1587
atmospheric heating, photodissociation rates, **38**,807
campaign, comparison of ground based and balloon results, **31**,707,811
Dobson G.M.B., spectrometers and the man, **37**,1485,1601
excitation, electronically, in atmosphere, **25**,1177
excitation, flash photolysis, laboratory, **34**,1147
global distribution, TOMS satellite, **37**,1555
heavy, stratospheric enhancement, **39**,945
impact on human activity, **37**,1653
Martian atmosphere, global distribution, **25**,839
mesospheric,
abundance, **19**,1583; **21**,273,963; **25**,165; **28**,1147; **36**,607; **39**,745; **40**,1391
changes during solar eclipse, **30**,507
density variations with temperature, **39**,745
depletion, associated $O_2(^1\Delta_g)$ emission, **35**,1087
depletion, implications for OI(557.7) emission, **36**,1077
measurements of attenuated moonlight, rocket, **22**,497
microwave measurements, **36**,607
NLTE processes and ir spectrum, **40**,989,1289
N-S asymmetry, rocket data, **34**,331
profiles, solar occultation, Solar Maximum Mission, **32**,503
variations, auroral, calculated, **16**,371, **21**,1969
SAGE I,II measurements, an overview, **37**,1567
satellite observations, a review, **37**,1539
stratospheric,
abundance in Earth's ancient oxygen-poor atmosphere, **36**,1391
abundance, distribution and transport, **26**,139; **36**,607
abundance, sunspot cycle and injected NO effects, **23**,247
Antarctic, associated chemistry, **36**,73
Antarctic, spring behaviour, **40**,7
asymmetric N-S distribution after solar particle events, **32**,857
chemical budget, 1-D model, **31**,1033

chemiluminescent sampler, **22**,19
chemistry, aeronomic, **36**,73; **37**,1606,1621
excited precursors, **27**,411
heavy, the symmetric isomer, **40**,1573
long-term polar losses, **40**,373,403
measurements, analysis, MAP/GLOBUS(1983), **35**,539,547,563,587,595,603
microwave measurements, **36**,607
seasonal and spatial variations, **37**,1509,1525
solar UV absorption measurement, **31**,767
thermospheric, stellar occultation, **22**,1337,1455
total ozone,
compared results from a variety of instruments, **31**,789
cross section of O_3 in 310-350nm range, **31**,1229
infra red measurements, NOAA6 satellite, **31**,779
mapping with TOMS, NIMBUS satellite, **31**,773
scanning filter photometer, compared with Dobson's results, **31**,735
trace species in the lower atmosphere, **31**,731
tropospheric, Arctic winter variations, **40**,203
vertical distribution,
chemiluminescent ozonometer, **31**,743
ground based microwave techniques, **31**,737
lidar measurements, **31**,717
rocket optical ozonesonde results, **31**,749,761
solar UV spectrometry, **5**,122; **11**,709; **16**,1189
Umkehr method, **31**,729
various techniques and results, **31**,729,791, 801,809,1053

PLANETARY PATROL PROGRAM
cumulative atmosphere, surface studies, **21**,1511

PLASMA
acceleration processes, **31**,25
adiabatic convection in tail plasma-sheet, **26**,1185
adiabatic potential transitions, **26**,925
anisotropic, rotational discontinuities, **19**,1693; **21**,475
astrophysical, turbulent, **23**,409
auroral, dynamics, wave generation, **39**,953, 1223,1343
cloud evolution in ionosphere, **35**,835; **38**,1375; **39**,1147
cold, interaction in confined magnetic field, **16**,1249; **17**,333; **20**,711; **27**,317
collisionless, interaction with electrostatic wave, **27**,933
collisionless, Radler effect and magnetotail currents, **30**,875
collisionless, total current to cylindrical collectors, **31**,275
convection, adiabatic, in dipole field, **23**,1527; **24**,805,821; **32**,1551; **39**,397
cosmic, shock waves, **24**,617
current signal, rectified, measured by rocket probes, **13**,725,969
cusp region, properties, **26**,993
cylindrically symmetrical enhancement, VLF, **23**,1649
decaying, properties, **11**,1
density diagnostics, **38**,269
density, spacecraft measurements, **22**,1041
depletion bubbles, topside ionosphere, **27**,593, 1187,1303; **31**,99
diffusion, ambipolar, along field lines, **19**,915
diffusion, multi-component, **31**,591
diffusion in terrestrial and lunar exosphere, **20**,103,149
drift in ionosphere, **19**,345; **22**,1,1131; **28**,407; **30**,581; **33**,773,1229; **38**,961,1567
dusty,
double layers, large amplitude, **40**,465
ion-acoustic waves, **40**,1,973
velocity modulation, **40**,763
vortices, **40**,647
dynamics of magnetospheric plasma, **13**,729; **14**, 223; **18**,349, 977; **21**,1713; **29**,391; **39**,1097, 1139,1223,1343
equations for anisotropic hydrodynamics, **31**,91
expansion in polar wind, **36**,753; **38**,723
flow around objects in space, **15**,155,463,1479, 1489,1847; **16**,145; **17**,685; **18**,793,901,1035; **20**, 1788; **22**,379; **23**,287,1081; **29**,1345; **38**,653; **40**,535
flow patterns in flux tubes, **38**,355
geosynchronous, analytical simulation, **27**,1101; **29**,1021,1045
hot, interaction with cold ionosphere, **19**,749; **20**,973; **23**,713
interaction with auroral electron beam, **31**,875
interaction with spacecraft, **22**,379; **27**,145
interplanetary, fluctuations, **19**,421
ion cloud expansion in geomagnetic field, **19**,1095; **20**,25,149
ionospheric *em*-emissive power, **40**,509
ionospheric waves, **20**,683; **21**,391,692; **40**,433
Langmuir turbulence, beam-plasma discharge, **40**,535
magnetospheric,
cold, plane of magnetic equator, **19**,107
correlation with pulsations, **31**,143
electron-acoustic double layer, **36**,1009
electron, oscillation fields, **13**,921; **26**,51
intensity variations at dawn, **28**,1163
interactions at magnetopause, **21**,1497,1713
particle density distribution, **19**,651
particle-wave interactions in neutral sheet, **29**,399
polar wind, topside ionosphere, **35**,703
proton dynamics, **14**,1207; **19**,1053; **26**,51
tail-like extrusion into confined magnetic field, **19**,869
thermal, protonosphere to ionosphere, **27**,603
viscosity between plasma streams, **18**,349
non-Maxwellian, characteristic frequencies, **29**,1251
polar, wind, temperatures, **22**,1193

probe-plasma interactions, **37**,21,873,1001
R wave cut-off propagation theory, **40**,433
Roche limit, **22**,757
scattering, bi-thermal ionosphere, **19**,1019
streaming in ionosphere, **16**,845; **18**,1843; **19**, 107,651; **26**,367
solar,
corona, particle streaming, **18**,1213; **38**,459
distant, geomagnetic field observations, **12**,87
energy, momentum flow to magnetosphere, **31**,247
injection mechanism into magnetosphere, **12**,209
shock front in interstellar space, **19**,1121
streams, **22**,841
three fluid model, **18**,199
temperatures, from electron density profiles, **24**,247
thermal,
effect of meridional E x B drift, **31**,411
environment of Space Shuttle, **32**,457,881
flow between protonosphere and ionosphere, **26**,753
turbulent, equations for ion transport, **32**,949
weakly ionized, whistler mode propagation, **22**,333

POLAR-CAP ABSORPTION
see RADIO WAVES or IONOSPHERE

POTASSIUM
mesospheric concentrations, by lidar, **26**,27

PRECIPITATION
auroral energy deposition rate, **40**,299
configuration, spatial, energetic influx, **13**,63
conjugate areas, total field maps, **16**,1357
corpuscular, correlations with optical emissions, **16**,1311,1418; **17**, 1961; **18**,187,661
correlations near solar minimum, **39**,557
correlation with ULF electric fields, **26**,833
current injection, double layer formation, **33**,853
DR-current development, **16**,891
during magnetic disturbance, **20**,1363; **21**,1699; **24**,487
dynamics of precipitation zone **16**,881
electric fields, effect of, **26**,833,1149
electrons,
auroral, **12**,722; **13**,225,1171; **14**,597; **15**,1287; **16**,371,567,737,1419; **17**,255,1051,1213,1257; **19**,313,540; **20**,233; **21**,2042; **22**,939,1067,1279; **27**,87,445; **28**,375; **31**,489,889; **32**,107,561; **33**,591; **36**,791; **40**,299,1043,1409
convection electric field properties, **30**,1083
D and E-regions, **23**,1321; **25**,991
energy deposition in atmospheric N_2, **36**,329
flux, from plasma line intensities, **27**,557; **33**,175
heating by charged particle streams, **15**,873; **16**,525; **17**,1709; **25**,123
inner radiation belt, high energy flux, **32**,1611; **38**,483
inverted V-events, **26**,673; **32**,379; **34**,255
magnetosheath to polar cusp region, **32**,41
magnetospheric cleft, **25**,1161
MHD wave associations, **33**,1277
oxygen and ozone concentrations, **16**,371
parallel electric-magnetic fields, **29**,915; **33**,591
photoelectron fluxes on AE satellite, **31**,221
pitch angle distributions, **36**,117; **38**,851
radiation belt, convection field effects, **34**,271
related to airglow, **16**,1418; **19**,540
relativistic, stratospheric evidence, **40**,413
signature of polar cusp, boundary layer, **36**,1219
slabs, auroral waves, **16**,1453; **17**,61,1391
storm related conditions, **29**,405; **34**,293; **38**,365,785,1051
suprathermal, **25**,5
VLF mode associations, **16**,1419; **34**,337
X-rays associations, **16**,1419; **17**,1565
electrostatic shock wave, **24**,1073
energy deposition, from auroral green line emission, **18**,187
energy deposition, O_2 1.27μm emission, **26**,619
energy spectrum and pitch angle distribution, **27**,193
flickering, 10 cps, in bright aurorae, **16**,1525
flux distribution from airglow data, **26**,339
fluxes inferred from long-period oscillations, **26**,171,1149
from interplanetary medium, thermospheric interaction, **21**,1317
generated by whistler-mode wave, **25**,395
ionospheric substorm, **20**,1375; **24**,409
ions, anisotropy, **19**,279; **25**,149; **26**,673
ions, pitch angle distribution in magnetotail, **38**,851
longitudinal scattering in radiation-belt, **8**,13
low energy, South pole, **14**,85
magnetic separation, origin of S_D field, **2**,49
modulation, hydromagnetic wave resonances, **33**,253
morphology, **8**,142; **9**,503; **10**,233; **12**,783; **13**, 565; **14**,807; **15**,301,1287; **16**,47; **17**,83,403,1657; **18**,479; **27**,841; **38**,355
near magnetospheric trapping boundary, **20**,1433; **27**,1523
nucleation, ion-induced, **28**,1003
particles in middle-atmosphere, effect of odd-H and odd-N, **29**,885
particles in high latitude, **23**,1597; **30**,1259
photoelectrons, pre-dawn enhancement, **18**,1011, 1335,1367
pitch angle, diffusion by bounce resonance, **26**,75; **30**,433
protons,
acceleration by interplanetary shocks, **38**,343
acceleration near X-point in magnetic field, **32**,313
arc, SAR, formation, **26**,245
associative detachment, **17**,731

bidirectional distribution, interplanetary shock event, **31**,1388
cyclotron frequency phenomena, **22**,793
diffusion at magnetospheric bow shock, **21**,971
during auroral break-up, **22**,735
effect on rf transmission, **17**,1329
energy loss in O_2, **29**,261
evening and forenoon sectors, **23**,1141
flux anisotropies, **19**,523; **27**,1035; **29**,1273
injection processes, **27**,165
intensity maps below radiation belt, **38**,483
ionospheric response, **25**,773; **30**,463
isotropic, ring-current, **22**,767
lateral dispersion, **22**,341
origin in region of bow shock, **27**,365
particle-wave interactions, **34**,1091
PCA events, **13**,583; **23**,787,935
pulsation effects, **28**,387
ring current, energy dependence, **25**,757; **36**,207
scattering in current sheet, **31**,1147; **33**,1433
showers, forecast by geomagnetic activity, **36**,205
solar, **20**,89,271,292,1051,1835,1979
solar, flares, emission and acceleration, **11**,613, 897
solar, conjugate, twilight, **13**,583
solar, ionospheric effects, **38**,1479
solar, propagation in IMF, **14**,745
solar, velocity distribution, **38**,1091
stormtime, recovery phase, **25**,2085; **33**,39
stormtime, sudden commencements, **25**,823
thermal, near equatorial plasmapause, **32**,351
transport equations in ionosphere, **27**,433
trapped, origin in neutron albedo, **11**,1151
trapping zones, **19**,525,1041; **24**,757
velocities, field aligned, **27**,297
pulsations, **15**,347; **17**,1141
reflections by rotational discontinuities, **22**,1571
ring current disruption, **15**,835,1225; **16**,703; **21**,1681; **36**,207
scattering, in current sheet, **33**,1433
scintillations, resulting, **20**,41; **23**,1035
South Atlantic anomaly, **23**,15
trajectory calculations, Williams and Mead field model, **19**,1016
VLF emissions, **20**,803
vorticity in atmosphere, **28**,419
X-ray emission, **10**,165; **16**,815,1419

RADAR

auroral, SABRE, STARE, micropulsation activity, **31**,573,1279; **32**,837,1291; **38**,603; **39**,1239
backscatter observations, F region, **12**,915; **13**, 1031; **15**,1387
echoes, Doppler spectrum, **35**,153
echoes, noctilucent cloud observations, **37**,1013
echoes, periodic, atmospheric transmission effects, **5**,50; **6**,186; **36**,423
incoherent scatter,
auroral brightening, **24**,425
auroral emissions, coordinated measurements, **37**,131,545
density, temperature, of F region, **18**,741,1225; **19**,1431; **23**,523
during geomagnatic activity, **40**,1371
E and F-regions, **40**,355
electric field during IPDP event, **36**,1103
energy deposition profile during break-up, **26**,619
field-aligned currents, **24**,479
hydrogen density and proton flux, **19**,1441
ion drifts, tidal winds, **20**,1269
ion flows and polar heating, **36**,1229
ion-molecule collision frequencies, temperatures, **37**,211
ion-neutral collision frequency, **35**,337
ionosphere, conductivity, substorm associated, **36**,1359
ionosphere, F-region, valley irregularities, **26**,1007
ionosphere, topside, data analysis, **19**,1431
ionospheric plasma, noise effects, **38**,903
mapping of electrostatic potentials, **31**,1329
neutral winds, ionospheric, **24**,541; **39**,657
PCA event, **35**,947
plasma line intensity, photoelectron distribution, **25**,123; **28**,661
proton fluxes, nocturnal, **26**,727
VHF backscatter, gravity wave and E_s signature, **32**,1455
interferometry, CW, localized auroral scatterers, **38**,933
lunar tides in middle atmosphere, **35**,445
negative ions, auroral mesosphere, **35**,27
thermospheric dynamics, comparison with FP spectroscopy, **39**,1511

RADIATION BELTS

anomalies,
south Atlantic, cosmic ray maximum, **9**,513
south Atlantic, van Allen belt, **13**,347,451
spurious, satellite measurement, **12**,163
belt, inner,
energetic electrons, **24**,643; **32**,1611; **35**,1281
energy distribution, **11**,317,567; **14**,569
multiple peaks in quiet-time spectra, **40**,89
position, Earth's magnetic field, **9**,841,861
belt, outer,
aurora borealis, **9**,829
charged particle flux, chromospheric, **9**,507
distribution in space, **9**,503,855
during magnetospheric substorm, **20**,1391
electrons, behaviour during storm, **22**,1249; **23**,913; **33**,1259
electron enhancement, processes, **23**,1495
motion and diffusion of particles, **20**,1025
belt deformation due to electrostatic fields, ionospheric winds, **13**,729

particle, charged, intensities, **9**,845
particle depletion by pitch angle scattering, **26**,75
particle, soft, 320km altitude, **11**,431
precipitation, *see* PRECIPITATION
properties of the upper atmosphere, **2**,165
scattering, longitudinal dependence, **8**,13
solar, *see* SUN
theory of origin, **13**,473; **14**,641
thermal, terrestrial albedo, **11**,663,681
trapped particles,
due to nuclear explosion, **10**,47
electrons, relation to IPDP, **15**,1239; **17**,389,1051
protons, generation of pulsations, **24**,465
protons, origin, albedo neutron theory, **11**,1151
resonance interaction with transverse wave, **15**,557; **17**,349
trapping in geomagnetic cavity, **14**,641; **15**,495
van Allen electron loss due to whistlers, **11**,591
van Allen, geomagnetic field cavity, **14**,641

RADIATIVE TRANSFER
atmospheric absorption,
Boltzmann equation in slab geometry, **39**,1435
microwaves, line shapes. **11**,1139
refraction and scintillation of solar rf energy, **1**,50
rf, ionosphere, satellite beacon data, **16**,1415
rf, related to electron profile equation, **16**,529
Schumann-Runge continuum absorption by O_2^*, **19**,1463; **24**,589
UV, by NO, gamma band emission, **25**,369
UV, extreme, cross section, **20**,161
UV, lunar, ozone determination, **20**,217
multidimensional, applications to planetary coronae, **25**,563
optical depth, atmospheric, computations, **12**,761
oxygen 130.4nm dayglow triplet, thermosphere, **13**,871; **18**,661,691
oxygen 63μm IR emission from atmosphere, **18**,271
penetration, solar X-rays to lower ionosphere, rocket phosphor, **11**,1489
radiation characteristics, from top-side Rayleigh atmosphere, **1**,265,277
scattering,
backscatter of solar resonance, **20**,829,1784
coefficient, atmospheric, sky brightness, **11**,417
in gas cloud from chemical release, **20**,165,663
Lyman-α, **9**,67,68; **18**,803
Rayleigh, Martian atmosphere, **12**,799
Rayleigh, tropospheric, 391.4nm twilightglow, **16**,693
resonant, N_2^+ in dayglow, **20**,549
resonant, sunlight, **19**,377
spherical atmosphere, **11**,657
thermal, terrestrial albedo, **11**,663,681
shadow height of Earth, effective **16**,1071
solar ionizing radiation, thermospheric intensity profile, **18**,1255
thermal balance, atmospheric transmission fluxes, **11**,701,839,983, 987,1091,1101

RADIO WAVES
atmospheric attenuation,
absorption and emission, **23**,61
auroral zone, day-to-night ratio, **25**,1031
auroral, electron precipitation, **27**,445
auroral, influence of IMF sector polarity, **28**,1155
correlation with Na nightglow, **25**,45
reflection and transmission coefficients, **29**,531
auroral, *see* AURORAE
Cerenkov, magnetospheric VHF emissions, **19**,813; **27**,959
chorus,
correlation with cosmic noise absorption, **15**,207
exospheric generation, **9**,69
fine structure, wave-particle interaction, **32**,425; **33**,385
generation and propagation, **38**,135
occurrence patterns and frequency, **24**,1007
review, **40**,681
study at Australian stations, **2**,238
triggered by hiss wavelets, **39**,1465
triple splitting in F_2 region, **2**,214
continuum storm from solar particles, **21**,17
decametric, Jupiter, *see* JUPITER
depolarization at rough conducting surface, **14**,563; **15**,1337
echoes,
auroral, drift measurements from auroragraph, **26**,519
auroral, ionization study, **5**,33,105
auroral, polarization of, **18**,655
ducted, delayed occurrence, **37**,935
from satellite, interpretation, **15**,611
meteor, 40-45 MHz, absorption in ionosphere, pre-storm, **1**,102
meteor train, **15**,1131; **17**,519,553,1519; **23**,1261; **26**,969; **38**,55
whistler-mode, **19**,739
ELF,
amplification by exospheric charged particles, **13**,391
associated with equatorial spread-F, **27**,127
daytime model, **35**,139
direction finding technique, **29**,365,515
full wave study in ionosphere, **23**,1155
goniometer receiver in Antarctica, **27**,1371
meteoritic ionization, **27**,533
narrow banded, southern polar region, **35**,745
quasiperiodic, analytical model, **35**,1267
radiation from overhead power systems, **27**,537
Faraday effect, *see* IONOSPHERE
HF, auroral storm begining, **17**,869
HF, synchrotron, from trapped electrons, **17**,389
hiss,
amplification, **27**,273
auroral, propagation of, ground data, **36**,259

auroral, rocket observations, **12**,11,751; **19**,1475
auroral, visual, and geomagnetic activity, **24**,375; **32**,809
auroral, X-ray correlations, **16**,1419
cyclotron generation, Doppler shifted, **11**,361
distinguished from discrete emissions, **19**.374
emission model, **32**,1263
magnetospheric disturbance, **1**,253; **23**,843; **25**,833; **40**,1325
topside ionosphere, **31**,389
wavelet triggered chorus, **39**,1465
lens effect of ionosphere on lunar signals, **16**,999
LF, ionospheric propagation, electron distribution, **2**,110; **15**,1717
magnetospheric propagation, ionization irregularities, **13**,1255; **15**,1059
noise,
atmospheric sources, **12**,1157; **13**,1137; **21**,443
continuum storms, μS-emissions, **23**,1344
cosmic, absorption, latitudinal variation, **19**,1579
cosmic, absorption, over solar cycle, **20**,253
cosmic, attenuation, auroral and magnetic storms, **2**,99; **11**,371
cosmic, attenuation, solar cosmic rays, **14**,277
cosmic, origin, **13**,861
electron beams in polar magnetosphere, **25**,899
electrostatic, auroral electrons, **27**,1491
electrostatic, magnetotail, ion-beam instability, **37**,145; **38**,695
magnetospheric, whistler influence, **25**,879
planetary emission, **11**,221; **14**,15, 1017
polar cap absorption,
conjugate observations, **13**,583; **18**,1005,1691
electron balance, **13**,339,1171
geomagnetic activity, influence of, **13**,1075
height, characteristics, **12**,579,1035
model for, in D-region, **15**,1111
precipitation effects, **17**,731,1313, 1329
proton energy deposition in O and O_2, **23**,787,935
recovery, midday, **15**,1667
review of characteristics, **12**,495
VLF emissions, consequences for detection, **13**,1165
propagation beyond the horizon, satellite to ground, **20**,1984
radar, *see* RADAR
radio star visibility fades, **16**,1155
scintillations,
airglow correlation, **20**,1982
causes, **20**,41
equatorial, **20**,1999
F-region irregularities, **20**,957
index, derivations, **17**,1056,1059,1066,1069
interplanetary, frequencies, motion, size, **14**, 1221; **16**,749; **17**,189,313; **18**,95; **35**,271; **38**,955
ionospheric, synopic study, **13**,51; **16**,21,775; **18**,1785
latitudinal variations, **17**,585,1557
morphology, **17**,1161
plasma irregularities, **19**,813
sources outside plane of ecliptic, **21**,1617
sporadic-E irregularities, **16**,1475
sky brightness rf, dipole measurements, **8**,68
sky brightness rf, rocket probe, **12**,1157
solar occultation, corona investigation, **18**,1213
solar radio activity, *see* SUN
transmission,
interaction with atmospheric plasma, **37**,229
partial reflections in antarctic mesosphere, **37**,889
through shock layer, *see* SATELLITES
VLF,
amplification, Cerenkov resonance interaction, **20**,2073
auroral correlation, **20**,803
banded and periodic structure, **31**,537
characteristics during great solar disturbance, **16**,1081
characteristics, storm related, **17**,1565: **25**, 261,353; **34**,225,1361; **36**,1305
D-region disturbance phenomena, **13**,175
direction finding technique, **29**,365,515
effects of PCA events, **17**,1329
eigenvalues for atmospheric waveguide propagation, **40**,1363
enhanced electron intensities, associated, **21**,239; **35**,1231
F-region formation mechanism, **26**,801
frequency-time structure, **23**,41
full wave modes, enhanced plasma density, **23**,1649
global, during great solar disturbance, **18**,944
goniometer measurements, **21**,899,913; **27**,1371
growth, affected by resonance phenomena, **17**,13,61,363
growth and damping in hot plasma, **36**,663
intensity peaks, low latitude, **40**,1425
ionospheric, by artificial electron beam, **18**,777; **28**,1131
ionospheric excitation, **28**,1051
magnetospheric, **18**,1753; **19**,567,1141; **25**,353; **32**,985
plasmasphere structure probing, **24**,987
post storm, in S.Atlantic anomaly region, **38**,633
power spectral density variations at Antarctica, **16**,1069
propagation characteristics, electron density, temperature, **25**,871; **26**,219; **31**,1083; **36**,833
proton precipitation, effects of, **38**,1479
quasi-longitudinal approximation, **36**,833,1111
quasi-periodic, model, **26**,399; **35**,1267; **38**,1555
radiation of terrestrial power-line origin, **29**,97

ring current electrons, **24**,341; **29**,825
scattering in magnetosphere, **21**,359
side-band instability, theory, **21**,67
theories and observations, **15**,1427
triggering by whistler morse pulses, **19**,1141
triggering, quasistatic theory, **32**,325
wave-normal directions in ionosphere, **21**,671
whistlers,
absence at equator, **28**,359
amplification in magnetosphere, **20**,639
attenuation and guiding in atmosphere, **5**,274; **24**,443
Cerenkov radiation from field-aligned particles, **38**,373
conjugate measurements, middle latitudes, **35**,1053
coupling fluxes, ionosphere-plasmasphere, **40**,1409
CW, noise effects, **25**,879
deduced radial plasma drifts, **32**,525
detection of magnetospheric electric field associated with substorm, **15**,395
dispersion characteristics, **25**,233; **40**,873,1185
dispersion, exospheric ionic distribution, **8**,71
dispersion, latitudinal characteristics, **5**,326; **25**,1087
duct life times, **23**,923
duct propagation, self-focussed, **36**,655
ducts, auroral precipitation and plasma waves, **16**,1297; **32**,1505
ducts, formation and lifetimes, **26**,375,423; **28**,645
echoes, satellite data, **19**,739
electron cyclotron waves from auroral reflections, **31**,499; **34**,337
electron loss in van Allen belt, **11**,591
exit point, bearing errors, **23**,1475
focussing and interference in spatially varying field, **26**,595
frequency shift, **24**,447,455
generation, current-jet hypothesis, **2**,72
generation, lightning discharge transients, **17**,1310
generation, precipitated protons, **33**,333
group delays, electron densities, **39**,1059
instability in anti-loss-cone plasma, **25**,598
instability, quasilinear model, **35**,753
ion cutoff, **23**,1155
L-dependence, **40**,1193
lightning discharge relation, **1**,173; **5**,46; **18**,1848
micropulsation 'nose' whistlers, **14**,1273
mode signals, **25**,957 monochromatic, frequency shift, **22**,859
morse pulses, magnetospheric triggers, **19**,1141
non-ducted, equatorial anomaly effect on reception, **28**,17
non-ducted, rocket measurements, **22**,638
oblique, in presence of electron beams, **38**,791
periodic emissions, theory, **15**,799
PL type, **25**,1037
polarization, **25**,233; **39**,725
propagation between conjugate points, **26**,171; **39**,425,611
propagation, effect of ring current, **20**,731
propagation through ionosphere, **2**,261; **16**,137, 863; **20**,1895; **21**,2113; **22**,333,1545; **40**,985,1339
quasielectrostatic propagation, **33**,295; **38**,311
quasilongitudinal approximation, **38**,1551
ray tracing propagation, **35**,1397
reflections, magnetospheric, **18**,1753
resonant interaction with cyclotron particle motions, **26**,75
rocket observations at night, **12**,11,751
self-consistent theory, **22**,349
sideband stability, non linear theory, **34**,429
single wave, particle precipitation, **25**,395
spectrum broadening, thermal electrons, **39**,1537
spin-modulation diagnostics, **38**,333
soliton, electron beam interaction, **24**,1093
source location, **25**,487
spectral characteristics, **25**,487
stationary turbulence, stability, evolution, **25**,309
Storey angle, **38**,327
storm-time characteristics, **21**,1797
study of plasmapause motions, **22**,1139; **25**,303
transequatorial, dependence on solar activity, **32**,955
wave injection experiment, **32**,1577
wave packets, particle trajectories, **18**,1799; **20**,1791
shock wave source, **13**,781

REACTION DYNAMICS

absorption cross-section,
bromoform, temperature dependence, **37**,1127
CH_2O, temperature dependence, **28**,675
electrons by argon, **25**,71
electrons by H_2, **23**,1059
extreme solar UV in atmosphere, **20**,161
O_2 Herzberg continuum, **36**,1469; **38**,287; **40**,185
O_2 Schumann-Runge bands, **18**,1639; **24**,589; **28**,85; **31**,339; **35**,1067; **36**,1201; **37**,419; **38**,287; **40**,185
O_3 in 238-335nm range, **36**,395
O_3 in 310-350nm range, **31**,1229
solar L_γ by N_2, **12**,656
solar UV flux in middle atmosphere, chemical reactions, **25**,1
adsorption of gas in snow of comet nucleus, **18**,717
associative detachment, mesosphere, PCA events, **17**,731
atom transport, proton-hydrogen in N_2, **40**,1503
atomic properties, O^{+++++}, **11**,1001
autoionization, absorption cross-sections, atomic

oxygen, **16**,1503
Boltzmann equation, flowing chemistry, **3**,4
branching ratio, OI 117.3/98.9nm, **33**,135; **36**,987
carbon, and dissociated gases, interactions, **3**,46
chain reactions, periodic pressure variations, **3**,94
charge exchange,
aeronomic, theoretical considerations, **37**,363
ion diffusion, **16**,1019
ion momentum transfer, **17**,1074; **21**,1975
He^+ to N_2, **15**,19
O^+ to H_2O, space-borne measurements, **40**,1695
$O^+(^2D)$ to N_2 in thermosphere, **25**,1171
chemical analysis of transient species, survey of methods, **3**,118
chemistry of O_3 in thermosphere, OI(557.7) excitation, **36**,1077
collision cross-section,
absorption, electrons in O, **19**,1653
absorption, Schumann-Runge continuum in O_2^+, **19**,1463
electron impact dissociation of O_2, **27**,753
electron impact for methane, **40**,1535
N_2^+ from e+N_2, **15**,1332; **19**,1192
reactive terms for fluid transport theory, **40**,47
collision dissociation, CO_3^- and NO_3^-, **29**,735
collision frequency,
charge exchange processes, **21**,1975
electron, energy transfer, **14**,1085; **20**,1121
electron-neutral, velocity power law, **23**,533
electrons in atmospheric gases, **19**,993
ions, energy transfer, **14**,1105; **21**,1975
ions in ionosphere, ion cloud observations, **19**,1
ion-neutral, velocity measurement, **37**,493
collision strengths, forbidden transitions in e-O and e-N scattering, **29**,377
collision vibrational quenching, atmospheric molecular ions, **31**,483
cooling, electron, D-region, **9**,439
Coulomb interactions, ionized gases, **3**,257; **15**,873
cross-section, oxidation, Ba and Sr, **21**,89
diffusion coefficients, E region, vapour trails, **8**,35
diffusion coefficients, topside ionosphere, **29**,851
electron collisions,
dissociation of O_2, **27**,753
dissociative excitation of SO_2, **31**,197
excitation of CO Cameron bands, **31**,317
fluorescence efficiency of air, **16**,1315
frequency and energy transfer, **14**,1085
N_2 excitation, line width measurements, **35**,1471
scattering spectrum of nitrogen, **17**,1527
survey of measurements, **3**,104
energy transfer,
auroral X-rays, **19**,1069
between excited oxygen species in mesosphere, **25**,79; **27**,341,717,925,1409; **33**,825; **34**,789; **35**,399; **36**,875,883,1077
charge exchange collisions, **21**,1975
distribution function, hot $O(^3P)$, **27**,1321
from electrons in ionosphere, **20**,1121
from electrons to CO_2, **27**,491
$N^2(A^3\Sigma_u^+)$ to $O(^1S)$, pulsating aurora, **21**,698
photoelectron to thermal electron, **19**,113
precipitating particles, *see* PRECIPITATION
excitation and quenching,
aeronomic deactivation, theoretical, **37**,363
airglow, aurorae, *see* AIRGLOW, AURORAE
$O(^1D)$, from $N(^2D)$+O_2, **40**,699
$O(^1D)$, from $O_2(B^3\Sigma)$, **40**,1719
$O(^3D^0)$, 3s and 3d levels, **27**,19
$O_2(^1\Delta_g)$, electric field excitation in aurorae, **18**,1043
oxygen bands, nightglow, **36**,875
quantum yield of $O(^1S)$ from O_2^+ dissociative recombination, **28**,1081; **36**,621
quenching of auroral H lines, collisional ionization **14**,1047
quenching of $N(^2D)$ by $O(^3P)$, 630nm emission, **37**,1145
quenching of $N(^2D)$ by thermal electrons, ionosphere, **34**,689
quenching of $NO(A^2\Sigma^+)$ by $O_2(X^3\Sigma_g^-)$, **20**,157
quenching of $O^+(^2D)$ by electrons in thermosphere, **28**,581
quenching of $O(^1D)$ by $O(^3P)$, 630.0nm airglow, **34**,1143; **38**,647
quenching of $O(^1S)$ in atmosphere, **21**,1757
quenching of precursors to $O(^1S)$ and $O_2(b^1\Sigma)$ in nightglow, **34**,789
vibrational, molecules, atmospheric, **10**,19
experiments, see LABORATORY EXPERIMENTS
fluorescence efficiency, electrons in N_2 and O_2, **16**,1315; **25**,555
fluorescence emission rates for NO gamma bands, **25**,369
Frank-Condon factors for H_2O^+ molecular bands, **31**,1371
Frank-Condon factors for O_2 band system, **19**,1009
fluid transport, reactive collision terms, **40**,47
heat transfer to surfaces in dissociated combustion gases, **3**,53
heating, decomposition, fluorocarbons at high temperatures, **3**,73
helium ions,
cross sections for collisions with N_2 and O_2, **16**,477
loss processes, **12**,1169
hydrogen ions,
collision model, results for ionosphere, **16**,759
cooling in helium gas, **16**,911
intermolecular potentials,
calculation of transport properties, **3**,205
diffusion in high temperature gases, **3**,221
diffusion, ambipolar, drift, F_2 region, **13**,959
interactions at high temperatures, **3**,253
ionic systems, **3**,217
ion collision frequency and energy transfer, **14**,1105

ionization,
auroral, incident energetic electrons, **11**,1209
critical ionization velocity in space, **37**,865
meteoritic elements, **17**,1233
N^+, in upper atmosphere, **2**,157; **15**,457
$N(^2D)$ and O in atmosphere, **27**,1233
oxygen, by electron impact, **30**,451; **33**,1303,1309
sulphur atoms by electron impact, **30**,1269
ionospheric processes, role of oxygen, **17**,1247
lifetimes,
$N^+(^5S)$, 214.5nm auroral feature, **29**,263
$N_2(A^3\Sigma_u^+)$, and diffusion, **15**,689
radiative, second positive system of O_2^+, **32**,1111
line strengths, dipole and quadrupole transitions, **13**,1131
mercury vapour, high temperature, low pressure, **3**,271
mobility, ions, in nitrogen afterglow, **13**,667
oscillator strengths, O_2, Schumann-Runge bands, **31**,339; **35**,1067; **36**,1201
photoabsorption coefficients for CO and CO_2, **23**,384
photochemistry of O and O_2 in aurorae, **16**,371
photodissociation,
H_2O_2, NO_2 and HNO_3, **22**,413
N^{+*} from $N_2+h\nu$, EUV emission, **39**,1197
O_2, NO, stratosphere and mesosphere, **28**,97
O_2, Herzberg continuum, **34**,1043; **36**,1069
O_2, Schumann-Runge system, **36**,819,1039; **37**,427,459
O_2, to produce odd oxygen, **35**,769
rates for O_2, O_3, CO_2, H_2O, solar irradiance in atmospheres, **29**,951; **31**,987; **36**,1059
water vapour in mesosphere, **32**,871
photoionization,
cross section, atomic oxygen, **12**,235; **15**,1747; **28**,165; **40**,1419
cross section, sodium, **12**,729
hydrogen, by extreme solar UV, **12**,905; **22**,143; **38**,1225
ionospheric rates at night, **28**,1027
photolysis,
CO_2, at 184.9nm and 213.9nm, **19**,1701
NO, far UV, quantum yields, **1**,333
twilight, available radiation field, **39**,671
reaction rates,
and thermal balance, **21**,159
Chapman's three-body, $O(^1S)$, **14**,113; **40**,1705
CO_2^+ with O, O_2 and NO, **18**,1267
energy transfer, ionospheric electrons, **20**,1121
He^+ with N_2 and O_2, **16**,477
ion-molecule reactions in N_2O_5 to HNO_3, **31**,185
ion-neutral reactions, laboratory, **15**,373,1349; **16**,701
ionospheric, measured in ionosphere and laboratory, **14**,33; **19**,15
neutrals in atmosphere, **15**,643
$N^+ + O_2$, $O(^1S)$, $O(^1P)$ production, **33**,1225
$N_2^+ + NO \rightarrow NO^+ + N_2$, **18**,1267
$N_2^+ + O \rightarrow NO^+ + N$, **13**,823; **18**,1267; **36**,307
$N_2^+ + O_2 \rightarrow N_2 + O_2^+$, **13**,919
NO production in atmosphere, **18**,1111
NO^+, O_2^+, N^+, N_2^+ with N_2 and CO_2, **31**,933
$NO_2^- + H \rightarrow OH^- + NO$, **20**,1984
oxygen, nitrogen ion-molecule reactions, **13**,219, 911; **15**,1349,1777,1781; **16**,243; **17**,1758; **25**,195
O^+ and vibrationally excited N_2, **15**,401
O^+ in He-O and He-O-N mixtures, **14**,1047
$O^+ + O_2 \rightarrow O_2^+ + O$, **13**,579,911; **15**,1777,1781
$O_2 + e \rightarrow O(^1D) + O$, **36**,47
$O_2 + e \rightarrow O(^1S) + O$, **36**,621
$O_2^+ + NO \rightarrow NO^+ + O_2$, **18**,1267; **31**,1181
recombination,
and ionization, atmospheric, **11**,1359
atomic N, on surfaces, **3**,38
coefficients, D-region, **21**,367
dielectronic, to N and O ions, **9**,77
dissociative, N_2^+, **33**,263; **39**,1297
dissociative, $O(^1S)$, $O(^1P)$ excitation. **23**,935
dissociative, O_2^+, **16**,1177; **28**,1081; **29**,999,1095; **36**,47,621; **38**,889
dissociative, electrons and NO^+, **31**,667
electron-ion, in nitrogen afterglow, **13**,667
electrons with H_3^+ and H_5^+, **32**,651
ion-ion, in atmosphere, **25**,433
ionospheric, historical resumé, **36**,55
radiative, coefficients for O, **40**,1705
rate for O+CO in solid CO_2, **23**,661
relaxation, vibrational, NO^*, **3**,86
scattering,
anisotropic, effect on planetary spectra, **24**,967
resonant, by N_2^+, **15**,1801
resonant, electron, by metastable nitrogen, **31**,843
resonant, sunlight in atmosphere, **19**,377
shock fronts,
electron densities, chemical and flux effects, **3**,99
oxidation rate of metals in high temperature gas flows, **3**,31
radiation, from O_2, N_2 and air, **3**,132
relaxation, thermodynamic, of atmospheric gases, **3**,113
spin change, H-H collisions, **14**,929
spin change, O-H collisions, **14**,937
snows, cometary, experimental properties, **18**,709
transition probabilities,
hydroxyl, importance for airglow, **37**,723
ionized p^2 and p^4 configurations, **13**,1131
OI 557.7nm emission, measured, **17**,1297
oxygen bands, nightglow, **36**,869; **37**,881
transport properties,
calculations, intermolecular potentials, **3**,205
diffusion coefficients from vapour trails, **8**,35
diffusion, gaseous, high temperature, intermolecular potentials, **3**,221,228
energy, gases at high temperature, **3**,238
hydrogen, **3**,236

mobilities of O^+, N^+, O_2^+ and NO^+ in O, N, O_2 and N_2, **18**,137
mobility, ions, nitrogen afterglow, **13**,667
water nucleation in spacecraft debris clouds, **18**,1387

RING CURRENTS
see CURRENT SYSTEMS

SATURN
atmospheric circulation, **14**,669; **20**,607
atmospheric superrotation, **31**,1339
auroral ions, electrons, outer magnetosphere, **38**,1295
brightness temperature, r.f. emissions, **14**,15,1017
eddy mixing coefficients, **30**,849
magnetosphere, asymmetry of tail region and IMF, **30**,1061
photographic survey, northern hemisphere, **36**,1381
rings, collisionless, **29**,1137
rings, formation and composition, **16**,1511; **17**,1312
rings, Voyager measurements, evolutionary implications, **34**,145
Titan, atmospheric origin and evolution, **30**,833,839
Titan, ion-molecule reaction rates for modelling, **32**,1301

SCALE HEIGHTS
atmosphere, terrestrial, see ATMOSPHERE, TERRESTRIAL

SCINTILLATIONS
see RADIO WAVES

SEEDING
beam injections,
AMPTE, solar wind-magnetosheath shock, **37**,1227
beam dynamics, **40**,153
electrons, accelerator, mother-daughter rockets, **36**,1509
electrons, auroral streaks, echo detection studies, **34**,411
electrons, ELF electric turbulence, **36**,235
electrons, em wave emission, **35**,11
electrons in ionosphere, Cerenkov emission, **18**,777
electrons in magnetosphere, conjugate echoes, **23**,1431
electrons, interaction with neutral gas, **35**,1123; **36**,399,469
Langmuir turbulence and plasma discharge, **40**,535
plasma interactions, **40**,143,1581
Polar 5, beam stimulates generation of waves, **28**,1131
Polar 5, charging, discharging of vehicle, **28**,291
Polar 5, electron accelerator, **28**,259
Polar 5, production of 391.4nm emission, **28**,309
Polar 5, scattering in atmosphere, **28**,279
spacecraft charging, **28**,291; **40**,153
chaff
D-region properties from cloud analysis, **20**,877; **21**,1131
needle satellites, orbit studies, **9**,153
chemical releases,
AlO bands, atmospheric density, **19**,1193
AlO bands, vibrational spectra, atmospheric temperatures, **12**,567; **15**,199; **19**,233
Ba^+, ionospheric dynamics, **15**,1,357; **19**,1,1095; **31**,849; **32**,1045
BaO spectra, temperatures, **17**,261; **19**,1,233, 669,1625
Ba cloud, (AMPTE), solar wind motion, **35**,493; **37**,1227
Ba clouds, emission rate calculations, **37**,1441
Ba clouds, ionospheric drifts and *Sq* currents, **21**,1237
Ba clouds, model, **21**,643
Ba clouds, lidar detection, **20**,440
Ba clouds, radiative transfer, **20**,663
Ba clouds, resonance fluorescence, **30**,897
Ba clouds, striations, **22**,67
CO_2 in F-region, OI(630.0nm) equatorial enhancement, **32**,1605
Cs in D,E-region, electron clouds, **2**,17,174,228
concepts and techniques, **1**, 227,291
dispersal of injected gases, **26**,605
expansion of neutral gas into vacuum, **19**,461
grenades, diffusion of, atmospheric density, **12**,317
grenades, spectra of luminous clouds, **11**,733
grenades, TMA and aluminium, thermospheric properties, **21**,1237
grenades, turbopause location **15**,811
ion clouds, spherical diffuse motion, **20**,149
ion clouds, velocity of neutral winds, **19**,1
Li cloud, (AMPTE), velocity distribution function, **35**,965; **37**,1227
Li ions, geomagnetic tail, **33**,685
Li, vapour trails, winds, **19**,1319
metal releases, interplanetary studies, **13**,95
metal vapors interaction with oxygen, **21**,89
metallic emissions, dynamics, **10**,117
Na, atmospheric density and temperature, **5**,84,185
Na, diffusion coefficients from vapour trails, E-region, **8**,35
Na, electron clouds, E-region, **2**,174; **2**,71
Na, vapour trails, winds, **11**,1309, 1311,1319; **19**,1319; **31**,369
NO at 100km, **14**,53
NO, stratospheric, meteorological circulation, **23**,247
nuclear explosion, *see* NUCLEAR EXPLOSION
observation methods, **20**,1348

potassium at 121km, **1**,306
shadow height of Earth, **16**,1071
Sr, cloud characteristics, **15**,357; **18**,1107; **20**,165
survey of physics, experiments and results, **3**,139
turbopause location, mixed vapour trails, **15**,811
volcanic, stratospheric ions from El Chichon, **32**,17

SHUTTLE
see SPACECRAFT, shuttle,

SILICON
ions in atmosphere, **29**,307; **30**,499

SKY BRIGHTNESS
rf field temperature, dipole measurements, **8**,68

SODIUM
chemical releases, see CHEMICAL RELEASES
mesospheric, concentration, D-line emissions, **18**,623; **26**,65
mesospheric, double-peaked layers, **37**,657
mesospheric, investigation by lidar, **25**,1093; **26**,511; **30**,169
mesospheric, seasonal variation, **27**,909
mesospheric, steady state model, implications, **34**,603; **40**,1607
photoionization cross section, **12**,729
sudden atmospheric layers, **40**,247

SPACECRAFT
ablation,
ammonium chloride, fabrication and evaluation, **4**,479
heat flow, materials and surface design studies, **4**,436,447,463,479
low Earth orbit, **36**,1497
plastics at high temperature, **3**,61,68,73,82,83
protective shield studies for manned vehicles, **4**,411,422
vaporization and thermodynamic properties of oxides, **3**,12
vaporization of refractory substances, **3**,24
aerodynamics,
aerodynamic lift, effect on orbits, **12**,1009; **33**,479
bow shock structure, **31**,615
drag coefficients, **13**,929
dynamic loading from liquid fuel motion in missile tanks, **4**,313
eddy torques, spin decay, cylindrical bodies, **26**,721
implications for atmospheric composition measurements, **36**,921
libration of satellite, **5**,83
motion relative to centre of satellite mass, **5**,79
pitching and yawing of nosecone configurations, **4**,328
rotation axis of tumbling cylindrical satellite, **27**,885,891
theory of dynamic effects, **5**,238
wake structure and effects, **18**,901,1843
antennas, see ANTENNAS
biology,
bioastronautics experiments, **7**,356,378
closed ecology systems, **7**,345,370
dog Laika in Sputnik II, **5**,80
human engineering, **7**,395
impact tolerance of mamals, **7**,386
man in space, **7**,301,309,345; **15**,1267
micro-organisms, viability in vacuum, **8**,30
space simulators, **7**,324,335,345
computers,
BIAX high speed magnetic element, **7**,184
missile simulation, **7**,179
design criteria,
aircraft launched satellite vehicle, **4**,249
cost effects on multi-stage rockets, **4**,242
Explorer XVII, instrumentation, **13**,593
spin stabilization of Able space probes, **4**,262
structural vibrational comparison of captive and free missile, **4**,301
vibration testing, support conditions and shaker arrangements, **4**,285
experiments,
see also SHUTTLE
AMPTE, ion releases at magnetosheath, **37**,1227
atmospheric structure, **5**,81,85; **9**,351; **13**,599; **23**,323; **25**,499
atmospheric temperatures, **7**,423,434; **13**,599
beam experiments, Polar 5, *see* SEEDING
cosmic rays, polar orbiting, **15**,1169
cosmic rays, synchronous satellite, **19**,1419
dayglow observations, **36**,963
electric field, magnetosphere, **20**,859; **30**,261
electron beam into atmosphere, **23**,1431; **36**,399,1509
electron content, ionosphere, **20**,11,353,395; **22**,1309; **26**,1179
heavy ion observations, **30**,1229
hydromagnetic waves, **30**,1209; **33**,365
injection events and plasmapause discontinuity, **30**,483,657
meteoritic dust impact data, **2**,121; **7**,417
mother-daughter pair, beam plasma study, **36**,1509; **39**,453
observation of faint sources, **17**,1089
occultation, planetary electron density, **20**,822
orientation measurements, **7**,445
ozone, effect of aerosols, **22**,1035
particle and magnetic field data, **22**,25
Phobos mission to Mars, **39**
plasma density, **22**,1041
pressure guages, adsorption effects, **15**,1329
probe, display of plasma parameters, **29**,1345

shuttle, electrical behaviour of tethered systems, **29**,139
shuttle, environmental plasma measurements, **32**,457,881
telescopes, particle anisotropies in space, **25**,799
tomography, rocket into auroral arc, **39**,895
trapped radiation at high altitudes, **7**,411
weightlessness, emptying, filling vessels, **11**,1343
guidance,
autopilot design, structural constraints, **7**,26
inertial components for astro-fixes, **7**,19
interplanetary space, theory, equations, **8**,97
manoeuvres with continuous thrust, **15**,103
navigation, round-trip, Venus to Mars, **7**,40
optical, vertical azimuth transfer, **7**,108
orientation measurements, **7**,445
powered-flight phase, interplanetary and lunar vehicles, **7**,64
rotation, influence of oblate Earth, **8**,173
stellar navigator, interplanetary, **7**,57
unmanned soft landings on moon, **7**,70
interactions with environment,
adsorption, effect on pressure guage measurements, **15**,1329
aerodynamic effects on composition measurements, **36**,921
bow shock structure, **31**,615
charging, discharging, **28**,291; **40**,153
effect on mass determination by mass spectrometers, **27**,1213
impact ionization and floating potential, encounter with Halley's comet, **33**,667
gas-surface interactions, **39**,729,1405
glow, surface, production of LBH N_2 bands, **38**,555; **39**,469; **40**,481
glow, *see also* shuttle
induced currents and orbital pertubations, geomagnetic field, **5**,85
ion releases, solar wind precipitated, **37**,535
meteoroid impacts on Gemini windows, **18**,953
outgassing, etc., local cloud implications for observations, **17**,143,1089
particle impacts, new analysis, **38**,567
pertubation, gas medium, satellite, **5**,81
plasma flow-past, **13**,285; **15**,155,463,1203, 1479,1489,1499,1847; **20**,1788, 2193; **22**,121,379; **27**,145,379; **29**,1345; **32**,457,881
potential discharge by positive ions, **35**,105
potential of metal sphere in space, **9**,259; **14**,1131; **17**,693
probe-plasma interactions, **29**,565; **40**,1063
radiation pressure, solar, effects, **18**,1499
radioactivity, induced by cosmic rays, **11**,167
ram, wake, measurements of plasma, rocket, **38**,653
reactions, see also REACTION KINETICS
sputtering, air impact on satellites, increased ionization, **5**,115
thermal impact, response of solids to intense radiation, **7**,427
wake characteristics in bi-thermal plasma, **18**,1843
wake effect, electron temperatures, **23**,1081
wake effect, ion distribution, **29**,975; **35**,1477
wake effect on antenna impedance, **18**,901
wake effect, plasma energization during beam injection, shuttle, **34**,555
wake effects in ionosphere, sounding rockets, **38**,395,653
water vapour nucleation in spacecraft debris, **18**,1387
orbit analysis,
aerodynamic resistance, pertubations, **5**,84
altitude determination, matrix transformation, **20**,1607
atmospheric densities, **1**,115,136,184,259; **5**,79, 314; **9**,529; **11**,261,1273; **12**,1111,1179; **13**,693; **18**,309,387,1573; **19**,297,685,1637; **20**,473,891, 1077,2153,2165; **22**,391,509,1045,1269; **23**,323, 1003,1301; **25**,1011; **26**,291,913; **27**,1361; **29**,35, 579,989; **30**,909; **31**,1501; **33**,23,721,735,965, 1125,1417; **35**,161,921,1039,1127; **38**,637
atmospheric oblateness, **29**,35
calculation methods, densities, **5**,314
capture, three-point circle problem, **5**,83
circular, calculation criteria, **9**,557; **14**,433
debris trajectory analysis, **40**,641
dynamic programming solution to trajectory problems, **7**,176
equations of disturbed Kepler motion, **8**,79; **12**,705,1001
equatorial, **11**,553
evolution, descriptive parameters, **12**,255
geophysical implications, **25**,511; **27**,1247
geostationary, perturbations, **11**,1325; **12**,283; **38**,241
gravitational perturbations, **5**,84; **7**,154; **8**,43; **9**,719; **11**,797,1325; **12**,289; **13**,1151; **14**,433; **17**,1505; **18**,1499; **20**,1213; **22**,645; **23**,229, 541,565,1239; **24**,711; **25**,337,343; **26**,611; **28**,1059; **30**,5,73,411; **33**,97,223,1145,1439; **34**, 47,58,183,1307,1319; **35**,79,937,997; **36**,449,569; **37**,351,693,795,805; **38**,407,1147,1409,1469; **39**, 685,961,1549; **40**,847
lifetimes and latitude effects, formulae, **2**,212; **14**,107; **15**,1549
lunar and solar influences, **9**,479; **14**,361
lunar satellite orbits, classification, **16**,285
lunar trajectories, **8**,107
miss distance, interplanetary missions, **7**,125
needle satellite belts for rf communication, **9**,153
new techniques, **24**,1
oblateness of Earth, pertubations, **5**,84
orbital decay, **14**,849; **16**,581
orbital elements and ephemerides, **12**,21,1121; **13**,1283; **14**,451,1173; **15**,775

orbital plane, rotation, **19**,1215; **20**,1797
orbital theory, large area-to-mass ratio, **11**,553
orbital transfer theory, **7**,132,164; **12**,17,639,721, 891; **13**,147,1233; **14**,773
orientation in space, optical method, **11**,1111
pertubation by solar radiation, **25**,809
position determination, computation and cameras, **12**,37
resonance with longitudinal gravity, **15**,53, 1829
rotation, atmospheric, effect of, **17**,217; **18**,1433,1585
rotational speed of upper atmosphere, **12**,835; **13**,169; **15**,775; **18**,1433,1585; **22**,1565; **23**,1003,1369,1573,1659; **29**,579,989
scale heights from orbit contraction, **11**,633; **12**,661; **13**,851; **16**,409; **35**,161
shadow and sunlit periods, **8**,159
Sputnik 1 rocket, re-entry, **1**,37, and spin decay, **1**,43
Sputnik satellites, dynamics and orbits, **5**,80
thermal accommodation coefficients, **29**,1089
trajectory charts and classifications, **7**,118; **9**,47
trajectory, gravitational field, **8**,86; **9**,491
trajectories for continuous propulsion, **7**,145
triangulation, ground observations, **11**,395
wind estimations, **23**,726; **25**,313; **31**,509; **35**,161; **36**,1085

power systems,
arcing at high altitudes, **7**,11
auxiliary, requirements for satellites, **4**,202
payload, from magnetospheric plasma, **25**,617
polonium thermoelectric generator, **4**,226
solar batteries, **5**,83
static inverter, design and performance, **7**,1

propulsion,
combustion chambers, fabrication, **4**,14
exhaust gas-jet expansion, high altitude, **4**,77
exhaust nozzle design, optimum thrust, **4**,92
fuel burn and bias, maximum range, minimum residual, **4**,34
fuel burn and bias, clustered rockets, **4**,194
fuel reservoir in space, air scooping vehicle, **4**,159
hydrogen peroxide attitude control system, **4**,184
non-chemical rockets, working fluids, thermodynamic performance, **4**,111
non-destructive testing, solid propellant, **4**,1
nuclear rockets, **4**,145
plasma accelerators, **4**,102,133
ramjet, atmospheric atomic oxygen, **4**,60
relativistic space flight, **11**,485
shaped charges for metal cutting, implications for solid propellant rockets, **4**,45

re-entry,
dynamics and thermodynamics, **4**,382; **40**,641
flight data analysis, epicycle techniques, **4**,486
hypersonics, see HYPERSONICS
rotation of orbital plane, **19**,1215
vehicles returning from satellite orbit, **4**,399

reliability,
ballistic missile systems, **7**,208
large solid rocket engines, **7**,217
monitoring and predicting, analytical techniques, **7**,230
random failure analysis, **7**,242

shuttle,
electrical behaviour of tethered systems, **29**,139
environmental plasma measurements, **32**,457,881
glow from surface-catalysed reactions, survey, **34**,665
glow, IR, excited NO as source, **33**,1119
glow, surface induced chemiluminescence, **34**, 421,879,1159; **35**,1367; **38**,555
heating of electrons in local turbulence, **33**,1023
ions from ambient-contaminant interactions, **33**,945; **38**,395,653
local neutrals and ions, contaminants and glow, **33**,421; **35**,501,1463
material changes in space, **34**,219
noise emission, electrostatic, **35**,1373
plasma parameters in vicinity, **34**,993; **36**,841; **37**,1001
spectrometry of atmospheric gases, **36**,291
wake effect, plasma energization during beam injection, **34**,555

signal propagation,
antenna impedance, satellite wake effects, **18**,901
antenna, transmitting characteristics in plasma sheath, **6**,116
auroral transmission and lunar reflection of UHF signals, **7**,272
beacon signals, electron content, ionospheric, **19**,1505
Faraday effect, influence of motion, **15**,1313
grid-sphere satellite, orbital behaviour, **16**,419
interference effects due to re-entry plasma sheath, **6**,1,207; **7**,286
ionization irregularities in magnetosphere, **13**,1255
long range, HF trans-ionospheric, **26**,37
microwave interaction with plasma sheath, **6**,100,105,186,196
occultation by planets, **18**,1769; **20**,822
pertubations, atmospheric phenomena, **1**,130; **5**,169,213
radio communications, **7**,254; **14**,155; **22**,1331
refraction in ionosphere, **20**,2015
resonant heating of ionospheric plasma, **38**,173
scintillations, ionospheric, **13**,51; **18**,1785; **19**,1588; **20**,957,965; **22**,617

surveys,
data on Soviet vehicles, **11**,277
experiments on IGY rockets and satellites, **1**,71
rocket research in Japan, **9**,355
space experiments, 1958 URSI meeting, **1**,238

tables of launchings,
1957-62, **11**,1053
1958-65, **14**,1167
1963, **12**,681
1964, **13**,707
1965, **14**,817
1966, **15**,1181
tracking,
echo area of plasma coated sphere, **6**,133
Doppler effect for orbital parameters, **5**,79; **9**,607
equivalent stellar magnitudes, flashing, tables, **12**,597; **13**,541
ground guidance, communication system, **7**,94
ground-satellite observation agreement, **38**,1533
isophote of transit, astronomical seeing, **15**,1799
laser ranging system, **38**,471
location by expectancy method, **5**,84
location for occurrence of scintillations, **22**,617
object crossing sun, **16**,818
optical characteristics, **5**,79,233; **12**,261; **13**,1289; **14**,839,1281; **15**,1535,1895; **19**,851
pass coverage from ground station, **14**,617
photographic, fast, large cameras, **7**,76; **9**,787
radar cross-section, plasma sheath effect, **6**,123
radar, Millstone, **7**,81
time recording of satellite photography, **11**,161

SPACE FLIGHT
lunar orbits, **11**,111
relativistic, to galactic civilizations, **11**,485

SULPHUR
ionization by electron impact, model, Io, **30**,1269
SO_2 dissociative excitation by electron impact, **31**,197

SUN
activity, general,
atmospheric absorption, chemical response, **25**,1
correlation, atmospheric airglow, **17**,1322
correlation, atmospheric density changes, **16**,675, 937,1161,1427; **17**,1581
correlation, ionospheric spread-F, **22**,1597
correlation, Lyman-α variability, **29**,907
correlation, Jupiter's decametric rf, **16**,1147; **20**,2051; **26**,1193
correlation, satellite rotation period, **12**,1121
correlation, Venus ionosphere, **17**,1923
descriptive indices, **12**,349
historical review of effects, **12**,333
indices, **31**,977
influence of solar and interplanetary sector structure, **21**,2003; **22**,1173
photospheric magnetic fields, **33**,863
SIDs, listing of observations, **12**,419
tropospheric influences, **12**,219,327,333
upper atmosphere influences, **12**,355; **17**,1581; **21**,1835; **33**,863,1451
violent disturbance, VLF emission, **16**,1081
corona,
effect of solar activity cycle, **14**,255
expansion, evidence of particle streaming, **12**,451
green line (530.0nm), cosmic ray correlation, **18**,81; **21**,1661
green line, geomagnetic activity, **22**,841
green line, solar magnetic sector structure, **21**,703
holes, solar plasma flows, **38**,459
hydromagnetic shocks, proton radiation, **13**,789
investigation by occultation of radio sources, **18**,1213
ion streams in solar wind, **29**,1235
mass ejections, **39**,737
noise storm spectra, cyclotron radiation, **14**,1139
structures, and recurrent geomagnetic patterns, **24**,381
transformation of plasma waves into em waves, **18**,479,867
corpuscular radiation,
chromospheric eruption, **9**, 507
continuum emission from, **21**,17
coronal expansion, **12**,451
correlated radio bursts, **12**,435
electrons, relativistic, flares, **18**,81
eruptive flows, sources, **39**,1031
events, exponential decay, **25**,1081
neutral hydrogen, energy source for geomagnetic storms, **12**,801,905
pertubation of satellite orbits, **25**,809
plasma characterisation of geomagnetic storms, **12**,87,573
plasma injection mechanism into magnetosphere, **12**,209
plasma, neutral hydrogen component, **14**,809
polar ionospheric disturbances, **5**,59
polar winter vortex, **14**,523
propagation in interplanetary space, **13**,435
protons, diffusion coefficient at bow shock, **21**,971
protons, diffusion mean free path, **19**,95
protons, flares from sunspots, **18**,33
protons, flares, oblique shock, **18**,333
protons, flares, radio bursts, **19**,1685
protons, flux anisotropies, **19**,533
protons, hydromagnetic shocks in corona, **13**,789
protons, into magnetosphere, **20**,89,1979,2113; **25**,1111
protons, PCA, **13**,583; **19**,1541; **20**,271,1835
protons, propagation in IMF, **13**,745; **14**,131; **17**,1313; **21**,23
protons, showers, plasma density variations, **35**,487
protons, temperature properties, **35**,185
trajectory calculations, **19**,1016
cosmic rays,
airglow-aurora intensity ratio, **12**,665
anisotropic diffusion, **13**,1301

cosmic noise absorption, **14**,277
diurnal variation over long term, **23**,961
Forbush decrease, **13**,435; **14**,791,979; **16**,1081, 1095; **17**, 1917; **19**,981
intensity, composition, **9**,195; **11**,427; **12**,665
intensity, coronal green line as monitor, **18**,81; **21**,1661
intensity, modulation influences, **17**,909,1173, 1749;**28**,177,195
interplanetary magnetic field effects, **15**,975
magnetic field polarity dependence, **37**,1421
nuclear abundance and rigidity spectra, **13**,867
cycle,
atmospheric variations, semi-annual, **18**,1051
atmospheric variations, 27 day, **18**,387
aurorae at solar maximum, **18**,1850
conductivity variations in ionosphere, **16**,353
correlation with coronal effects, **14**,255
cosmic ray anisotropy, **16**,29; **18**,81,509; **19**,981
gamma radiation in atmosphere, **18**,939
heliospheric oscillation, **30**,307
influence on mesospheric temperatures, **33**,795
K_p-index variations, **22**,537
lunar magnetic variation effects, **21**,1923
nightglow variations, **16**,1311; **17**,797,879; **18**, 641
scale heights at sunspot max and min, **16**,409
eclipse,
flux attenuation, **29**,601
Lamb wave generation, **21**,1843
long term geomagnetic effect, **30**,587
observation at 100 cm wavelength, **16**,363
spectrophotometry of dayglow, **12**,875
X-ray penetration to lower ionosphere, **11**,1489
electric charge, **5**,70; **11**,1501
flares,
auroral consequences of, **18**,525; **32**,925
center-limb effect on cosmic ray and geomagnetic storms, **13**,435
class 3, associated sunspot activity, **13**,163
class 3B, VLF and other disturbances, **16**,1081
consequences for zodiacal light, **23**,1329
enhancement of nightglow green line, **12**,867
EUV observations, Phobos mission, **39**,39
geoeffectiveness, new classification, **38**,189
geomagnetic phenomena, **11**,597,897; **12**,393, 419,657; **17**,1183; **30**,1183
hydromagnetic shocks, coronal, **13**,789, **16**,309,1483; **33**,1251
IMF associations, **36**,669
magnetic field lines, reconnection rate, **23**,813
neutral gas glow, interplanetary space, **37**,369
nightglow association, **24**,99
origin of, **19**,1289
particles, electrons, relativistic, **20**,1229
particles, heavy nuclei, acceleration, **23**,955
particles, high energy, **21**,793
particles, protons, **18**,33,333; **19**,1685
shock wave and magnetic bottle, **22**,493; **24**,951
streams, configuration at 1AU, **35**,793
X-ray flux and D-region recombination, **21**,367
interior, revised model with neutrino spectrum, **12**,119
ionizing radiation,
absorption, photodissociation, atmospheric, **24**, 589; **29**,951; **30**,67
airglow effects, **13**,947; **16**,1311; **17**,879,1322
atmospheric density changes, **16**,1427
atmospheric heating and geomagnetic activity, **16**,231,1531; **17**,815, 1737; **18**,1745; **20**,1745,1761; **33**,1451
current knowledge and future needs, **26**,347,355
D-region evidence for, **15**,1035
D-region ionization, X-rays, **17**,609,1855
radiances, measured, **31**,977,987,1001
radiation pressure on satellites, **18**,1499
resonance scattering by N_2^+, **15**,1801
thermospheric variations, **17**,1581,1709; **18**,1255
twilight effects, **14**,1321
M-region,
nature of, **14**,1193; **15**,1603
shocks, recurrent geomagnetic storms, **11**,505; **12**,113,487; **13**,675,1111; **23**,143
travel times associated with activity centres, **15**,941
magnetic field,
field configuration, **29**,313
field lines, reconnection rate, **23**,813
field polarity, and cosmic rays, **37**,1421
field, sunspots, coronal holes, **37**,1027
quasi-periodic variations, **40**,741
sector structure, inferred from storm statistics, **21**,2003
parallax, **5**,71
polar-cap absorption, **12**,495; **15**,1111,1667; **23**, 787,935
radio activity,
absorption, refraction and scintillation, **1**,50
air density increases, **17**,985
auroral and magnetic disturbances, **1**,325,223; **11**,608,897
auroral luminosity, radio star visibility fades, **16**,1155
bursts and corpuscular radiation, **12**,435; **13**,781
burst, type II, **13**,781
burst, type III, data, theory, **17**,267; **18**,867
burst, type IV, proton flares, **19**,1685
corpuscular emissions, correlation, **12**,435; **17**, 1449
cosmic rays, correlation, **2**,104
eclipse observation at rf 100 cm, **16**,363
decimeter flux, **15**,231; **17**,181,1737; **18**,1850
solar-terrestrial models, applications software, **40**,541
solar tides, induced heating in atmosphere, **33**,283
solar tides, thermal, airglow variations, **25**,711

solar wind,
alpha particle heating and acceleration, **38**,1305
asymmetries, interstellar wind causes, **38**,383
auroral oval, **18**,501; **27**,973
Chapman-Euskog model, **25**,203
characteristics, review, **12**,463; **17**,295
Compton-Getting anisotropies, **21**,1802
coupling function to magnetosphere, **38**,627
degradation by interplanetary dust, **15**,593; **17**,155; **20**,1949
effect on polar cap electric field, **29**,205
effect on solar rotation, **16**,1
energetic particle fluxes, **39**,57,557
energy changes in cosmic rays, **15**,975,1375; **16**,15,818
expansion beyond heliosphere, **20**,445
expansion, including heat-loss function, **22**,1637
flare origin, structure, **15**,39,942; **31**,1435
flow characteristics at sector boundaries, **36**,1025
geoactive zones, **23**,627
geomagnetic bay development, **17**,1795
heating of interplanetary medium, **31**,1157
heliospheric current sheet, **39**,1123
H and He^+ content, **20**,841
hydrogen, consequences at Earth, **14**,95
hydrogen, consequences at Venus, **12**,1143
hydrogen, outside heliosphere, **16**,783
hydromagnetic flow around magnetosphere, **14**,223,1207; **18**,1,1143; **25**,201
hydromagnetic pulsations, associated, **28**,535; **33**,933
hydromagnetic shocks, **16**,309,1483; **35**,329
ion streams related to coronal conditions, **29**,1235
interaction with comets, **12**,719; **15**,137; **17**,1413; **21**,1647; **24**,289
interaction with geomagnetic field, **12**,1187; **17**,1183; **18**, 1381; **20**,1909; **30**,669,1079; **35**,329
interaction in interplanetary region, **28**,799; **35**,271
interaction with ionosphere, **18**,1832; **38**,1479
interaction with large obstacles, **16**,145; **26**,99; **35**,1221
interaction with lunar atmosphere, **12**,1075
interaction with neutral and ion exosphere, **21**,2181
interaction with magnetosphere, **11**,505; **12**,45, 113,209,227; **15**,787; **16**,587; **17**,333; **18**,407; **21**, 499,1191; **22**,1075; **23**,27,75,817; **26**,229; **27**, 47,1055,1087; **28**,495,823,933; **30**,81,367,371,537, 627,1007; **31**,247; **33**,891,1091; **38**,627,765,841
interaction with planets, atmospheres, **15**, 515; **17**,595; **18**,1281; **21**,463,507,1475,1647; **22**,1501; **25**,621; **27**,243,1111; **35**,1213; **38**,539; **39**,75,123; **40**,121,131,1033
K_p index correlations, **21**,2139; **30**,1079
large-scale properties, variations, **40**,741
latitude effects, **22**,439
lunar magnetic field, induced, **17**,685
lunar magnetic tail and wake, **16**,142
lunar surface observations, **20**,1577
magnetic classification of streams, **27**,1451
magnetic clouds, **35**,329
magnetic N-S asymmetry, geomagnetic effects, **39**,751
magnetospheric wake, **17**,321; **18**,1143
mass loss, wind induced, magnetic-field free planets, **19**,1580; **27**,243
Maunder Minimum, **27**,1001
model equation (two fluid), viscous solutions, **24**,799
plasma streams, **22**,841; **33**,831; **36**,205,775, 1343
plasmoids into geomagnetic field, **40**,193
power spectrum of irregularities, **21**,1367
pressure variations, field-line resonances, **38**,1517
proton acceleration by coronal shock waves, **13**,789
proton velocity distribution, **14**,1207; **38**,1091
pulsations, correlated ground measurements, **26**,547; **40**,1399
radiation pressure at Venus, **37**,1063
rotational discontinuities, **19**,1693; **21**,475,1571
scintillations due to plasma irregularities, **16**,749; **17**,189,313; **18**,95; **21**,1617; **35**,271
shock front, location in IMF, **19**,1121; **36**,301
southward motion, magnetic cause, **35**,493
speed, heliographic structure, **36**,1329
speed, transverse velocity in, **17**,909
sputtering and erosion of planetary bodies, **11**,885,1257; **28**,511
streaming pattern in declining activity, **37**,297
structure and ion-temperature anisotropies, **18**,321
structure, relationship with corona, **39**,1351
tail associated phenomena, **39**,1039
tangential discontinuity, distribution, **24**,621,1043
temperature anisotropy, **17**,1009; **19**,1609
three fluid model, **18**,199
transport equations, bi-Maxwellian, **39**,435
transients and interplanetary shocks, **36**,301
transition zone, **14**,143
velocity fluctuations, **19**,421
wave generation at bow shock, **24**,261
spectrum,
continuum rf from energetic particles, **21**,17
corona, **12**,55;
cyclotron radiation, coronal noise storm, **14**,1139
HeII (30.4nm) backscattered from interplanetary He^+, **21**,1795
helium emission, far UV, **11**,73
hydrogen L_γ absorption by N_2, **12**,656
in region of 557.7nm and 630nm, **15**,945

irradiances between 120 and 900nm, **37**,1249
Lamb waves generated by solar eclipse, **21**,1843
microwave bursts and PAC, **21**,707
microwaves, flares, origin in pion decay, **15**,1303
neutrino, revised model of interior, **12**,119
radiation inferred from cosmic ray modulation, **28**,177,195
rf emission, 4700 MHz, terrestrial data, **1**,50
skylight during partial eclipse, **16**,647
solar limb effect, extreme red shift, **19**,659
sunspots,
activity, and spread-F, **23**,899
cycle, stratospheric ozone modulation, **23**,247
cycle, tropospheric influence, **12**,327
magnetic field stability, **19**,1289
maximum, heating effect, **15**,1821
maximum predicted from preceding minimum, **29**,73
max and min, effects on air density scale heights, **16**,409
plasma outflow from coronal holes, **37**,1027
vertical distribution, **33**,275
Yule analysis, auroral associations, **36**,99
UV radiation, **9**,969,977; **11**,73,333; **12**,167,379
X-rays, **9**,969,977; **11**,61,1489; **12**,167; **13**,807; **15**,231,681,931,1035; **17**,609,1855; **19**,1069; **21**,367; **32**,31; **39**,1,7,13,15

TELESCOPES
micro-meteorite impact damage on optics, **12**,77
optimum resolving power in UV, **5**,207
satellite tracking, **12**,261

TIDES, ATMOSPHERIC
airglow emissions, **25**,711; **27**,1409; **32**,897; **35**,1389
classical theory, (1,1,1) type oscillations, **31**,67
classical theory, vertical structures, **30**,219
dissipation, effect of mean winds, **37**,197
dissipation, upward propagation, **37**,669
diurnal, associated energy fluxes, **31**,67,1183; **36**,579
electron density, lunar-solar effects, **19**,1349
evidence for, **5**,196
generation of electric-potential field, **22**,569
gravitational-thermal theories, **10**,79
ionosphere, incoherent scatter, **20**,1269
ionospheric dynamo, **18**,121,423,1075,1091
lunar, middle atmosphere, **18**,367,1075; **35**,445
mesosphere and thermosphere, **30**,1283
meteor zone, **14**,1253
middle atmosphere, radar data, **32**,1087; **38**,1431
modulation effects, **20**,1613
partial reflection drift observations, **25**,441
solar effects, **18**,1091
stratopause, hemispheric similarities, **16**,1011
S_q currents, **17**,471,889; **18**,121,423,1075,1091
thermal, effect of turbulent dissipation, **32**,1559

TIDES, OCEANIC
sea, geomagnetic variations, **18**,1597

TRAPPED PARTICLES
see RADIATION BELTS

URANUS
aurora, Faraday dics dynamo mechanism, **31**,1187
bow shock, energetic particles, Voyager, **36**,311
condensable species, abundance at cold trap, **37**,151
internal constitution, **15**,1609
magnetic dipole, inclination, eccentricity, **39**,1259
magnetic tail, neutral sheet topology, **19**,483
model atmosphere, **21**,1601

UREY EQUILIBRIUM
temperature dependence, **11**,1303

VAN RHIJN FORMULA
see AIRGLOW, NIGHT

VENUS
accretion of ions from solar wind, **40**,121,131
aeronomy, some problems, **23**,763
airglow, EUV emissions, Venera spacecraft, **29**,149
airglow, night, terrestrial-based observations, **1**,32; **5**,163; **16**,343
Ashen light, **16**,1417; **17**,1081; **19**,1049
atmospheric composition,
cloud composition, **33**,109
CO_2, **8**,23; **11**,1303
density, escape of atomic isotopes, **26**,949
dust ring, satellite observations, **27**,951
hydrogen, exospheric distribution and escape, **32**,1235
hydrogen, non-thermal, **26**,817,1063
image intensifier, solar specrograph, **15**,1211
ion density and chemistry, 55 to 100km, **22**,525
neutral gases, vertical distribution, **11**,269
nitric oxide, **31**,1363
outgassing history, He UV emission, **34**,585
atmosphere-surface interactions, **30**,803
atmospheric evolution, **17**,1021
atmospheric interaction with solar wind, **22**,967; **35**,1213
cloud production, solar hydrogen and Venusian atmosphere, **12**,1143
contribution to zodiacal light, **37**,1141
CO_2 photolysis at 184.9nm and 213.9nm, **19**,1701
dynamics,
circulation and temperature, atmosphere, **5**,141
cloud motions by meteoroid capture, **23**,551
rotation, 4-day, upper atmosphere, **21**,1559
super-rotation, thermospheric models, **37**,701, 707
energy transport in atmosphere, **23**,1293
exosphere structure and solar radiation, **28**,687; **37**,1063

gravitational spectrum, **28**,443
heating efficiencies in thermosphere, **36**,37
ionosphere,
dayside, theoretical model, **19**,443
currents and fields, **29**,635
currents induced by solar wind, **25**,621
effect of solar cosmic rays, **17**,1923
holes, mass spectrometer data, **40**,33
interaction with solar wind, **27**,1111
ionopause, observations of energetic ions, **30**, 1107
nightside chemistry, **27**,1403; **40**,1663
plasma clouds above ionopause, **30**,29
topside, plasma transport, **25**,921
VLF bursts, magnetic field effect, **36**,1211
lightnings in atmosphere, **31**,1363
microwave opacity, dielectric relaxation, **15**,204
radar echoes, solar parallax, **5**,71
radar echoes, determination of astronomical unit, **12**,1129
scale height of haze layer, **15**,1817
solar wind flow past, **18**,1281; **23**,713
temperature,
brightness temperature, r.f. emissions, **14**,15, 1017; **15**,907
microwave temperature, **5**,166
temperature and circulation, **5**,71

VOLCANO
El Chichon eruption, stratospheric ions, **32**,89

WATER VAPOUR
cooling of electrons, rotational, vibrational excitation, **34**,961
mesosphere, ion-induced nucleation, **28**,1003; **30**,55
mesosphere, photodissociation, **32**,871
mesosphere, Spacelab spectrometer data, **34**,1067
microwave measurements, **36**,607
stratosphere, 6-7μm satellite data, **5**,202; **22**,1265

WAVES
atmospheric, basic formulation, **25**,1045
atmospheric, generation by auroral forms, **16**,993
atmospheric, mesosphere and thermosphere, **29**,615; **33**,1013
atmospheric, relaxational dissipation, **25**,1061
auroral, observed, **16**,993,1453
compressional, ionospheric scintillations, **20**,41
electric field component, auroral, **18**,847
electrostatic, Coulomb collisions, space plasma, **18**,155; **24**,1097
gravity,
acoustic, O_3 variations, temperature pertubations, **39**,74
airglow, **23**,896; **25**,200; **31**,331; **33**,381,1013; **35**,413,815; **36**,975; **38**,1105,1431; **39**,1363
auroral thermosphere, **32**,667,685
due to auroral currents, **18**,565
dynamic model, mean flow interaction, **31**,1465
interactions with diurnal tides, **39**,1249
ionospheric, winds, **16**,273; **17**,749; **18**,1793; **19**,561; **20**,613; **21**,147,653; **22**,181,504,505; **23**,487; **28**,119; **37**,967; **39**,1421
mesospheric, photogrammetry and lidar, **30**,611
numerical calculations of wave-fields, **24**,1199
origins in weather disturbances, **23**,493
partial reflection drift observations, **25**,441
photographic evidence, OH emissions, **25**,265
signatures on VHF backscatter radar, **32**,1455
stratospheric lidar studies, **39**,1541
thermospheric composition, photochemistry, **27**,1469
tidal effects and wind oscillations, **38**,1431
vertical, thermospheric, during magnetic storm, **35**,1157
wave-like structures in trace gas measurements, **35**,673
hydromagnetic, *see* MAGNETOHYDRODYNAMICS
infrasonic, auroral generation, **18**,591,599; **22**,151; **27**,1195; **29**,57
ion-acoustic, cause of radio aurora, **16**,449; **18**,1813
ion-cyclotron, **25**,643; **27**,691
magnetosonic, excitation near plasmapause, **23**,279
mesospheric, planetary, tidal and gravity, **25**,441
oscillations, mechanical, atmospheric, **18**,1393, 1719; **20**,1627
plasma, non-linear interaction, **20**,711
radio, *see* RADIO WAVES
wave experiment on satellite, electric and magnetic fields, **27**,317
zonal and meridional, solar tides, **33**,283

WHISTLERS
see RADIO WAVES

WINDS
airglow line widths, **16**,211,431; **17**,957; **30**,1025; **35**,1255; **36**,197,225,677,851; **40**,1599
airglow, spatial emission characteristics, **26**,893
atmospheric helium bulge association, **16**,1103
auroral line widths, **19**,1225
chemical releases, **11**,1309,1311,1319; **16**,159; **19**,1,1319; **20**,761; **23**,973
comparison, Thompson scatter and meteor radar data, **29**,345
cusp region, optical analysis, **33**,305
diurnal, seasonal variations, dynamo region, **26**,705
electrostatic field, radiation belt deformation, **13**,729
exospheric, zonal, satellite orbit analysis, **24**,529; **36**,1385; **40**,223
F region,
asymmetric global pressure system, **17**,97,1097,1269,1691; **18**,1485

atmospheric rotation rate, **16**,557
auroral arc and oval, **33**,373,425,869
cause of downward motion, **19**,1327
correlated with $h'F$, **17**,957
current systems resulting from, **19**,263
drifts and electrical coupling, **22**,743
equatorial, **17**,97,957; **19**,357
F_2 layer shape, **18**,1181
mid-latitude, **29**,1367
polarization fields resulting from, **19**,357
theoretical model, **23**,401
ion trough, supersonic, **20**,1923
ionospheric, **21**,147; **23**,389
ionospheric particles in geomagnetic field, **13**,469
ionospheric warming, **19**,731
meridional, from SAR arc observations, **35**,1077
meridional, incoherent scatter, **39**,657
meteor trail observations, **1**,94; **5**,196; **16**,61; **17**,553; **18**,1623; **20**,301; **23**,389,509; **26**,893
meteorological, *see* METEOROLOGY
morphology of, predawn enhancement, **18**,1335
neutral, E-region, auroral, **24**,541
neutral, electron content of ionosphere, **31**,53,377
neutral, meridional, **24**,69
occultation and refractivity experiment, **22**,789
oscillations and tidal effects, **38**,1431
polar, hydrogen depletion, **26**,873
polar, temperatures, **22**,1193
radiation belt deformation, **13**,729
response to magnetic activity, **33**,461
shear effects, **14**,53; **15**,27; **17**,1207; **21**,653, 1815,1817
shears, radio meteor echoes, **20**,301
sporadic-E ionization, **12**,1173; **13**,1161; **14**,909: **15**,123; **17**,1207; **39**,1421
thermospheric,
auroral electrojet heating, **19**,1010,1225
effect of gravity waves, **22**,181
high latitude, **30**,1095,1259
low g accelerometer measurements, **22**,1036
jet stream, **33**,425
model, 3-d time-dependent, **28**,919
neutral, at 23°, **40**,767
particle precipitation, **30**,1259
related to displaced geomagnetic and geographic poles, **22**,623
rocket and ground-based observations, **28**,919; **31**,303; **33**,305,373,461,817,869,1049; **35**,1255
satellite orbit analysis, **23**,726
storm-time, **20**,511; **40**,595
structure and fluctuations, **38**,675
systematic behaviour, **23**,879
tides, *see* TIDES
zonal, **20**,2099; **22**,391,545; **25**,313; **29**,35,349,505; **31**,509; **35**,161; **40**,223

ZODIACAL LIGHT

brightness integral, inversion, **27**,551,1043; **31**,1381
brightness observations and small-scale structure, **38**,517
brightness variations, solar flare effect, **23**,1329
celestial pole, **13**,1311
characteristics, observations, **11**,1015; **15**,1081
charged interplanetary grains, implications, **17**,155
cloud structure, symmetry surface, **38**,1461
counterglow from Earth-Moon libration points, **23**,173
density, phase function of interplanetary dust, **28**,657
dust cloud, motion of charged particles, **27**,1269
dust cloud profile out of ecliptic, **31**,871
H_β absorption contamination, **16**,795,803
intensity gradient, with heliocentric distance, **23**,1235
light brightness integral, inversion of, **28**,1077
measurement from space probe, proposed, **17**,949
models, colour dependence, **21**,2061
nightglow contamination, O(557.7nm) polarized component, **16**,1291
observations from spacecraft, **17**,143; **21**,2173
optical properties, **21**,513
optical scattering, interplanetary, **15**,1641; **21**,2149
photometry, absolute, **13**,207
photometric axis, observations, **13**,237
scattering along line of sight, **33**,1
Venusian contribution, **37**,1141

SEND FOR A FREE SAMPLE COPY OF...

ACTA ASTRONAUTICA

JOURNAL OF THE INTERNATIONAL ACADEMY OF ASTRONAUTICS

Editor: **JEAN-PIERRE MAREC**, *International Academy of Astronautics, BP 1268.16, 75766 Paris Cedex 16, France*

Acta Astronautica publishes original contributions in all fields of basic, engineering, life and social sciences and of space technology related to:
(1) the peaceful scientific exploration of space
(2) its exploitation for human welfare and progress
(3) the conception, design, development and operation of space-borne and Earth-based systems.
The journal publishes selected proceedings of the Annual IAF Congress in a special volume. In addition to regular issues of contributed papers the journal publishes the Transactions of the Academy and special issues on topics of current interest such as microgravity, Space Station technology, geostationary orbits, and space economics. Other major subject areas regularly covered include satellite technology, space transportation and communications, space energy, power and propulsion, astrodynamics, extraterrestrial intelligence and Earth observations.

A Selection of Papers
P. R. CHOUDHURY & M. GERSTEIN (USA), Particle agglomeration and fuel decomposition in burning slurry droplets.
H. T. HEMDAN (Saudi Arabia), Hypersonic flows over slender circular cones at small angles of attack.
N. S. VENKATARAMAN & D. G. SEPULVEDA (USA), Thermal resistance in satellite mounting plates due to conductive heat transfer.
A. NAKAJIMA, M. ABE, Y. NISHIO & H. YAHAGI (Japan), Space experiments of Deployable Boom and Umbrella Test satellite (DEBUT).
W. ALBERY & D. REPPERGER (USA), Time and mass perception in non-terrestrial environments.
C. MACCONE (Italy), Relativistic interstellar flight communication theorems.
A. ALDRICH, R. ROSEN, M. CRAIG & J. C. MANKINS (USA), Exploration Technology Program plans and directions.
T. K. YANEV (Bulgaria), Probability density functions of vegetation indices.
A. K. MISRA & V. J. MODI (Canada), Three-dimensional dynamics and control of tether-connected *N*-body systems.

Indexed/Abstracted in: *Appl Mech Rev, Curr Cont ASCA, BIOSIS Data, Cam Sci Abstr, Chem Abstr Serv, Curr Cont/Engng Tech & Appl Sci, Engng Index, INSPEC Data, PASCAL-CNRS Data, Curr Cont SCISEARCH Data, Murdoch Magazine*

(00310)
Subscription Information
1993: Volumes 29 - 31 (14 issues)
Annual subscription (1993) **£810.00** **US$1539.00***
ISSN: 0094-5765

PERGAMON PRESS
Pergamon Press Ltd, Headington Hill Hall, Oxford OX3 0BW, UK
Pergamon Press Inc., 660 White Plains Road, Tarrytown, NY 10591-5153, USA
A member of the Elsevier Science Publishing Group

First price quoted is definitive. Prices include postage and insurance. * Asterisked price is quoted for convenience only and is subject to exchange rate fluctuation.

SEND FOR A FREE SAMPLE COPY OF...

ADVANCES IN SPACE RESEARCH

THE OFFICIAL JOURNAL OF THE COMMITTEE ON SPACE RESEARCH (COSPAR), A SCIENTIFIC COMMITTEE OF THE INTERNATIONAL COUNCIL OF SCIENTIFIC UNIONS (ICSU)

Chairman: **W. I. AXFORD** FRS, *MPI für Aeronomie, Postfach 20, D-3411, Katlenburg-Lindau, Germany*

COSPAR is an interdisciplinary scientific organization concerned with the progress on an international scale of all kinds of fundamental research carried out with the use of balloons, rockets, or rocket propelled vehicles. Operating under the rules of ICSU, COSPAR ignores political considerations and considers all questions solely from the scientific viewpoint. The COSPAR journal *Advances in Space Research* includes the proceedings of COSPAR organized symposia and other scientific meetings organized by this Committee, containing the latest scientific information in this area. Fields covered are: Space Studies of the Earth's Surface, Meteorology and Climate; Space Studies of the Earth-Moon System, Planets and Small Bodies of the Solar System; Space Studies of the Upper Atmospheres of the Earth and Planets, including Reference Atmospheres; Space Plasmas in the Solar System, including Planetary Magnetospheres; Research in Astrophysics from Space; Materials Sciences in Space; Life Sciences as Related to Space. Individual issues of *Advances in Space Research* are self-contained topic research works and available for separate purchase.

A Selection of Issues

M. FULCHIGNONI (Italy), **L. W. ESPOSITO** (USA), **G. NEUKUM** (Germany) & **M. J. S. BELTON** (USA), Planetary Studies.

R. W. SHORTHILL, G. M. KEATING (USA) & **R. LUNDIN** (Sweden), Recent Results on Mars and Venus.

R. TORBERT (USA), Active Experiments in Space.

J. M. FORBES (USA), **F. VIAL** (France), **T. FULLER-ROWELL** (UK), **A. MANSON** (Canada), **W. K. HOCKING** (Australia), **R. R. MEIER** & **C. R. PHILBRICK** (USA),The Earth's Middle and Upper Atmosphere.

R. P. SINGH (India), **A. TABBAGH** (France), **J. F. R. GOWER** (Canada), **W. L. SMITH, A. E.MACDONALD** (USA), **M. J. MANTON** (Australia), **J. PAILLEUX** (UK), **K. TSUCHIYA** (Japan) & **J. DOZIER** (USA), Remote Sensing of the Earth's Surface and Atmosphere.

G. M. KEATING, F. A. HERRERO, S. CHAKRABARTI (USA) & **L J. GRAY** (UK), Middle and Upper Atmosphere Results.

K. RAWER (Germany) & **W. R. PIGGOTT** (UK), Enlarged Space and Ground Data Base for Ionospheric Modelling.

Indexed/Abstracted in: *Chemical Abstracts, INSPEC Data, Geo Bib & Index, Geol Abstr, Geogr Abstr*

(00644)

Subscription Information

1993: Volume 13 (12 issues)

Annual subscription (1993)	**£925.00**	**US$1758.00***

ISSN: 0273-1177

PERGAMON PRESS

Pergamon Press Ltd, Headington Hill Hall, Oxford OX3 0BW, UK
Pergamon Press Inc., 660 White Plains Road, Tarrytown, NY 10591-5153, USA

A member of the Elsevier Science Publishing Group

First price quoted is definitive. Prices include postage and insurance. * Asterisked price is quoted for convenience only and is subject to exchange rate fluctuation.

SEND FOR A FREE SAMPLE COPY OF...

CHINESE ASTRONOMY AND ASTROPHYSICS

Translation Editor: **WANG SHOUGUAN**, *Beijing Astronomical Observatory, Chinese Academy of Sciences, Beijing 100080, People's Republic of China*

The vigorous growth of astronomical and astrophysical science in China led to an increase in papers on astrophysics which *Acta Astronomica Sinica* could no longer absorb. Translations of papers from two new journals the *Chinese Journal of Space Science* and *Acta Astrophysica Sinica* are added to the translation of *Acta Astronomica Sinica* to form the new journal *Chinese Astronomy and Astrophysics.*

"The latest issues of the journal reflect keen interest in new ideas in cosmology - massive neutrinos, phase transitions and elementary particles ....The most impressive articles appearing regularly in the journal are those on the history of astronomy - any scholars with interests in the history of astronomy will find remarkable and otherwise inaccessible archival material published here. All astronomy and history of science libraries should consider subscribing, especially since the subscription is moderate and over eighty articles appear in an annual volume."

Nature

Chinese Astronomy and Astrophysics brings English translations of notable articles to astronomers and astrophysicists outside China.

A Selection of Papers

WANG MIN, XIE RUI-XIANG & WANG CONG-YUN (PRC), Observation and analysis of solar decimetric spike radiation.
QIN ZHI-HAI, LI CHUN-SHENG, WEI SHUANG-LING & CHEN YUN-XIA (PRC), The quasi-periodic fine structures in a solar radio burst at 3.2 cm wavelength on 23 May 1990.
WANG JING-XIU & SHI ZHONG-XIAN (PRC), Direct indication of magnetic reconnection in solar photosphere.
DING YOU-JI & HONG QIN-FANG (PRC), An emerging current/magnetic flux system with delta structure in AR 2372.
LI ZONG-YUN & DING YUE-RONG (PRC), The variation of ultraviolet continuum in 5 Cet and its interpretation.
GAO HENG, CHEN PEI-SHENG, BAO MENG-XIAN & CHEN YAN-KANG (PRC), Infrared properties and evolution of MSC stars.
LUO SHAO-GUANG (PRC), Infrared emission of Canis Major OB1/R1 star forming region.
PAN RONG-SHI, ZHAO JUN-LIANG, CHEN LI, TIAN KAI-PING &
HE YAN-PING (PRC), Photometry and HR diagram of the open cluster NGC 2286.
WANG GANG (PRC), The IRAS colors of galaxies.

Indexed/Abstracted in: *Math R, Astronomy and Astrophysics Abstracts, INSPEC*

(00585)
Subscription Information
1993: Volume 17 (4 issues)
Annual subscription (1993) **£370.00** **US$703.00***
ISSN: 0275-1062

PERGAMON PRESS

Pergamon Press Ltd, Headington Hill Hall, Oxford OX3 0BW, UK
Pergamon Press Inc., 660 White Plains Road, Tarrytown, NY 10591-5153, USA

A member of the Elsevier Science Publishing Group

First price quoted is definitive. Prices include postage and insurance. * Asterisked price is quoted for convenience only and is subject to exchange rate fluctuation.

SEND FOR A FREE SAMPLE COPY OF...

JOURNAL OF ATMOSPHERIC AND TERRESTRIAL PHYSICS

Editor-in-Chief: **MICHAEL J. RYCROFT**, *College of Aeronautics, Cranfield Institute of Technology, Cranfield, Bedford MK43 0AL, UK*
Editor Emeritus: **SIR GRANVILLE BEYNON, FRS**

The *Journal of Atmospheric and Terrestrial Physics* is an international journal concerned with the interdisciplinary science of the Earth's atmospheric and space environment. Papers are published on the results of experiments and their interpretations, and on theoretical or modelling studies. Papers dealing with remote sensing carried out from the ground or with *in situ* studies made from rockets or from satellites orbiting the Earth are particularly suitable. Plans for future research, often carried out as an international programme, are also discussed. Besides original research papers, discussion papers and short reports, the journal includes commissioned review papers on topical subjects and special issues arising from chosen scientific symposia or workshops.
The journal covers the physical processes operating in the troposphere, stratosphere, mesosphere, thermosphere, ionosphere, magnetosphere and heliosphere. Phenomena occurring in other `spheres` and supporting laboratory measurements are also considered. The journal deals especially with the coupling between the different regions. Regarding the upper atmosphere, the subjects of aeronomy, geomagnetism, auroral phenomena, radio wave propagation and plasma instabilities are examples within the broad field of solar-terrestrial physics which emphasise the energy exchange between the solar wind, the magnetospheric and ionospheric plasmas, and the neutral gas. In the middle and lower atmosphere, the topics covered include dynamics, radiation and chemistry, atmospheric electricity and electrodynamic effects, including lightning and its effects, and anthropogenic changes. Helpful, novel schematic diagrams are encouraged as is the use of colour.

A Selection of Papers
R. G. ROBLE (USA), On modeling component processes in the Earth's global electric circuit.
H. A. VON BIEL (New Zealand), Ionisation in the Antarctic stratosphere.
A. S. RODGER, R. J. MOFFETT & S. QUEGAN (UK), The role of ion drift in the formation of ionisation troughs in the mid- and high-latitude ionosphere - a review.
W. K. TOBISKA (USA), Revised solar extreme ultraviolet flux model.
R. H. M. MIESEN (The Netherlands), Applying weakly nonlinear internal wave theories to solitary waves in the atmosphere.
M. LOCKWOOD (UK), The excitation of ionospheric convection.

Indexed/Abstracted in: *Curr Cont, ASCA, Cam Sci Abstr, Curr Cont/Phy Chem & Earth Sci, INSPEC Data, Curr Cont Sci Cit Ind, Curr Cont SCISEARCH Data*

(00211)
Subscription Information
1993: Volume 55 (14 issues)
Annual subscription (1993) **£750.00** **US$1425.00***
ISSN: 0021-9169

PERGAMON PRESS
Pergamon Press Ltd, Headington Hill Hall, Oxford OX3 0BW, UK
Pergamon Press Inc., 660 White Plains Road, Tarrytown, NY 10591-5153, USA
A member of the Elsevier Science Publishing Group

First price quoted is definitive. Prices include postage and insurance. * Asterisked price is quoted for convenience only and is subject to exchange rate fluctuation.

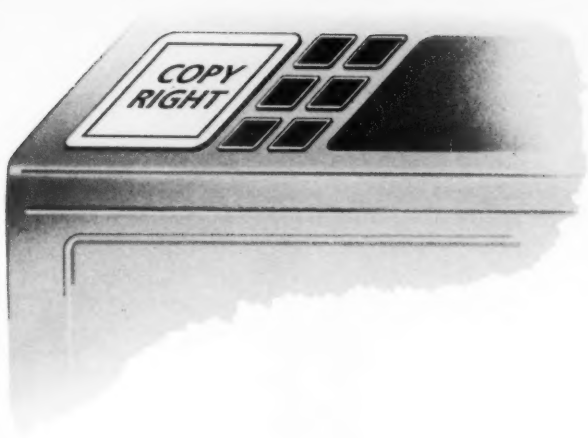

THE ~~AN~~ MOST IMPORTANT PART OF YOUR PHOTOCOPIER ISN'T PART OF YOUR PHOTOCOPIER

Having the machine does not permit you to photocopy
books, journals and magazines.
The Copyright Clearance Center DOES.
Contact us to find out
how you too can Copy Right.

COPYRIGHT CLEARANCE CENTER

27 Congress Street, Salem, MA 01970 □ Tel. (508) 744-3350 □ Fax (508) 741-2318

© 1991 Copyright Clearance Center

From January 1993

PLANETARY AND SPACE SCIENCE

will become the Official Journal of the

European Geophysical Society Planetary and Solar System Sciences Section

Editor-in-Chief:
MARCELLO CORADINI,
Observatoire de Paris-Meudon, 5 Place Jule Janssen, 92195 Meudon Cedex, France

Associate Editor:
W-H IP, *Taiwan*

Subject Editors:
Cosmology and Origin:
H WÄNKE, *Germany*

Small Bodies, Dust and Rings:
M FULCHIGNONI, *Italy*

Terrestrial Planets and Satellites:
P MASSON, *France*

Outer Planets:
D GAUTIER, *France*

Planetary Atmospheres:
F TAYLOR, *UK*

Planetary Magnetospheres and Ionospheres:
D SOUTHWOOD, *UK*

Exobiology:
G HORNECK, *Germany*

Celestial Mechanics:
A E ROY, *UK*

History of Planetary and Space Research:
D HUGHES, *UK*

New Aims and Scope

Planetary and Space Science publishes original articles as well as short communications (letters). Ground based and space borne instrumentation and laboratory simulation of solar system processes will be included. The following fields of planetary and solar system research are covered:

***cosmochemistry and origin, including all aspects of the formation and initial physical and chemical evolution of the solar system**

small bodies, dust and rings, including asteroids, comets and zodiacal light and their interaction with the solar radiation and the solar wind

***terrestrial planets and satellites, including the physics of the interiors, geology and morphology of the surfaces, tectonics, mineralogy and dating**

outer planets and satellites, including formation and evolution, remote sensing at all wavelengths and *in situ* measurements

planetary atmospheres, including formation and evolution, circulation and meteorology, boundary layers, remote sensing and laboratory simulation

planetary magnetospheres and ionospheres, including origin of magnetic fields, magnetospheric plasma and radiation belts, and their interaction with the sun, the solar wind and satellites

***exobiology, including origin of life, detection of planetary ecosystems and pre-biological phenomena in the solar system and laboratory simulations**

***celestial mechanics, including dynamical evolution of the solar system, gravitational captures and resonances, relativistic effects, tracking and dynamics**

***history of planetary and space research**

* New Features

Subscription Information
1993 Volume 41 (12 issues)
Annual Subscription (1993)
£745.00 US$1192.00
ISSN: 0032-0633

Special Rate for EGS Members
1993: £50.00

CALL FOR PAPERS
Contributions are invited. Please send four complete copies of your manuscript to Dr Coradini at *Observatoire de Paris-Meudon, 5 Place Jule Janssen, 92195 Meudon Cedex, France*

PERGAMON PRESS
A member of the Elsevier Science Publishing Group
Oxford New York Seoul Tokyo

EA/19/12/92

PRINTED IN GREAT BRITAIN BY BPCC-AUP ABERDEEN LTD